

Rochester Institute of Technology

**RIT Digital Institutional Repository**

---

Theses

---

4-25-2017

## **Overcoming the Challenges for Multichip Integration: A Wireless Interconnect Approach**

Md Shahriar Shamim  
ms5614@rit.edu

Follow this and additional works at: <https://repository.rit.edu/theses>

---

### **Recommended Citation**

Shamim, Md Shahriar, "Overcoming the Challenges for Multichip Integration: A Wireless Interconnect Approach" (2017). Thesis. Rochester Institute of Technology. Accessed from

This Dissertation is brought to you for free and open access by the RIT Libraries. For more information, please contact [repository@rit.edu](mailto:repository@rit.edu).

OVERCOMING THE CHALLENGES FOR  
MULTICHIP INTEGRATION: A WIRELESS  
INTERCONNECT APPROACH

BY

MD SHAHRIAR SHAMIM

A DISSERTATION SUBMITTED IN PARTIAL FULFILLMENT OF THE REQUIREMENTS  
FOR THE DEGREE OF DOCTOR OF PHILOSOPHY IN COMPUTING AND  
INFORMATION SCIENCES

B. THOMAS GOLISANO COLLEGE OF COMPUTING AND INFORMATION SCIENCES

DEPARTMENT OF COMPUTING AND INFORMATION SCIENCES-PHD

ROCHESTER INSTITUTE OF TECHNOLOGY

ROCHESTER, NEW YORK

April 25, 2017

# *Overcoming the Challenges for Multichip Integration: A Wireless Interconnect Approach*

*By*  
*Md Shahriar Shamim*

## **Committee Approval:**

We, the undersigned committee members, certify that we have advised and/or supervised the candidate on the work described in this dissertation. We further certify that we have reviewed the dissertation manuscript and approve it in partial fulfillment of the requirements for the degree of Doctor of Philosophy in Computing and Information Sciences.

---

Dr. Amlan Ganguly  
Dissertation Advisor, Dept. of Computer Engineering, R.I.T.

Date:

---

Dr. Andres Kwasinski  
Dissertation Committee Member, Dept. of Computer Engineering, R.I.T.

Date:

---

Dr. Satish G. Kandlikar  
Dissertation Committee Member, Dept. of Mechanical Engineering, R.I.T.

Date:

---

Dr. Minseok Kwon  
Dissertation Committee Member, Dept. of Computer Science, R.I.T.

Date:

---

Dr. Dorin Patru  
Dissertation Defense Chair, Dept. of Electrical & Microelectronic Engineering, R.I.T.

Date:

Certified by:

---

Dr. Pengcheng Shi  
Ph.D. Program Director, College of Computing and Information Sciences, R.I.T.

Date:

© [2017] [Md Shahriar Shamim]

All rights reserved.

# *Overcoming the Challenges for Multichip Integration: A Wireless Interconnect Approach*

*By*  
*Md Shahriar Shamim*

## **ABSTRACT**

The physical limitations in the area, power density, and yield restrict the scalability of the single-chip multicore system to a relatively small number of cores. Instead of having a large chip, aggregating multiple smaller chips can overcome these physical limitations. Combining multiple dies can be done either by stacking vertically or by placing side-by-side on the same substrate within a single package. However, in order to be widely accepted, both multichip integration techniques need to overcome significant challenges.

In the horizontally integrated multichip system, traditional inter-chip I/O does not scale well with technology scaling due to limitations of the pitch. Moreover, to transfer data between cores or memory components from one chip to another, state-of-the-art inter-chip communication over wireline channels require data signals to travel from internal nets to the peripheral I/O ports and then get routed over the inter-chip channels to the I/O port of the destination chip. Following this, the data is finally routed from the I/O to internal nets of the target chip over a wireline interconnect fabric. This multi-hop communication increases energy consumption while decreasing data bandwidth in a multichip system. On the other hand, in vertically integrated multichip system, the high power density resulting from the placement of computational components on top of each other aggravates the thermal issues of the chip leading to degraded performance and reduced reliability. Liquid cooling through microfluidic channels can provide

cooling capabilities required for effective management of chip temperatures in vertical integration. However, to reduce the mechanical stresses and at the same time, to ensure temperature uniformity and adequate cooling competencies, the height and width of the microchannels need to be increased. This limits the area available to route Through-Silicon-Vias (TSVs) across the cooling layers and make the co-existence and co-design of TSVs and microchannels extremely challenging.

Research in recent years has demonstrated that on-chip and off-chip wireless interconnects are capable of establishing radio communications within as well as between multiple chips. The primary goal of this dissertation is to propose design principals targeting both horizontally and vertically integrated multichip system to provide high bandwidth, low latency, and energy efficient data communication by utilizing mm-wave wireless interconnects. The proposed solution has two parts: the first part proposes design methodology of a seamless hybrid wired and wireless interconnection network for the horizontally integrated multichip system to enable direct chip-to-chip communication between internal cores. Whereas the second part proposes a Wireless Network-on-Chip (WiNoC) architecture for the vertically integrated multichip system to realize data communication across interlayer microfluidic coolers eliminating the need to place and route signal TSVs through the cooling layers. The integration of wireless interconnect will significantly reduce the complexity of the co-design of TSV based interconnects and microchannel based interlayer cooling. Finally, this dissertation presents a combined trade-off evaluation of such wireless integration system in both horizontal and vertical sense and provides future directions for the design of the multichip system.

## ACKNOWLEDGEMENTS

The completion of this dissertation and the research behind it would not be possible without the guidance, support, and encouragement from many individuals. I would like to take this opportunity to express my earnest and heartfelt gratitude towards them.

First and foremost, I would like to give special thanks to my advisor, Dr. Amlan Ganguly, for his constant support and mentorship throughout my Ph.D. tenure at Rochester Institute of Technology. He has taught me how to become a good and effective researcher. The meaningful discussions that we have shared during my research have been truly inspirational to me. My thoughts and ideas were always more thorough and well developed after he refined them. I cannot thank him enough for his efforts on revising my manuscripts for journal and conference publications. His positive attitudes in both research and life have influenced me deeply, which will certainly benefit me for the rest of my career.

I would also like to express my sincere appreciation to my Ph.D. dissertation committee members, Dr. Andres Kwasinski, Dr. Satish G. Kandlikar, Dr. Minseok Kwon, and Dr. Dorin Patru for agreeing to serve on my dissertation committee and giving me feedback and suggestions to improve my dissertation. A special thanks to Dr. Jayanti Venkatarman for helping us with all the antenna modeling and simulations. I would also like to thank Dr. Pengcheng Shi and Dr. Shanchieh Yang for their support throughout my Ph.D. tenure.

I would like to thank all my lab mates, co-authors, and friends at Multi-core System Lab, especially Rounak Narde, Ashraf Mitul, and Meraj Ahmed for their support. I would like to express my special gratitude to my research sibling, Naseef Mansoor, whom I am very fortunate to work

with from the beginning of my Ph.D. career. I cannot thank him enough for his companionship and contributions to my research throughout last four years. Our brainstorming and conversation over the many cups of coffee helped me to strengthen the foundations of my conceptual understanding of the problems. Without any doubt, caffeine and research make the perfect blend!

My internship at Intel Corporate Quality Network (CQN) Lab during my Ph.D. has been an invaluable experience, and I appreciate the support, guidance, and the pleasant working atmosphere my colleagues at Intel have provided. I particularly thank my mentors, Dan Bockelman, Steven Chen, and Tim Pifer, as it has been a pleasure to work with them during the time I spent at Intel.

I would like to thank my parents, Md Ghias Uddin and Sarifun Nahar, who have sacrificed a lot to get me well educated. They have always encouraged my curiosity and my passion to follow my dreams. None of this would happen without their support and inspiration. I would also like to thank my younger brothers, Kashfi & Mashfi, my elder brother Shahrish Shuvo, his wife Susmita Karim, and Sabrina's family, who always have supported and inspired me. I feel extremely blessed to have such a wonderful family.

Last but most importantly, I would like to thank my wife and best friend, Sabrina Afrin, who always had my best interest in her heart; who motivated, and endured my constant nagging (with occasional yelling ☺) during the course of my Ph.D. She has made me the person I am today, taught me to have faith in myself, and reminded me what is important in life.

The research that forms the basis of this dissertation has been supported in part by the US National Science Foundation (NSF) CAREER grant CNS-1553264 and grant CCF-1162123, and by the department of Computer Engineering, RIT.

The text of Chapter 3 is in part a reprint of the material from the paper, *M. S. Shamim, N. Mansoor, R. S. Narde, V. Kothandapani, A. Ganguly and J. Venkataraman, "A Wireless Interconnection Framework for Seamless Inter and Intra-Chip Communication in Multichip Systems,"* in IEEE Transactions on Computers, vol. 66, no. 3, pp. 389-402, March 1, 2017. The dissertation author was the primary researcher and author, and the co-authors involved in the publication assisted the research which forms the foundation for that manuscript. The zigzag antennas are modeled and simulated by Rounak Singh Narde under the supervision of Dr. Jayanti Venkatarman.

The text of Chapter 4 is in part a reprint of the material from the paper, *M. S. Shamim, A. Ganguly, C. Munuswamy, J. Venkatarman, J. Hernandez, and S. Kandlikar, "Co-design of 3D wireless network-on-chip architectures with microchannel-based cooling,"* in Sixth International Green and Sustainable Computing Conference (IGSC), Las Vegas, NV, 2015, pp. 1-6. The dissertation author was the primary researcher and author, and the co-authors involved in the publication assisted the research which forms the foundation for that manuscript. The microchannels are modeled and simulated by Jose-Luis Gonzalez-Hernandez under the supervision from Dr. Satish G. Kandlikar. The zigzag antennas for the 3D wireless NoCs are modeled and simulated by Chetan Munuswamy and Rounak Singh Narde under the guidance of Dr. Jayanti Venkatarman.

# DEDICATION

*To my parents and Sabrina,  
for their boundless love and support.*

# TABLE OF CONTENT

<b>ABSTRACT .....</b>	<b>IV</b>
<b>ACKNOWLEDGEMENTS .....</b>	<b>VI</b>
<b>DEDICATION .....</b>	<b>IX</b>
<b>TABLE OF CONTENT .....</b>	<b>X</b>
<b>LIST OF FIGURES.....</b>	<b>XIV</b>
<b>LIST OF TABLES .....</b>	<b>XVI</b>
<b>LIST OF ABBREVIATIONS .....</b>	<b>XVII</b>
<b>CHAPTER 1 INTRODUCTION.....</b>	<b>1</b>
1.1 MULTICHIP SYSTEM .....	1
1.2 CHALLENGES OF THE MULTICHIP SYSTEM .....	4
1.2.1 <i>Horizontal Integration of the Multichip System</i> .....	4
1.2.2 <i>Vertical Integration of the Multichip System</i> .....	6
1.3 POSSIBLE SOLUTION: WIRELESS INTERCONNECTS.....	8
1.4 SUMMARY OF RESEARCH OBJECTIVES.....	10
1.5 CONTRIBUTIONS.....	12
1.6 DISSERTATION ORGANIZATION.....	13
<b>CHAPTER 2 BACKGROUND AND STATE-OF-THE-ARTS .....</b>	<b>15</b>
2.1 INTRA AND INTER-CHIP INTERCONNECTION FOR HORIZONTALLY INTEGRATED MULTICHIP SYSTEM .....	15
2.2 VERTICALLY INTEGRATED MULTICHIP SYSTEM AND MICROCHANNEL BASED COOLING .....	18
2.3 WIRELESS TECHNOLOGY: A PROMISING INTERCONNECT PARADIGM.....	21

<b>CHAPTER 3</b>	<b>DESIGN OF A WIRELESS INTERCONNECTION FRAMEWORK FOR SEAMLESS INTER AND INTRA-CHIP COMMUNICATION IN HORIZONTALLY INTEGRATED MULTICHIP SYSTEMS .....</b>	<b>24</b>
3.1	WIRELESS INTERCONNECTION FRAMEWORK FOR MULTICHIP SYSTEMS.....	25
3.1.1	<i>Topology .....</i>	25
3.1.2	<i>Physical Layer.....</i>	28
3.1.3	<i>Flow Control and Routing .....</i>	30
3.1.4	<i>Wireless Communication Protocol.....</i>	32
3.2	EXPERIMENTAL RESULTS .....	36
3.2.1	<i>Simulation Platform .....</i>	36
3.2.2	<i>Wireless Channel Characteristics and Wireless Link Budget Analysis .....</i>	38
3.2.3	<i>Comparative Performance Evaluation .....</i>	41
3.2.4	<i>Deployment of the Wireless Interconnection with Scaling of System Size.....</i>	51
3.2.5	<i>Performance Evaluation with Non-uniform Traffic Patterns .....</i>	54
3.2.6	<i>Comparative Evaluation with Respect to Emerging Multichip Integration Technologies.....</i>	56
3.2.7	<i>Area Overheads .....</i>	61
3.3	SUMMARY .....	62
<b>CHAPTER 4</b>	<b>WIRELESS INTERCONNECT AS AN ENABLER FOR DATA COMMUNICATION ACROSS MICROCHANNEL BASED COOLING LAYER IN VERTICALLY INTEGRATED MULTICHIP SYSTEM.....</b>	<b>63</b>
4.1	INTEGRATED DESIGN METHODOLOGY FOR WIRELESS 3D NOC WITH MICROCHANNEL BASED LIQUID COOLING .....	67
4.1.1	<i>Design of Microchannel Cooling Layer.....</i>	67
4.1.2	<i>Proposed Topology of the 3D Wireless NoC Architecture .....</i>	70
4.1.3	<i>Physical Layer.....</i>	71
4.1.4	<i>Seamless Flow Control and Routing.....</i>	73
4.1.5	<i>Wireless Communication Protocol and Transceiver.....</i>	74
4.2	EXPERIMENTAL RESULTS .....	75
4.2.1	<i>Dimensions of the Cooling Channels.....</i>	76

4.2.2	<i>Evaluation of the Hybrid 3D NoC Architecture in the Presence of Microchannel based Liquid Cooling...</i>	81
	.....	
A.	Wireless Channel Modeling and Link Budget Analysis .....	83
B.	Temperature and Performance Characteristics of 3D Wireless NoC Architectures with Synthetic Workload .....	87
4.2.3	<i>Temperature and Performance Characteristics of 3D NoC Architectures with Real Application-based Workloads.....</i>	92
4.2.4	<i>Increasing Cooling Capacity of the Interlayer Coolers and its Impact on Performance of the 3D Wireless NoC .....</i>	94
4.2.5	<i>Comparison with Alternative Wireless Communication Mechanism .....</i>	95
4.2.6	<i>Area Overheads .....</i>	98
4.2.7	<i>Trade-off Analysis .....</i>	99
4.2.8	<i>Holistic Comparison of the Vertically Integrated Wireless System with Horizontally Integrated Wireless Multichip System .....</i>	101
4.3	SUMMARY .....	104
<b>CHAPTER 5</b>	<b>CONCLUSION AND FUTURE RESEARCH DIRECTIONS .....</b>	<b>106</b>
5.1	CONCLUSION .....	106
5.2	FUTURE RESEARCH DIRECTIONS .....	109
5.2.1	<i>Energy-Efficient Multi-gigabit Transceiver Design for Intra and Inter-Chip Wireless Interconnects .....</i>	109
5.2.2	<i>Traffic-Aware Medium Access Mechanism for Multi-Chip System .....</i>	110
5.2.3	<i>A Wireless Interconnection Framework for Multichip System with In-Package Memory.....</i>	111
5.2.4	<i>60 GHz mm-wave Wireless Interconnects to Enable Contactless Testing.....</i>	113
APPENDIX A.....		116
PUBLICATIONS .....		116
JOURNALS: .....		116
CONFERENCES: .....		117
WORK-IN-PROGRESS (WiP)/POSTER PRESENTATION: .....		118

**BIBLIOGRAPHY..... 119**

# LIST OF FIGURES

FIGURE 1.1. A TYPICAL COMPUTING ORGANIZATION IN HPC ENVIRONMENTS I.E. DATA CENTER/SERVERS .....	2
FIGURE 1.2. THE RANGE OF DIFFERENT INTERCONNECTION ARCHITECTURES. ....	3
FIGURE 1.3. SCALING OF I/O PITCH AND MINIMUM GLOBAL INTERCONNECT PITCH [6] .....	5
FIGURE 2.1. CONCEPTUAL DIAGRAM OF A WIRELINE MESH BASED NOC AND ITS MULTIHOP COMMUNICATION NATURE.....	15
FIGURE 2.2. CONCEPTUAL DIAGRAM OF A MULTICHIP SYSTEM INTERCONNECTED WITH C4 BUMPS AND IN-PACKAGE TRANSMISSION LINE.	17
FIGURE 2.3. VERTICALLY STACKED DIES WITH CONVENTIONAL AIR-COOLED HEAT SINK. ....	18
FIGURE 2.4. (A) INDUCTIVE COUPLING (B) CAPACITIVE COUPLING BASED INTERCONNECTED FOR VERTICALLY STACKED DIES [50]. ....	20
FIGURE 3.1. CONCEPTUAL DIAGRAM OF THE WIRELESS MULTICHIP SYSTEM. ....	27
FIGURE 3.2. SPECIFIC DIMENSIONS OF THE ANTENNA AND FEED STRUCTURE. ....	29
FIGURE 3.3. BLOCK DIAGRAM OF MM-WAVE TOKEN-BASED WIRELESS INTERFACE.....	34
FIGURE 3.4. (A) TOP VIEW OF THE MODEL (B) SIDE VIEW OF THE MODEL .....	38
FIGURE 3.5. (A) RADIATION PATTERN, (B) RETURN LOSS, AND (C) WORST CASE PATH LOSS FOR WIRELESS MULTICHIP SYSTEM.....	40
FIGURE 3.6. CONCEPTUAL VIEW OF (A) BUS I/O AND (B) NETWORK I/O BASED WIRELINE CONFIGURATION .....	42
FIGURE 3.7. PEAK ACHIEVABLE BANDWIDTH PER CORE WITH VARYING SYSTEM SIZE FOR DIFFERENT CONFIGURATIONS WITH UNIFORM TRAFFIC.....	45
FIGURE 3.8. AVERAGE PACKET LATENCY OF VARIOUS MULTICHIP SYSTEMS. ....	46
FIGURE 3.9. PACKET ENERGY WITH VARYING SYSTEM SIZE FOR DIFFERENT CONFIGURATIONS WITH UNIFORM TRAFFIC.....	48
FIGURE 3.10. RELATIVE GAIN IN BANDWIDTH AND PACKET ENERGY WITH DIFFERENT FLIT WIDTH FOR 2-CHIP SYSTEM.....	50
FIGURE 3.11. BANDWIDTH PER CORE AND AVERAGE PACKET ENERGY FOR 1, 2, 4-CHIP SYSTEMS FOR TWO DIFFERENT DEPLOYMENT APPROACHES OF WIS. ....	51
FIGURE 3.12. RELATIVE GAIN IN BANDWIDTH AND AVERAGE PACKET ENERGY WITH DIFFERENT SYSTEM SIZES. ....	52
FIGURE 3.13. (A) BANDWIDTH PER CORE AND (B) PACKET ENERGY WITH NON-UNIFORM TRAFFIC FOR I/O BASED AND WIRELESS MULTICHIP SYSTEMS.....	54
FIGURE 3.14. BANDWIDTH PER CORE AND PACKET ENERGY FOR 2-CHIP I/O BASED AND WIRELESS MULTICHIP SYSTEMS WITH VARYING LOCALIZATION.....	55

FIGURE 3.15. BANDWIDTH PER CORE AND AVERAGE PACKET ENERGY FOR DIFFERENT INTERCONNECT TECHNOLOGIES FOR 4-CHIP SYSTEM	58
FIGURE 3.16. AREA OVERHEADS OF DIFFERENT WIRELINE AND WIRELESS ARCHITECTURE CONSIDERED IN THIS PAPER	61
FIGURE 4.1. SIDE VIEW OF PROPOSED 3D WIRELESS NOC ARCHITECTURE WITH THE INTERLAYER COOLING LAYER	65
FIGURE 4.2. TOP VIEW OF ONE ACTIVE LAYER	70
FIGURE 4.3. THERMAL RESISTANCE VARIATION FOR THE MICROCHANNELS	77
FIGURE 4.4. PRESSURE DROP VARIATION FOR THE MICROCHANNELS	78
FIGURE 4.5. PUMPING POWER VARIATION FOR THE MICROCHANNELS	79
FIGURE 4.6. (A) FULL SIDE VIEW (B) VIEW INSIDE THE BOX	82
FIGURE 4.7. DIMENSIONS OF THE DESIGNED ZIG-ZAG ANTENNA	84
FIGURE 4.8. RETURN LOSSES OF ALL 16 ANTENNAS	85
FIGURE 4.9. THE INSERTION LOSS OF ANTENNA 1 IN LAYER1	86
FIGURE 4.10. PEAK BANDWIDTH AND ENERGY COST PER BIT FOR DIFFERENT 3D NOC ARCHITECTURES	91
FIGURE 4.11. NORMALIZED PEAK BANDWIDTH AND ENERGY COST PER BIT IN THE PRESENCE OF REAL APPLICATION TRAFFIC	92
FIGURE 4.12. PEAK CHIP TEMPERATURE IN PRESENCE OF REAL APPLICATION TRAFFICS	93
FIGURE 4.13. THE IMPACT OF FREQUENCY OF THE COOLING LAYERS	94
FIGURE 4.14. PEAK BANDWIDTH AND ENERGY COST PER BIT FOR DIFFERENT WIRELESS COMMUNICATION MECHANISMS	96

# LIST OF TABLES

TABLE 3.1. MULTICHIP SYSTEMS WITH DIFFERENT INTER-CHIP INTERCONNECTION CONSIDERED IN THIS PAPER .....	44
TABLE 3.2. ENERGY PER BIT AND AGGREGATE BANDWIDTH FOR DIFFERENT INTERCONNECT TECHNOLOGIES.....	57
TABLE 4.1. SUMMARY AND COMPARISON OF THE SINGLE-PHASE MICROCHANNEL GEOMETRIES IN THE LITERATURE .....	80
TABLE 4.2. PEAK TEMPERATURE OF TWO ARCHITECTURES CONSIDERED HERE .....	89
TABLE 4.3. ENERGY PER BIT FOR A SINGLE POINT-TO-POINT LINK AND POSSIBLE AGGREGATE BANDWIDTH FOR DIFFERENT WIRELESS COMMUNICATION PROTOCOLS.....	97
TABLE 4.4. AREA OVERHEAD FOR THE SIGNAL TSVS THROUGH MICROCHANNEL COOLING LAYER. ....	98
TABLE 4.5. PERFORMANCE COMPARISON WITH THE HORIZONTALLY INTEGRATED WIRELESS MULTICHIP MODULE.....	101
TABLE 4.6. HOLISTIC COMPARISON OF BOTH MULTICHIP INTEGRATION TECHNIQUES IN VARIOUS DOMAINS. ....	103

## LIST OF ABBREVIATIONS

<i>3D-CHiWiNoC</i>	<i>CDMA based 3D Wireless NoC</i>
<i>3D-HiWiNoC</i>	<i>3D- Hierarchical Wireless NoC</i>
<i>3D-ICs</i>	<i>Three-dimensional Integrated Circuits</i>
<i>3D-MTSV</i>	<i>3D Mesh NoC with TSV</i>
<i>3D-THiWiNoC</i>	<i>Token based 3D Wireless NoC</i>
<i>APUs</i>	<i>Accelerated Processor Units</i>
<i>AR</i>	<i>Aspect Ratio</i>
<i>A-TDMA</i>	<i>Asynchronous TDMA</i>
<i>ATE</i>	<i>Automatic Test Equipment</i>
<i>BER</i>	<i>Bit-Error Rate</i>
<i>CDMA</i>	<i>Code Division Multiple Access</i>
<i>CNT</i>	<i>Carbon Nanotube</i>
<i>CSMA/CD</i>	<i>Carrier Sense Multiple Access/Collision Detection</i>
<i>CTE</i>	<i>Coefficient of Thermal Expansion</i>
<i>DSSS</i>	<i>Direct Sequence Spread Spectrum</i>
<i>DUT</i>	<i>Device-Under-Test</i>

<i>DVFS</i>	<i>Dynamic Voltage and Frequency Scaling</i>
<i>EDA</i>	<i>Electronic Design Automation</i>
<i>EMF</i>	<i>Electromotive Force</i>
<i>FDMA</i>	<i>Frequency Division Multiple Access</i>
<i>HPC</i>	<i>High-Performance Computing</i>
<i>ITRS</i>	<i>International Technology Roadmap for Semiconductor</i>
<i>MAC</i>	<i>Medium Access Control</i>
<i>MAD</i>	<i>Minimum Average Distance</i>
<i>MCM</i>	<i>Multi-Chip Module</i>
<i>MIMD</i>	<i>Multiple Instruction Multiple Data</i>
<i>mm-wave</i>	<i>Millimeter-Wave</i>
<i>MWCNT</i>	<i>Multi-Walled Carbon Nanotube</i>
<i>NoC</i>	<i>Network-on-Chip</i>
<i>OOK</i>	<i>On-Off Keying</i>
<i>PCB</i>	<i>Printed Circuit Boards</i>
<i>RFI</i>	<i>Radio Frequency based Interconnects</i>
<i>SiP</i>	<i>System-in-Package</i>

<i>SNR</i>	<i>Signal-to-Noise Ratio</i>
<i>SW</i>	<i>Small-World</i>
<i>TSV</i>	<i>Through-Silicon-Vias</i>
<i>UWB</i>	<i>Ultra-Wide Band</i>
<i>VCs</i>	<i>Virtual Channels</i>
<i>WDM</i>	<i>Wavelength Division Multiplexing</i>
<i>WI</i>	<i>Wireless Interfaces</i>
<i>WiNoC</i>	<i>Wireless Networks-on-Chip</i>

# Chapter 1 INTRODUCTION

## 1.1 Multichip System

Moore's law, the primary guiding principle for the chip development, states that the numbers of transistors on a chip will roughly double in every technology generation. Because of this scaling, billions of transistors are now packed tightly into each microprocessor. Until recently, dynamic power was considered as the most significant source of power consumption with technology scaling, and Dennard's scaling has helped to control it by reducing supply voltages. Since dynamic power is proportional to the square of the supply voltage, reducing the voltage decreases dynamic power consumption significantly. However, with technology scaling, sub-threshold leakage and gate-oxide leakage increase in an exponential manner which are the main sources of leakage current. As a result, static power is now starting to dominate total power consumption. This upsurge in power consumption is not only increasing chip temperature and cooling cost but also decreases chip reliability and performance. The multicore system has appeared as a feasible solution to address the power and frequency limitations of the uniprocessor system. According to Flynn's taxonomy of parallel computer classification, the multicore system is an example of Multiple Instruction Multiple Data (MIMD) computing organization where different cores execute different threads (Multiple Instructions), working on different parts of memory (Multiple Data) concurrently [1]. As a result, instead of running at the higher clock frequency, multicore system improve overall performance by running more tasks in parallel. This, in turn, helps to reduce the rapid growth of power consumption of uniprocessors. The Network-on-Chip (NoC) paradigm has emerged as an enabling methodology for interconnecting hundreds of cores on the same die by designing separate scalable interconnection fabrics to support high-speed communication between

cores [2] and has captured the attention of both the academia and the industry. Tiler's 64-core TILE64 [3], Intel's 80-core Polaris [4], 48-core Single-chip Cloud Computer [5] are some examples of such NoC based multicore chips.

However, demand for performance improvement is still quite high, and according to the projection from International Technology Roadmap for Semiconductor (ITRS), it is expected to grow to 300x by 2022 [6]. This growth will result in an integration of 100x more cores than the current state of art multicore system. Designing such large multicore chip will not come without any price. Larger chip size usually results in lower yield. For example, let us consider two different die sizes, one with 20 mm × 20 mm and another with 10 mm × 10 mm. A round wafer with a diameter of 300 mm, it can pack 143 and 640 dies of those two sizes respectively. If we consider only 20 manufacturing defects due to process and fabrication variations (In reality, it can be more than that), larger die size results in 14% yield loss whereas in smaller die size, it is only 3.12%. Although, smaller die size improves yield and provides fine-grained granularity regarding binning, per die fixed costs i.e. packaging, assembly, and test can increase the total combined cost of

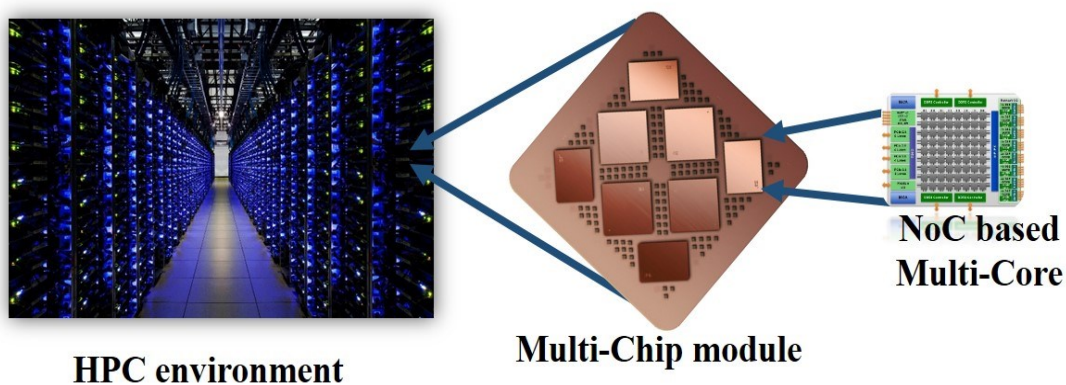
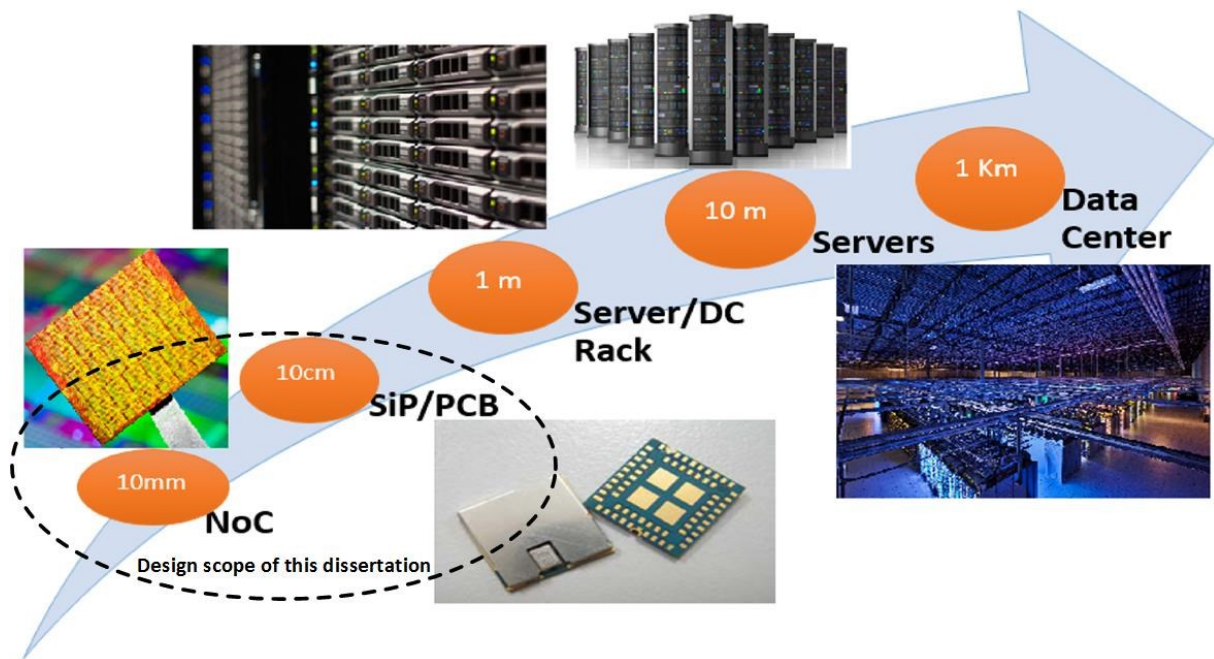


Figure 1.1. A typical computing organization in HPC environments i.e. data center/servers

development [7]. It also provides less functionality as a relatively small number of cores can be packed into that small area. Aggregating multiple moderately smaller dies within a package can provide the functionality of a large chip and at the same time can provide significant advantages in terms of higher yield and better packing of rectangular die on a round wafer [8]. Moreover, the disintegration allows easier reuse by supporting different system sizes. Combining multiple chips in a single package can be done either by vertically stacking several chips with Through Silicon Vias (TSVs) i.e. 3D integration [9] or by placing them horizontally on the same substrate within the package i.e. multichip module [10][11]. Computing modules with the multichip system are all-pervasive in hardware infrastructures from servers to data centers. A typical computing organization in High-Performance Computing (HPC) environment like data centers/clusters is shown in Figure 1.1. Due to scaling up of a number of individual computing nodes by several



**Figure 1.2. The range of different interconnection architectures.**

orders of magnitude in the HPC systems, the interconnection between them has become increasingly sophisticated. For example, inter-chip interconnections vary from solder bumps or C4 interconnects in the multichip module within a System-in-Package (SiP) spanning 10cm in range on one end to Ethernet used in data center warehouses spanning about a kilometer on the other as shown in Figure 1.2. While intra-chip communication infrastructure is seeing a paradigm shift from bus-based systems to NoC architectures [2], inter-chip communication also needs to evolve at a rapid pace to cater to increasing bandwidth demands within the strict power and thermal envelopes.

## **1.2 Challenges of the Multichip System**

The multichip system presents new opportunities to overcome the floorplan restriction, yield, and scalability limitations of the traditional single-chip multicore system. However, to be widely accepted, the multichip system requires high bandwidth, low latency, and energy-efficient communication across the distinct chips and at the same time, needs to operate within a thermal budget while maintaining high performance. Depending on the integration methodology, the challenges of designing multichip system can be different. Volume production and commercial exploitation of multichip system will only be feasible after addressing these concerns.

### **1.2.1 Horizontal Integration of the Multichip System**

In environments like data center or servers, the lower level cache is physically distributed between all cores. Hence, cache or memory access eventually requires communication between components in different chips. However, recent trends according to the ITRS predict that the pitch of the I/O interconnects in ICs is not scaling as fast as the gate lengths or pitch of on-chip interconnects [6]

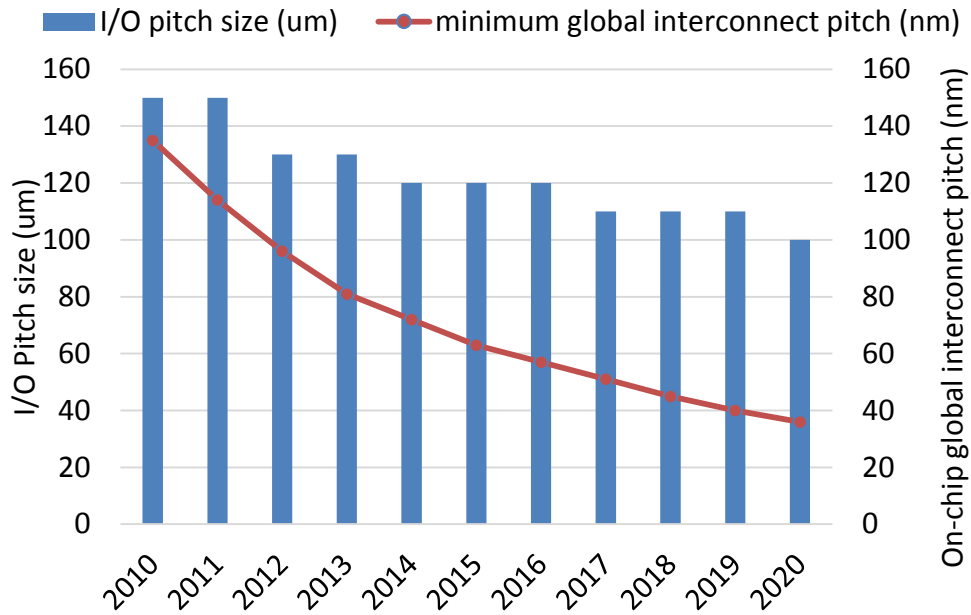


**Figure 1.3. Scaling of I/O pitch and Minimum global interconnect pitch [6]**

as shown in Figure 1.3. This implies a gap in density and performance of traditional I/O systems relative to on-chip interconnections. The wiring complexity of both on-chip and off-chip interconnects exacerbates the problem by presenting design challenges, crosstalk and signal integrity issues [10]. Additionally, because of different interconnection frameworks for on-chip and off-chip communication, data from cores located within the chips need to travel to the I/O blocks, traverse the inter-chip link and then be routed to the final destination inside the target chip. Besides, switching between protocols is necessary if the off-chip communication protocol is different from the on-chip one. All these factors reduce the efficiency in terms of energy consumption as well as latency and bandwidth of the data transfer between cores in a multichip system. Integrated inter and intra-chip photonic interconnections [12] [13] is a promising solution to the off-chip interconnection challenges of traditional I/Os. However, the pitch of photonic interconnects do not scale well due to the limitations in size of silicon photonic devices. Also, the

optical loss of silicon waveguides (typically 3.6 dB/cm) [14] makes routing long inter-chip optical channels impractical. Thus, to be widely accepted, the horizontally integrated multichip system requires high bandwidth, low latency, and energy efficient communication across the different chips.

### **1.2.2 Vertical Integration of the Multichip System**

Vertically stacking several dies with TSVs i.e. 3D integration is another alternative way to overcome the physical limitations of single chip multiprocessor system [9]. However, utilizing the third dimension to provide additional device layers poses significant thermal challenges. Higher power density is already a major problem in single chip system, and stacking vertical layers increases the power dissipation density and the thermal footprint per unit area substantially. This fact augmented with the slow lateral diffusion of heat in silicon creates localized thermal hotspots. Also, conventional cooling techniques are limited in ability to extract heat only from the top or bottom layer of the entire 3D stack. Conventional thermal management techniques adopted in a single planar chip like Dynamic Voltage and Frequency Scaling (DVFS) or Clock/Power gating sacrifice performance to control the thermal behavior by slowing down or turning off the processors when a critical temperature threshold is exceeded. On the other hand, task scheduling or task reallocation based dynamic thermal management technique redistributes existing processes to available cores based on the current thermal profile of the chip. However, the effectiveness of such DTM technique depends on the availability of relatively cooler processors or cores, which might be difficult to find in 3D integration due to relatively high power density and shorter inter-chip distance. Moreover, technology scaling is pushing the limits of affordable cooling, thereby requiring suitable design techniques to reduce peak temperatures [15]. The design of sophisticated

cooling mechanisms like liquid cooling through microfluidic channels can provide cooling capacities necessary for effective management of chip temperatures in 3D ICs [16][17][18][19]. In liquid cooling, embedded inter-layer microchannels or a cooling chip is inserted in between layers of the 3-D chip and a coolant fluid (i.e., water or other liquids) is pumped through the microchannels to extract the heat from the interlayer regions effectively. However, pumping liquid through the microchannels can cause high-pressure drops compromising the mechanical integrity of the thin walls between TSVs and microchannels [20]. Lowering the coolant flow rate to reduce the pressure drop has another disadvantage of higher temperature non-uniformity in the silicon substrate along the flow length. Moreover, large thermal gradients along the fluid flow direction inside microchannels can affect the structural reliability of the TSVs by inducing temperature related expansion and contraction due to a mismatch in Coefficient of Thermal Expansion (CTE) between copper and silicon. To reduce the mechanical stresses and at the same time, to provide temperature uniformity and adequate cooling capabilities, the height and width of the microchannels need to be increased. Several dimensions of microchannels are suggested in literature ranging from 50  $\mu\text{m}$  to 1000  $\mu\text{m}$  in height and 100  $\mu\text{m}$  to 1000  $\mu\text{m}$  in width depending on desired pressure drop and cooling capabilities [21][22]. This, in turn, imposes significant restrictions on where and how many TSVs and microchannels can co-exist together. TSVs with Aspect Ratio ( $AR=Height/Diameter$ ) greater than 10 are tough to manufacture at high yield due to challenges related to etching, sidewall passivation, and formation, insulation, and filling of vias [6] and co-dependency of the microchannels and electrical design makes the process even more complex. Wider microchannels occupy a significant portion of the floor area of the vertically integrated multichip system severely restricting the freedom of placement and routing of TSV based links. Moreover, increasing the microchannels height will eventually increase the die

thickness and consequently, the height of TSVs, which in turn will increase the diameter of the TSVs to maintain a fixed AR. Also, to reduce voltage drop, TSVs used for power delivery network require higher diameter and pitch than the signal TSVs. All these factors restrict the area available to route TSVs across the cooling layers and make the co-existence and co-design of TSVs and microchannels challenging especially when thousands of TSVs are required for interconnections in large chips with die areas higher than  $100 \text{ mm}^2$  [23]. Contactless interconnects in 3D ICs through inductive and capacitive coupling based vertical links have been proposed in recent years [24][25][26]. However, their feasibility across microchannel based cooling layers is unknown. Moreover, these inductive/capacitive coupling links have larger area overheads compared to TSVs [26]. In addition, energy per bit of such links increases significantly with the communication distance [26], making these contactless interconnects inefficient for communication across the microchannels with a height greater than  $50 \text{ }\mu\text{m}$ .

### **1.3 Possible Solution: Wireless Interconnects**

Research in recent years has demonstrated that on-chip and off-chip wireless interconnects are capable of establishing radio communications within as well as between multiple chips. The absence of the need for physical layouts makes wireless interconnects stand out from other emerging interconnects. Wireless data communication links up to 10 m in length with multi-GigaHertz bandwidths in millimeter wave (mm-wave) bands are fabricated and demonstrated in [27]. Using such on-chip antennas embedded in the chip Wireless Networks-on-Chip (WiNoC) architectures have been proposed [28][29]. These wireless NoCs are shown to improve energy efficiency and bandwidth of on-chip data communication in multicore chips [29][30]. On-chip antennas like Carbon Nanotube (CNT) or Graphene-based structures are predicted to provide high

bandwidth wireless communication channels [30][31]. However, integration of these antennas with standard CMOS processes needs to overcome significant challenges. Whereas mm-wave antennas fabricated using top layer metals are CMOS process compatible making them suitable for near-term solutions to the wired interconnect problem [29]. In mm-wave wireless interconnects, bandwidth is limited by the state-of-the-art transceiver design and on-chip antenna technology. To improve performance, multiple wireless transceivers need to access the wireless medium to communicate with other wireless transceivers without interference. Medium access mechanisms in WiNoCs using mm-wave transceivers range from simple token passing based protocol to more sophisticated Code Division Multiple Access (CDMA) based mechanisms [29][32][33][34]. The chosen on-chip antenna has to provide the best power gain for the smallest area overhead. A metal mm-wave zigzag antenna has been demonstrated to possess these characteristics as they are more compact compared to other antenna structures such as a patch antenna. Such mm-wave 60GHz antennas are shown to have a bandwidth of 16GHz for both intra-chip and inter-chip [28][35] communications links. It has been noted in many earlier works that the mm-wave wireless antennas are not directional and hence can be used for broadcast type transmission over the shared wireless channel. This property gives an additional advantage as wireless interconnects can provide a broadcast-capable medium to distribute any kind of control messages faster efficiently.

This work proposes to utilize mm-wave wireless interconnect to overcome the challenges of the multichip system. Few cores inside the chips will be equipped with wireless transceivers, which will be capable of establishing direct one-hop communication with other such cores in the same as well as other chips. Depending on the target integration technology, the dissertation proposes design principles and methodologies to use wireless interconnect for multichip based

system. The first part proposes the design methodologies to use wireless interconnect to provide high bandwidth, low latency, and energy efficient communication across the distinct chips for the horizontally integrated multichip system. Whereas the second part addresses the co-design challenges of TSVs and microchannels in vertically stacking multichip system by utilizing wireless interconnects for data communication across microchannels coolers eliminating the need to place and route signal TSVs through the cooling layer. In conclusion, this dissertation performs a comparative evaluation of horizontally and vertically integrated wireless multichip systems in terms of performance, energy-efficiency, and temperature and points towards various promising future directions initiating from this research work. The design scope of this dissertation is encircled in Figure 1.2.

## **1.4 Summary of Research Objectives**

### **1. Design of a Wireless Interconnection Framework for Seamless Inter and Intra-chip Communication in Horizontally Integrated Multichip System**

This research objective proposes to use wireless interconnects to establish a seamless communication backbone which enables data exchange between cores in a single chip as well as between chips in a multichip system with dimensions spanning up to a few tens of centimeters. The same communication protocols used for on-chip data transfer in the intra-chip NoC will be utilized for off-chip data as well, eliminating the need for protocol transfer. By deploying the wireless transceivers in the internal nodes of the chips such that all cores are within a short distance from their nearest transceivers, energy-efficient inter and intra-chip communication can be achieved. The design methodologies for such multicore multichip systems will be developed, and

comparative system-level performance evaluation with traditional I/O based multichip system will be completed.

## **2. Wireless Interconnect as an Enabler for Data Communication across Microchannel based Cooling Layer in Vertically Integrated Multichip System**

The objective of this research goal is to investigate design methodologies and suitable architecture for vertical integration to realize the data communication across the cooling layers with on-chip wireless interconnects depending upon the dimensions of the microchannels for best trade-offs in thermal and hydraulic performance. Integration of wireless interconnects in 3D integration for data communication across microchannel-based interlayer will eliminate the need for accommodating signal TSVs through the cooling chip while providing energy efficient data communication. Therefore, the only TSV based links to be placed and routed across the cooling layers would be the power and clock delivery networks. This integration methodology will significantly reduce the complexity of the co-design challenge of TSV based interconnects and microchannels based interlayer cooling.

## **3. Holistic Comparative Evaluation of the Horizontally Integrated Multichip System with Vertically Stacked Multichip System**

For first two research goals, depending on the target integration technology, the design methodologies and architectures will differ. However, both research activities propose to use wireless interconnect to overcome the limitations of horizontal and vertical integration of the multichip system. The final research goal aims to perform a holistic comparative evaluation of these two different integration approaches in terms of performance, energy-efficiency, and temperature and to provide future directions for design of the multichip system.

## 1.5 Contributions

In this dissertation, we develop design principles and methodologies to utilize wireless interconnect for horizontally and vertically integrated the multichip system. The principal contribution of this dissertation can be summarized as below:

### **1. Design of a Wireless Interconnection Framework for Seamless Inter and Intra-chip Communication in Horizontally Integrated Multichip Systems**

As part of this objective, this thesis explored the advantages possible if inter-chip communication in horizontally integrated multichip modules can be realized with state-of-the-art mm-wave wireless links operating in the 60GHz band. The specific contributions of this research goal are:

- Proposed two different interconnect frameworks to utilize wireless interconnects for seamless inter and intra-chip communication. This proposed framework eventually extends the NoC spanning to multiple chips.
- The design of suitable on-chip antennas to establish wireless interconnection in a multichip system.
- Evaluated the performance of the wireless multichip system and compare it with several traditional I/O based multichip systems.
- Proposed a methodology to deploy wireless interconnects when system scales up.
- Comparative evaluation of emerging multichip integration technologies.

### **2. Wireless Interconnect as an Enabler for Data Communication across Microchannel based Cooling Layer in Vertically Integrated Multichip System**

As part of this research goal, this dissertation accomplished the following tasks:

- The design of 3D wireless NoC architectures for 3D ICs with microchannel based cooling to eliminate the need for TSVs across the cooling layers.
- The design of suitable on-chip antennas to establish wireless interconnection in vertical stacking multichip integration.
- Evaluate the performance and thermal characteristics of 3D wireless NoCs equipped with microchannel cooling layers and compare with respect to traditional 3D interconnection systems using TSVs.

### **3. Holistic Comparative Evaluation of the Horizontal and Vertical Integration of Multichip Integration with Wireless Interconnect**

As part of this research goal, this dissertation compared the horizontally integrated wireless multichip system with respect to the vertically stacked 3D wireless system in terms of interconnect performance, energy-efficiency, and temperature and provided future directions for the design of such multichip system.

## **1.6 Dissertation Organization**

The dissertation is organized in five chapters. **Chapter 1** introduces the complexity of the horizontal and vertical integration of the multichip system and an overview of the possible means of addressing those issues. **Chapter 2** discusses the background and summarizes the current state of knowledge in this field. **Chapter 3** presents design methodologies for a seamless, hybrid wired and wireless interconnection network for horizontally integrated multichip systems with dimensions spanning up to tens of centimeters with on-chip wireless transceivers. The same communication protocols used for on-chip data transfer in the intra-chip NoC will be utilized for off-chip data as well, eliminating the need for protocol transfer. Few cores inside the chips will be

equipped with wireless transceivers, which will be capable of establishing direct one-hop communication with other such cores in the same as well as other chips. By deploying the wireless transceivers in the internal nodes of the chips, such that all cores are within a short distance from their nearest transceivers, energy-efficient inter and intra-chip communication can be achieved. With system-level simulations, this chapter demonstrates that such a design increases the bandwidth and reduces the energy consumption in comparison to state-of-the-art wireline I/O based multichip communication. **Chapter 4** proposes to realize the vertical interconnects for data communication across the cooling layers with on-chip wireless interconnects and presents energy-efficient wireless 3D NoC architectures designed for optimal dimensions of microchannels for best thermal cooling capability and pressure drop characteristics. This chapter demonstrates that the proposed 3D wireless NoC is capable of establishing data communication across the cooling layers using wireless interconnects with lower energy consumption and reduces chip temperatures due to interlayer cooling channels. This chapter also presents holistic Comparison of the horizontally integrated wireless multichip system with respect to the vertically stacked 3D wireless system in terms of interconnect performance, energy-efficiency, and temperature. Finally, **Chapter 5** summarizes the important conclusions and points out the direction of future research.

## Chapter 2      **BACKGROUND AND STATE-OF-THE-ARTS**

The research activities proposed in this dissertation are inspired and founded upon the current state of knowledge in three main directions. Here we discuss the most recent activities in these directions.

### **2.1 Intra and Inter-chip Interconnection for Horizontally Integrated Multichip System**

In the last few years, intra-chip communication infrastructure has seen a paradigm shift from bus-based systems to Network-on-Chips (NoCs) architectures [2]. The NoC paradigm aims to mitigate global wire delays by designing separate scalable, plug-and-play interconnection fabrics to support high-speed communication between cores. In this network-centric approach, packetized data is routed from source to destination through a series of switches and links. Commonly, wormhole switching is adopted for NoCs, where data packets are broken down into flow control units or flits. The first flit or the header flit contains routing information that helps to establish a path from the

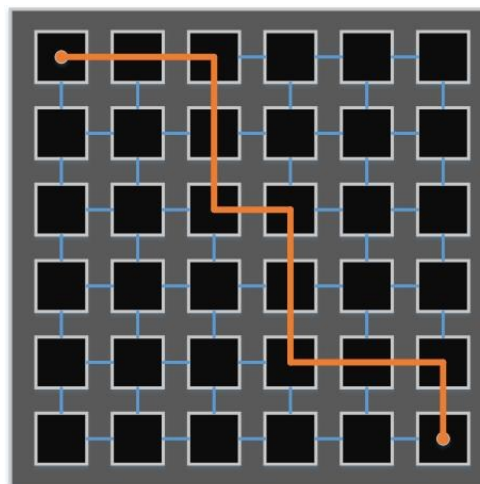


**Figure 2.1. Conceptual diagram of a wireline Mesh based NoC and its multihop communication nature.**

source to destination, and all the other payload or body flits follow that path [36]. Grid based Mesh topology shown in Figure 2.1 is most widely used NoC topology as it is relatively easy to design, manufacture, and test [3][4][5]. However, as can be seen from Figure 2.1, data transfer between two distant nodes happens in multi-hop fashion due to its regular structure. This can cause high latency and energy dissipation in metal wireline based traditional mesh architecture limiting the possible performance gain of NoCs. Insertion of long range links using conventional metal wires [37] or ultralow-latency and low-power express channels between communicating cores [38] have been proposed in the literature to alleviate this problem. However, with technology scaling, the gap between the global wire delays and gate delays increases significantly [6] and consequently, restricts the performance benefits from these approaches. Hence, to enhance the performance of metal wireline based NoC architectures, few radically different interconnection technologies such as photonic interconnects [39], multi-band RF transmission line interconnects [40], or wireless interconnects [29][30] are currently being explored. The on-chip photonic interconnects are implemented using on-chip optical waveguides, micro-ring resonators, and laser sources and are capable of achieving low latency and low power dissipation due to single hop communication between distant cores. However, the challenges regarding integration of photonic devices, precise thermal tuning of electro-optic modulators and demodulators, the signal noise due to coupling between waveguides, and manufacturing process involving a separate photonic plane [39] need to resolve for the photonic interconnects. While RF-interconnects (RF-I) [40] are compatible with CMOS technology, they require long on-chip transmission lines to enable data transmission which can lead to routing challenges and significant area overhead. On the other hand, on-chip wireless interconnects enable long distance, energy efficient, high bandwidth, and low-latency communication over long-range paths. Moreover, the absence of the need for physical

interconnection layouts makes wireless interconnects a promising alternative to the performance limitations seen by long-distance wired links. In addition, such mm-wave antennas fabricated using top layer metals are CMOS process compatible making them suitable for near-term solutions to the wired interconnect problem. More detailed literature survey on wireless interconnect is discussed in Section 2.3.

In a parallel direction, conventionally C4 bumps coupled with in-package transmission lines are used to interconnect chips within a multichip system [41] as shown in Figure 2.2. However, signal quality deteriorations due to microwave effects, crosstalk coupling effects, signal reflections, and frequency-dependent lines losses in the transmission line limit the number of concurrent, high-density inter-chip I/O [10]. This, in turn, restricts the possible off-chip bandwidth. Moreover, the pitch of chip-to-chip I/O does not scale in the same proportion as on-chip global wires [6]. This creates a gap in performance of on-chip interconnections with respect to the off-chip communication. Different interconnect technologies such as photonic interconnects [12][13], inductive or capacitive coupling based interconnects [24][25], and wireless interconnects [42] are being explored to mitigate the performance issues of conventional I/O based multichip systems. In [13], onboard integrated intra and inter-chip photonic network are proposed. In [43] transceivers

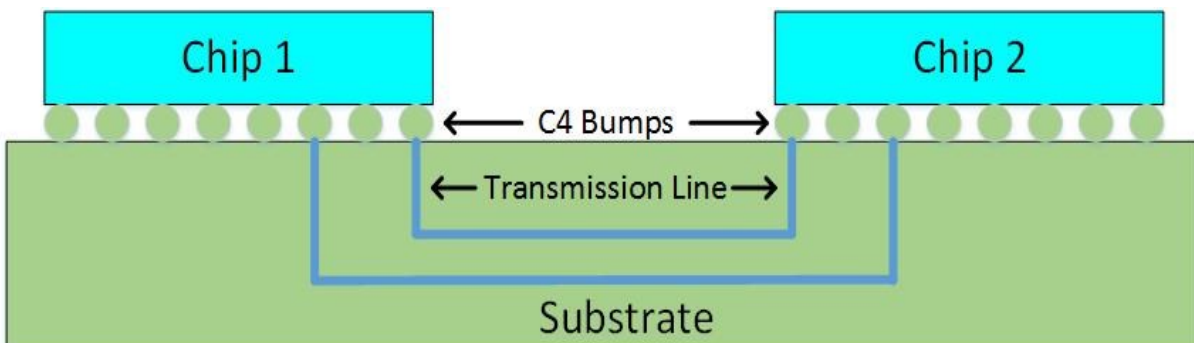


**Figure 2.2. Conceptual diagram of a multichip system interconnect with C4 bumps and in-package transmission line.**

for 60 GHz inter and intra-chip communications are designed. However, system-level performance gains are not evaluated in this work. In [44], wirelessly connected multichip modules are proposed for a High-Performance Computing (HPC) environment.

## 2.2 Vertically Integrated Multichip System and Microchannel based Cooling

Vertically stacked multichip integration or commonly known as 3D integration, provides promising solutions to the challenges of footprint, device density, and energy cost of the planar single-chip multicore system. The problem with metallic interconnect is not severe in 3D integration because of the smaller footprint. Through-Silicon-Vias (TSVs) are most often used to realize the interconnections between dies in the multichip system. TSV is a metallic interconnect that passed through silicon substrate to provide high bandwidth and energy efficient die-to-die interconnection due to its short length. However, One of the major issues in the implementation of 3D integration is the excessive heat flux generated by stacking multiple chips, giving rise to an

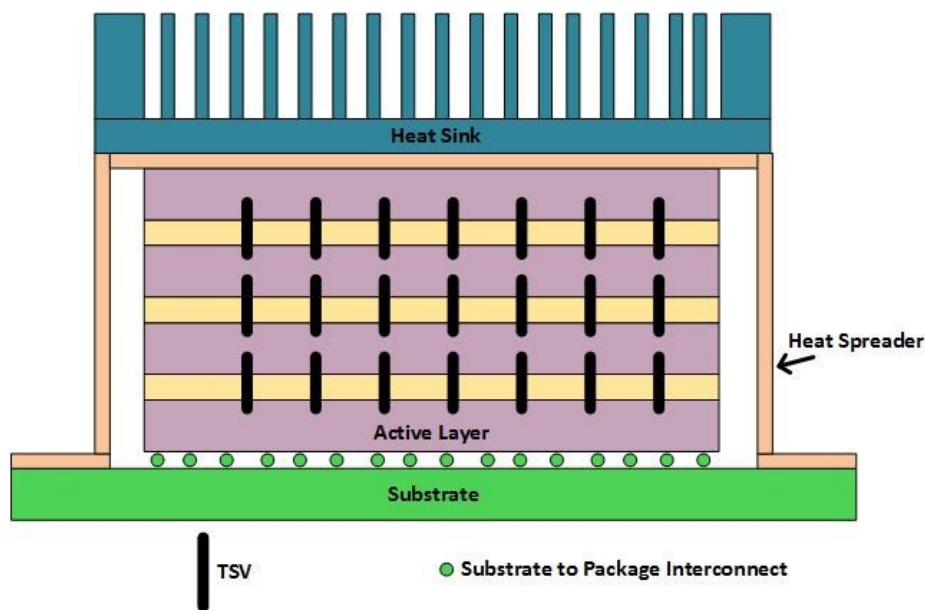
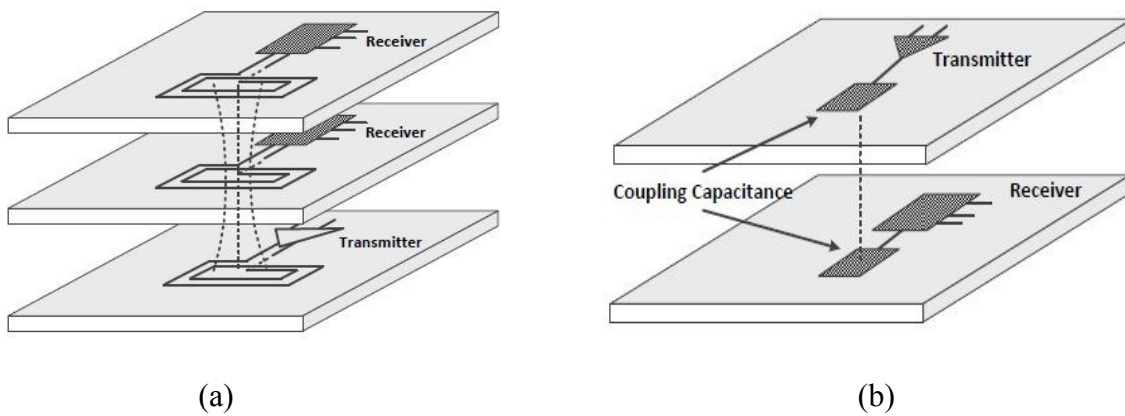


Figure 2.3. Vertically stacked dies with conventional air-cooled heat sink.

increase in the power generated per unit surface area as well as in the peak temperature [16][18]. Conventional cooling techniques are limited in ability to extract heat only from the top or bottom of the entire 3D stack as shown in Figure 2.3. Moreover, the conventional air-cooled heat sink requires heat flux from the vertically stacked dies to travel through a longer conductive path in order to dissipate through the heat sink, increasing the overall thermal resistance. For aggressive cooling of 3D ICs, interlayer liquid cooling methods have been investigated by several researchers. Tuckerman and Pease [17] first proposed the use of microchannels to cool ICs effectively. Tuckerman and Pease [17] were able to dissipate  $790 \text{ W/cm}^2$  with a thermal resistance of  $0.09 \text{ K/W}$  by using microchannels with a height of  $302 \text{ }\mu\text{m}$  and a width of  $50 \text{ }\mu\text{m}$ . However, the flow rate required was  $8.6 \text{ ml/s}$ , which resulted in a pressure drop of  $214 \text{ kPa}$ . In [45], authors decreased the pressure drop from  $25$  to  $1.01 \text{ kPa}$  by increasing the microchannel height from  $50$  to  $300 \text{ }\mu\text{m}$ . They reported that it is possible to achieve low-pressure drops ( $< 10 \text{ kPa}$ ) and relatively low substrate temperatures by having flow rates between  $2$  and  $5 \text{ ml/s}$  in a  $100 \text{ }\mu\text{m}$  tall microchannel. In [46], authors noted that the fluid temperature increases significantly for microchannels widths beyond  $300 \text{ }\mu\text{m}$  under low flow rates. However, increasing the flow rate reduces the fluid temperature rise. Kandlikar [20] presented a review of the available cooling schemes for 3D IC stacks and identified that 3D IC cooling is suitable for hotspot management and proper thermal regulation of the chip components. Comprehensive thermal management techniques are developed in [47] where combined approach utilizing dynamic voltage frequency scaling (DVFS), temperature-aware task allocation and liquid cooling is proposed. In [48], authors analyzed the impact of the liquid cooling on a 3D multi-core processor compared to the conventional air cooling and showed that integrating interlayer cooling improves the lifetime reliability of a chip significantly by reducing the peak temperature. However, from a thermal viewpoint, to provide

adequate cooling capabilities at the low-pressure drop, microchannels are required to be wide and taller which in turn complicated the placement and routing of TSVs. Two different approaches exist in literature to address the co-design problem. In microchannels first approach, microchannels dimensions are optimized first to get the best cooling capabilities and then, TSVs are placed in the remaining area [21][22]. Whereas in TSV-constrained placement approaches, TSVs are placed first to reduce the average wire length and then, microchannels are employed in the remaining area [49]. However, in both methods, whatever is placed first occupy a significant silicon area leaving the lesser area for other and consequently, can result in either lower performance or cooling capabilities.

Contactless wireless interconnects in 3D ICs through inductive and capacitive coupling based vertical links have been proposed in recent years [24][25][26]. In inductive coupling, a planar spiral transmitter and receiver inductor pairs are placed on the silicon dies and time-varying current is passed through the transmitter coil to generate magnetic flux as shown in Figure 2.4 (a). This coupled magnetic field, in turn, induces an Electromotive Force (EMF) in the receiving coil, and the receiver coil converts this EMF into an electrical signal. However, these inductive coupling



**Figure 2.4. (a) Inductive coupling (b) Capacitive coupling based interconnect for vertically stacked dies [50].**

links have larger area overheads compared to TSVs [26]. In addition, energy per bit of such links increases significantly with the communication distance [26]. On the other hand, in the case of capacitive coupling links, small metal plates are placed on two silicon dies which create parallel plate capacitance between them as shown in Figure 2.4 (b). However, these dies are required to be close to each other to create this electrical field. Due to this proximity requirements, the capacitive coupling based links require the dies to be face-to-face [50]. This limits the number of dies to be connected with capacitive coupling based interconnects.

The idea of using wireless interconnects using mm-wave on-chip antennas in 3D NoC was explored in [51]. However, how it affects the design methodology in a 3D IC with liquid cooling was not discussed. Unlike capacitive/inductive coupling links, the energy consumption of mm-wave wireless interconnects do not increase with the distance. This makes mm-wave wireless interconnect more viable solution for data communication across microchannels cooling layers with heights more than 50  $\mu\text{m}$ . Enabling 3D NoC with wireless interconnects will eliminate the need for place and route of signal TSVs across the cooling layer for data transfer. This integration technique will ease the restrictions on the dimensions of the microchannels, reduce the complexities of co-design challenges of microchannels & TSVs, and make the fabrication of the cooling layer more flexible.

### **2.3 Wireless Technology: A Promising Interconnect Paradigm**

On-chip wireless interconnect is a promising alternative to the performance limitations seen by long-distance wired links. The absence of the need for physical interconnection layouts makes wireless interconnects stand out from other emerging interconnects. Moreover, wireless interconnect are capable of enabling high bandwidth and low latency communication over long-

range paths which is beneficial for the inter-chip communication. A comprehensive survey regarding various WiNoC architectures and their design principles is presented in [29]. Notable examples include the design of a WiNoC based on CMOS ultra-wideband (UWB) technology [32], hierarchical mm-wave WiNoC architecture [28], 2D concentrated mesh-based WCube architecture using sub-THz wireless links [52], and the inter-router wireless scalable express channel for NoC (iWISE) architecture [33]. In [44], on-chip wireless transceivers are used to facilitate quick pre-bonding wafer testing enabled by direct accesses to components under test within the ICs. On-chip antennas from graphene or Carbon Nanotube (CNT) based structures are predicted to provide high bandwidth wireless communication channels [30][31]. However, integration of these antennas with standard CMOS processes needs to overcome significant challenges. On the other hand, mm-wave CMOS transceivers operating in the sub-THz frequency ranges is a more near-term solution. However, the bandwidth of the mm-wave wireless channels is limited by the state-of-the-art in transceiver design. The design of multiple non-overlapping channels enabling Frequency Division Multiple Access (FDMA) is a non-trivial challenge from the perspective of transceiver design and is not easily scalable. Hence, to efficiently utilize the available bandwidth, several WIs need to share the wireless bandwidth for data communication. A synchronous and distributed medium access mechanism is proposed in [32] for the Ultra-Wide Band (UWB) wireless NoC. In [34], a Code Division Multiple Access (CDMA) based medium access scheme is proposed by utilizing orthogonal codewords to enable simultaneous wireless transmission through the wireless channel. In [30], a hybrid medium access scheme combining both Time Division Multiple Access (TDMA) and FDMA is proposed for WiNoCs based on CNT antennas. A distributed MAC protocol is proposed in [53]. The proposed mechanism uses simple orthogonally coded request packets, processing the request packets and granting permission to the channel by a priority based

mechanism. However, this mechanism has an overhead of maintaining the state of current transmission at each transceiver. In [54], authors discussed the performance of ALOHA and CSMA for graphene-based WiNoCs. A comparative performance evaluation of CSMA and Token-based MAC is presented in [55]. For WiNoCs utilizing mm-wave transceivers, a token passing based medium access mechanism is used in [29][56].

# **Chapter 3      DESIGN OF A WIRELESS INTERCONNECTION FRAMEWORK FOR SEAMLESS INTER AND INTRA-CHIP COMMUNICATION IN HORIZONTALLY INTEGRATED MULTICHIP SYSTEMS**

In this chapter, we propose to use wireless interconnects to establish a seamless communication backbone which enables data exchange between cores in a single chip as well as between chips in a multichip system with dimensions spanning up to a few tens of centimeters. The same communication protocols used for on-chip data transfer in the intra-chip NoC will be used for off-chip data as well, eliminating the need for protocol transfer. Few cores inside the chips will be equipped with wireless transceivers, which will be capable of establishing direct one-hop communication with other such cores in the same as well as other chips. By deploying the wireless transceivers in the internal nodes of the chips, such that all cores are within a short distance from their nearest transceivers, energy-efficient inter and intra-chip communication can be achieved. Here, we present the design methodologies for such multicore multichip systems and demonstrate that the proposed design out-performs traditional wired I/O based multichip systems through system-level simulations. The specific contributions of this chapter are:

1. Proposed two different interconnect frameworks to utilize wireless interconnects for seamless inter and intra-chip communication.
2. The design of suitable on-chip antennas to establish wireless interconnection in a multichip system.

3. Evaluated the performance of the wireless multichip system and compare it with traditional I/O based multichip system.
4. Proposed a methodology to deploy wireless interconnects when system scales up.
5. Comparative evaluation with respect to emerging multichip integration technologies.

### **3.1 Wireless Interconnection Framework for Multichip Systems**

The interconnection fabric of the proposed multichip system with wireless interconnects is a hybrid network with both wired and wireless links. Each core in all the multicore chips is connected with a NoC switch. The switches within a single chip are interconnected in an intra-chip NoC architecture. Certain switches in the NoC are equipped with Wireless Interfaces (WIs) to realize the inter-chip communications. These switches can directly communicate with their counterparts in the other chips. Figure 3.1 shows the conceptual architecture of the multichip system interconnected with inter and intra-chip wireless network.

#### **3.1.1 Topology**

In the proposed wireless interconnection framework, cores within each chip are interconnected using an intra-chip NoC. We discuss the interconnection architectures for the multichip systems with two different intra-chip NoC topologies as case studies to exhibit their role in the overall system. The topology of the chosen two intra-chip NoCs is Mesh and a Small-World topology. The Mesh is selected as it is a conventional NoC topology used in several multicore-based products [4][5][3] and is relatively easy to design, verify, and manufacture. The Small-World topology is chosen, as it is suitable to design wireless NoCs as noted in [57] and is demonstrated to outperform

the Mesh-based NoC [37]. The multichip systems with the two chosen intra-chip NoCs are described below.

#### ***A. Multichip System with Intra-chip Mesh***

In the first multichip interconnection framework the intra-chip interconnection topology is a traditional Mesh-based NoC. For inter-chip communication, traditional chip I/O is connected to the periphery of the chip in one of the corner switches. This requires inter-chip data between cores embedded inside the chips to travel to the periphery then be transferred to over the I/O resulting in high latency and high-energy consumption. To alleviate this problem, we equip NoC switches associated with cores embedded within the chip with WIs. To deploy the WIs each intra-chip mesh NoC in each chip is further subdivided into a certain number of logical subnets. The WIs are deployed in a switch at the center of the subnets as shown in Figure 3.1, to avoid long multi-hop paths from all cores in its subnet. This WI deployment strategy corresponds to the approach that achieves Minimum Average Distance (MAD) between all switches in an intra-chip NoC in [58]. This improves the connectivity of the entire multichip system by establishing direct wireless links between internal switches eliminating the need to travel to and from the periphery of the source and destination chips respectively to access the traditional I/O modules.

#### ***B. Multichip System with Intra-chip Small-World***

Insertion of bypass paths or long-range shortcuts realized with metal interconnects is shown to improve the performance in a traditional Mesh-based NoC [37]. Small-World networks are a type of complex networks often found in nature that is characterized by both short-distance and long-range links. This improves the efficiency of the network as they have a very low average number of hops between nodes even for very large network sizes. Hence, such network topologies are

suitable for designing scalable, hybrid intra and inter-chip interconnection networks using wireless links in [56][57].

To establish the wireline links within each intra-chip NoC while satisfying the properties of Small-World graphs, we generate the wireline topology according to the following inverse power law to minimize wiring costs [59]

$$P(i, j) = \frac{l_{ij}^{-\alpha} f_{ij}}{\sum_{i=1}^n \sum_{j=1}^n l_{ij}^{-\alpha} f_{ij}} \quad (3.1)$$

Where,  $P(i, j)$  is the probability of establishing a link, between two switches  $i$  and  $j$ ,  $l_{ij}$  is the Manhattan distance,  $f_{ij}$  is the frequency of communication between switch  $i$  and  $j$  and  $n$  is the total number of switches. As can be seen from (3.1), the probability of a link insertion between two switches  $i$  and  $j$  where  $l_{ij}$  separates them is proportional to the distance raised to a finite negative power. The value of  $\alpha$  is chosen such that optimal wiring costs [59] are obtained. The distance is obtained by considering a tile-based floor plan of the cores on the die. The frequency of traffic

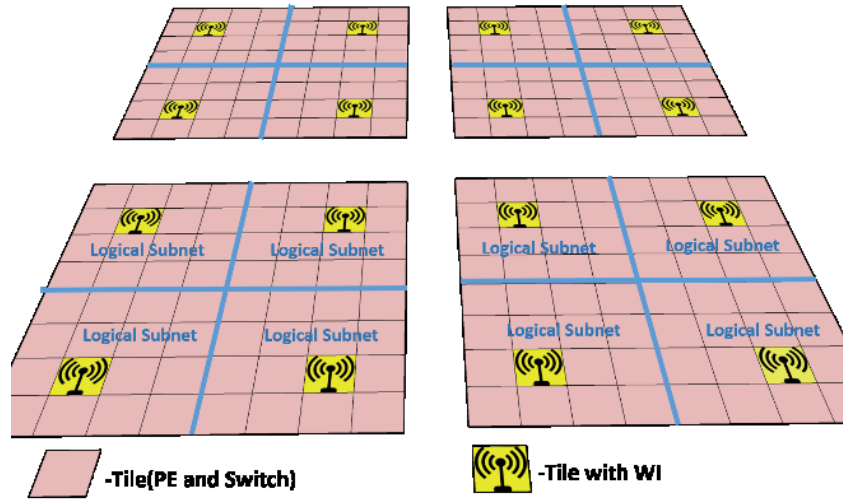


Figure 3.1. Conceptual diagram of the wireless multichip system.

interaction between the cores,  $f_{ij}$ , is also factored into (3.1), so that more frequently communicating cores have a higher probability of having a direct link optimizing the topology for application-specific traffic. This power-law based link distribution results in both short distance connections and long-range links due to the non-zero probability of links between far-away nodes. The total number of these wireline links is considered same as that in a mesh of the similar size to ensure no undue advantage is granted to the small-world architecture due to additional links. Also, an upper bound of 7 is imposed on the number of links attached to a particular switch so that no particular switch becomes unrealistically large [57]. The link setup method is repeated until no core or groups of cores are left unconnected. In this way, the intra-chip wireline small-world NoC topology is created. In addition to these wireline links, the wireless transceivers are deployed to form the WIs at the same switches as in the Mesh-based intra-chip NoC. This method is followed to form the same overlaid inter-chip wireless interconnect topology between the mesh and small-world based multichip systems.

### **3.1.2 Physical Layer**

The main enabling technology for such inter and intra-chip wireless interconnection is the physical layer design comprising of the transceiver circuits and antennas. We envision the multichip system where wireless interconnects will enable seamless intra and inter-chip communications. On-chip communication will happen over the hybrid wireline and wireless NoC. Wireline links are realized with traditional global-wire based interconnects depending on the specific topology adopted.

Several alternative technologies exist for realizing on-chip and off-chip wireless interconnections [29] [30][31][32][35]. We envision the use on-chip embedded miniature antennas operating in the 60 GHz mm-wave band that can be fabricated within the chip to establish direct

communication channels between internal switches of the chips. To realize such wireless channels, we choose on-chip metal zig-zag antennas which have been shown to be effective in establishing both on-chip and off-chip communication [27]. The chosen on-chip antenna has to provide the best power gain for the smallest area overhead. Several on-chip antenna designs in the mm-wave bands have been investigated [29][30][31][32][35]. A linear dipole occupies a large area proportional to the wavelength of the carrier frequency. A patch antenna is directional mostly radiating perpendicular to its plane. A log-periodic antenna is highly directional [60][61]. We intend the chosen antenna to be compact as well as not directional. This is because we want to communicate

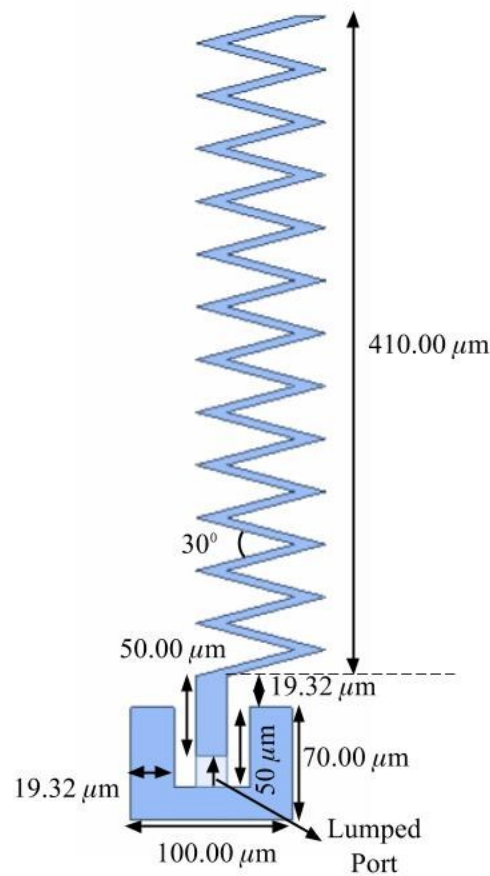


**Figure 3.2. Specific dimensions of the antenna and feed structure.**

between antennas, which are located in different chips and potentially at different angles with respect to each other's axes. A metal mm-wave zigzag antenna has been demonstrated to possess these characteristics as they are more compact compared to a linear dipole due to the zig-zag folding of the arms. Also, such mm-wave antennas fabricated using top layer metals are CMOS process compatible making them suitable for near-term solutions to the wired interconnect problem [29]. Such mm-wave 60GHz antennas are shown to have a bandwidth of 16GHz for both intra-chip [28] and inter-chip [35] communications links. We have designed mm-wave zig-zag on-chip antennas to resonate in the 60GHz frequency and studied its characteristics in terms of return loss and path loss in a multichip system. A coplanar feed structure is chosen for the antenna as it has low losses compared to other feed structures such as microstrips. These antennas are also shown not to be directional. This enables the WIs to communicate with any other WI in the system making the wireless medium a shared channel. Figure 3.2 shows the specific dimensions of the antenna and its coplanar feed structure. A trace width of 5 $\mu$ m is used for all arms of the antenna.

The WI transceiver circuitry has to provide a very wide bandwidth as well as low power consumption to ensure high throughput and energy efficiency. Hence, we adopt the transceiver design from [28] where low power design considerations are taken into account at the architecture level. Non-coherent On-Off Keying (OOK) modulation is chosen, as it allows relatively simple and low-power circuit implementation.

### **3.1.3 Flow Control and Routing**

The routing protocol for the proposed multichip system is a seamless intra and inter-chip data communication mechanism. We adopt wormhole switching for both inter and intra-chip data where data packets are broken down into flow control units or flits [36]. Wormhole switching is

known to reduce the buffering requirements at the switches as unlike packet switching; whole packets are not stored and forwarded. This makes the on-chip NoC switches consume low power and occupies lesser area. All switches have bidirectional ports for all links attached to it. All cores in the system have unique addresses. As the overall system is not a regular network, we adopt the shortest path routing to optimize network performance. For the wireless links, we adopt the same wormhole switching with simple modifications to enable the energy-efficient token-based sleep/awake transceiver modes of operation as discussed in the next subsection.

We use a forwarding table based routing over pre-computed shortest paths determined by Dijkstra's algorithm. Dijkstra's algorithm extracts a minimum spanning tree, which provides the shortest path between any pair of nodes in a graph. The exact minimum spanning tree depends on the chosen start node for the algorithm but the length of paths between any particular pair, along the tree does not rely on the start node. Hence, it is chosen randomly from among all the switches in the system. However, for a specific start node, the shortest path along the extracted tree is always unique as the minimum spanning tree eliminates loops inherently. Consequently, deadlock is avoided by transferring flits along the shortest path routing tree extracted by Dijkstra's algorithm, as it is inherently free of cyclic dependencies. As a result of using shortest path routing, the wireless links can also be used for intra-chip communication if they reduce the path lengths compared to a complete wireline path. Each switch only forwards the header flits to the next switch in the path to the final destination. The body flits simply follow the path laid out by the header according to the adopted wormhole switching protocol. Hence, each switch only has local forwarding information eliminating the need for maintaining non-scalable global routing information.

### 3.1.4 Wireless Communication Protocol

In mm-wave interconnects, wireless bandwidth is limited by the state-of-the-art transceiver design and on-chip antenna technology. To improve performance, multiple wireless transceivers need to access the wireless medium to communicate via the energy-efficient wireless interconnects. Consequently, multiple transceivers share a single wireless frequency channel. Therefore, an efficient and collision-free Medium Access Control (MAC) mechanism is needed.

#### *A. Wireless Medium Access Control (MAC) Scheme*

Several MAC protocols have been investigated in the context of wireless NoCs. To enable Frequency Division Multiple Access (FDMA) using mm-wave bands transceivers tuned to multiple carrier frequencies need to be designed. Power efficient design of such transceivers is a non-trivial challenge. The system-level performance of Code Division Multiple Access (CDMA) based on-chip and off-chip wireless interconnection architectures have been evaluated in [34][42]. However, such CDMA schemes require precise synchronization between the transceivers to avoid inter-channel interference by preserving the orthogonality of the code channels. Such a synchronization is difficult to achieve in transceivers distributed across multiple chips. Similarly, synchronized classical Time Division Multiple Access (TDMA) is difficult to adopt in a multichip system for the same reason. Therefore, Asynchronous TDMA (A-TDMA) based on token passing [29] or Carrier Sense Multiple Access/Collision Detection (CSMA/CD) [62] are proposed. However, CSMA-based A-TDMA does not perform well in the presence of the high traffic density due to exponential back-off [63][64]. A token-based medium access mechanism is proposed in [29] for WiNoCs to access the wireless channel in a distributed fashion while avoiding a collision. Hence, in this work, we adopt a similar token-based medium access mechanism for the multichip

systems using wireless interconnection. In a token-based medium access mechanism, the access to the wireless medium is granted by the possession of a token. Only the WI possessing the token can transmit via the wireless medium. No separate request mechanism or priority is considered as a part of the token passing scheme to avoid the need for a central grant or arbitration unit enabling a distributed access mechanism.

To enable autonomous token passing among the WIs with fairness in accessing the wireless medium, the WIs are numbered sequentially in a virtual token ring. The token circulates autonomously between the WIs as a wireless flit in a round robin fashion. Each WI holds the token for a variable number of time slots (i.e. token possession period) where the one-time slot is same as the system clock cycle. The WI currently possessing the token passes it to the WI next in the virtual token ring when it does not have any more packets to send or the maximum token possession period expires. The maximum token possession period is given by

$$T_{max} = (n \times \eta_{flit} + 1)t_{flit}. \quad (3.2)$$

Where  $\eta_{flit}$  is the number of flits in a packet (packet size),  $t_{flit}$  is the time (number of cycles) required to transmit a single flit over the wireless medium and  $n$  is the number of Virtual Channels (VCs) in the wireless port of the WI. This method allows the adoption of wormhole switching in the wireless links. The buffer depth of the VCs in the wireless ports need to same as that of the maximum packet size (in the case of variable packet size) to hold entire packets before they can be transmitted via the wireless channel to adopt the modified wormhole switching in the wireless links for a seamless communication. This also helps in increasing the energy-efficiency by using power gating of the wireless transceivers as discussed in the next subsection. From (3.2), the maximum token possession period is the time required to send all the packets in  $n$  VCs in the WI

as well as the token as a wireless flit. The architecture of the WI to enable the token-based medium access is shown in Figure 3.3. The Token Unit is the main logical unit responsible for managing the token passing mechanism. The Token Unit contains three registers,  $ID_{self}$ ,  $ID_{next}$ , and  $HasToken$ . The  $ID_{self}$  and  $ID_{next}$  stores the address of the WI itself and the address of the next WI in the round robin circulation of the token. The  $HasToken$  indicates the presence of the token in the WI. The Token Unit also contains a token possession period counter. When a token flit with a destination address set to  $ID_{self}$  is received at a WI, the Token Unit sets the  $HasToken$  and triggers the token possession period counter. On the other hand, when the token possession period counter expires indicating the end of the token possession period, a token flit containing the fields  $TokenID$ ,  $NextWI$ , and  $PrevWI$  is constructed. The WI currently possessing the token then transmits it over the wireless medium. The field  $TokenID$  is an identifier to differentiate the token flit from data flit. The  $ID_{next}$  and  $ID_{self}$  are used to set the field,  $NextWI$ , and  $PrevWI$  respectively. Although the token is circulated among the WIs in a round robin fashion, all these fields are necessary for the token to

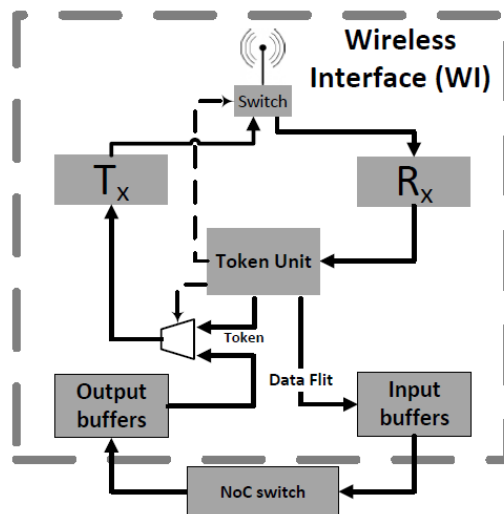


Figure 3.3. Block diagram of mm-wave token-based wireless interface.

enable a distributed token passing mechanism without relying on synchronization between the WIs distributed in different chips.

### ***B. Improving Energy-Efficiency of the Wireless Interconnect Using MAC***

The energy efficiency of the wireless interconnects can be further increased by using sleep transistor based power-gated transceivers instead of keeping them always awake. In [65][66] such a sleepy transceiver is implemented where control signals to turn them on/off are sent over specialized low-latency wired global line wires. However, in a multichip environment where WIs are distributed across different chips communicating the sleep/awake control signals using wired lines is challenging as it will require an additional pin and I/O overhead. Therefore, to enable a power-efficient sleep mode in the transceivers when they are not used we modify the wireless communication protocol. Each header flit to be sent across the wireless medium from a transmitting WI contains the number of flits in the packet and the address of the destination WI. All other WIs, which are not the destination of that particular header, will receive the header due to the broadcast nature of the non-directional antennas. On decoding the number of flits contained in that packet, all WIs except the source and destination WIs will go to sleep for the duration of the packet transmission. It will wake up after this duration to receive the next header (if there are other packets to send from other VCs) or token (if the token is being passed) and react accordingly. The flit type field in the header, body or token flits will enable this feature. As the VCs contain entire packets as noted in the previous subsection, only full packets will be transmitted together over the wireless medium. Therefore, a new header or a token flit is transmitted and received by all WIs when they wake up. In this mechanism, wormhole switching is modified as flits of a packet

are not transmitted over the wireless channel unless the whole packet is available for continuous transmission in the VCs.

## **3.2 Experimental Results**

In this section, we evaluate the performance and energy efficiency of the wireless multichip systems. We compare the wireless interconnect based multichip system with both conventional I/O and alternative emerging interconnection based multichip system. The chip-to-chip I/O is adopted from [67] and is shown to have a bandwidth of 15 Gbps and an energy consumption of 5 pJ/bit. On the other hand, the delay and energy dissipation on the intra-chip wireline link is obtained through Cadence simulations taking into account the specific lengths of each link based on the established topology in the 20 mm x 20 mm dies. The wireless transceiver adopted from [28][65] is designed and simulated using the TSMC 65-nm CMOS process and is shown to dissipate 2.31 pJ/bit sustaining a data rate of 16 Gbps with a Bit-Error Rate (BER) of less than  $10^{-15}$  while occupying an area of 0.3 mm<sup>2</sup>. The network switches and the Token Unit are synthesized from an RTL level design using 65-nm standard cell libraries from CMP [68], using Synopsys.

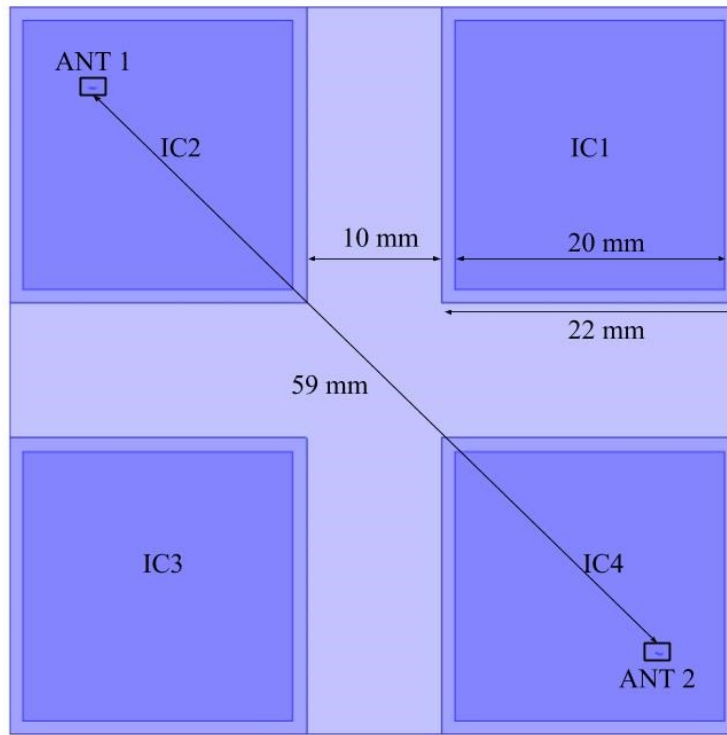
### **3.2.1 Simulation Platform**

The delay and power dissipation including both dynamic and static power consumption of the digital components are incorporated in an in-house cycle accurate simulator to evaluate the performance and energy efficiency of different multichip systems. This cycle-accurate simulator is written in MATLAB. This simulator takes network topology, flit injection rates, traffic information, the number of switches, simulation cycles, and message length as input, processes

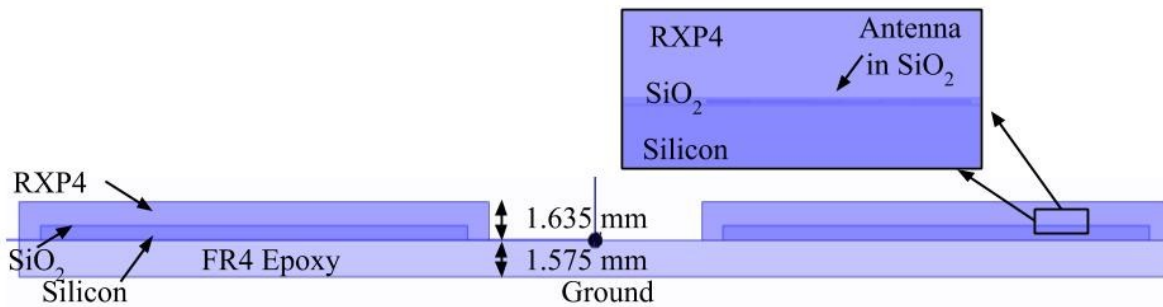
the messages at flit level, implements routing policies and flow control, and outputs performance metrics i.e. peak bandwidth, packet energy, and latency. The simulator characterizes the multichip architecture and models the progress of the flits over the switches and links per cycle accounting for those flits that reach the destination as well as those that are stalled. Each core is considered to be connected to a three-stage pipeline network switch [69]. The three stages correspond to input buffering, routing/arbitration, and output buffering operations, respectively. Each switch can have a number of VCs, which can be set by the user. The user can also configure the buffer depth of each VC (in terms of number of flits it can store). In our experiments, ten thousand iterations were performed eliminating transients in the first thousand iterations. The switches are connected to other switches according to the topology. The conventional I/O is modeled as a high-speed serial I/O port [67]. Similarly, the WI is also modeled as a port connected to the network switches where they are deployed. We consider each input and output port of a switch to have 4 VCs with a buffer depth of 2 flits for all the architectures considered in this paper. To avoid an excessive number of packets being stalled while waiting for the token, the ports associated to the WIs have an increased buffer depth of 8 flits. We consider a representative packet size of 64 flits with a flit size of 32 bits in our experiments unless otherwise mentioned. All the digital components are driven by a 2.5 GHz clock and 1V power supply, which are the nominal frequency and voltage for the 65nm technology node. In the Mesh-based NoCs, all wired links are considered being single-cycle links whereas the long intra-chip wireline links in the Small-World architectures are pipelined by insertion of FIFO buffers such that between any two stages it is possible to transfer an entire flit in 1 clock cycle.

### 3.2.2 Wireless Channel Characteristics and Wireless Link Budget Analysis

In this subsection, we present a link budget analysis to determine the transmitted power that is required to achieve an acceptable BER on the intra and inter-chip wireless links. Figure 3.4 shows the 4-chip system that we have used to design the on-chip antennas required for inter and intra-



(a)



(b)

Figure 3.4. (a) Top view of the model (b) Side view of the model

chip communication. As seen in Figure 3.4 (a) the individual chips are 20 mm X 20 mm and are separated from each other by 10 mm. Figure 3.4 (b) shows the side-view of the multichip system with various layers and materials considered in our evaluation model. We have considered the chips to be housed on a substrate of FR4 Epoxy material, which typically is the material for Printed Circuit Boards (PCBs) [70]. The individual chips are considered to be packaged in a dielectric material called RXP4 [71], which allows electromagnetic wave propagation to enable the inter-chip wireless communication. The antennas are considered to be embedded in a 2  $\mu\text{m}$  layer of silicon dioxide (silica) over a 633  $\mu\text{m}$  thick substrate of silicon of the chips.

The transmitted power,  $P_t$  in dBm on the wireless channels is given by the following equation:

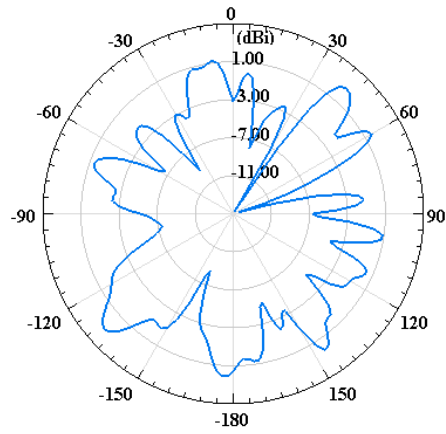
$$P_t = SNR + PL + N_f. \quad (3.3)$$

Where  $SNR$  is the signal to noise ratio at the receiver in dB,  $PL$  is the path loss in dB and  $N_f$  is the receiver noise floor in dBm. The relationship between Signal-to-Noise Ratio (SNR) and BER for non-coherent OOK modulation [72] is given by:

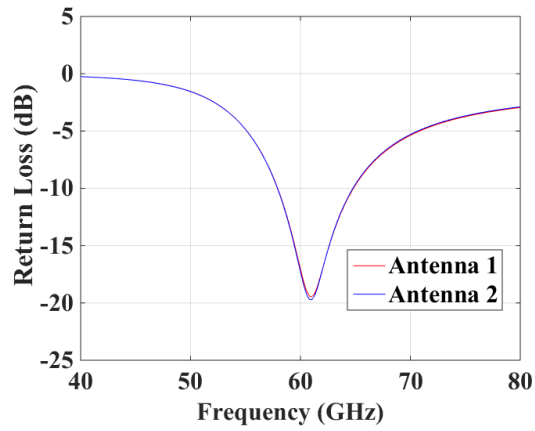
$$\text{BER} = \frac{1}{2} \left( 1 - Q \left( \sqrt{2SNR}, \sqrt{2 + \frac{SNR}{2}} \right) + \exp\left(-\frac{(2+\frac{SNR}{2})}{2}\right) \right). \quad (3.4)$$

Where  $Q(\cdot)$  is the Marcum-Q function. An SNR of 15 dB results in a BER of less than  $10^{-15}$  for the OOK modulation scheme adopted here. A BER of  $10^{-15}$  is comparable to wireline data transfer in current technologies. Hence, we consider a required SNR of 15 dB in our link-budget analysis. Figure 3.5 (a), (b), and (c) show the radiation pattern, return loss, and worst-case path loss respectively of the designed mm-wave antennas in a 4-chip system, which we use for system level

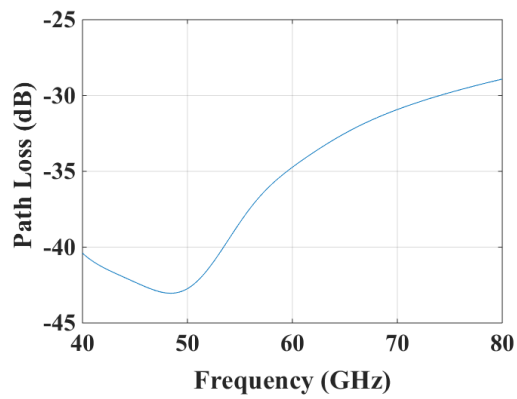
analysis in this work. The characteristics of the antennas are simulated using HFSS [73]. The



(a)



(b)



(c)

Figure 3.5. (a) Radiation Pattern, (b) return loss, and (c) worst case path loss for wireless multichip system

insertion loss shows that the antennas are tuned to resonate at 60 GHz. The antennas are designed and tuned by Rounak Singh Narde under the supervision of Dr. Jayanti Venkatarman [74].

The worst-case path loss, PL between two antennas, which are farthest apart in the 4-chip system as illustrated in figure 3.4 (a), is 34.9 dB. The noise floor of the receiver is -59 dBm [75]. Consequently, the output power of the transmitter is -19.43 dBm in the worst case. The power consumption of the transceivers, which is capable of generating this transmitted power as shown in [28], is considered in the following sections for system-level performance evaluation. We have observed that the return loss of the antennas is 0 dB at low frequencies between 0 to 10 GHz. This eliminates the possibility of interference with digital signals in the ICs due to their non-overlapping operational bands.

### **3.2.3 Comparative Performance Evaluation**

We evaluate the wireless multichip systems in terms of bandwidth per core and energy efficiency and compare with several wireline I/O based multichip systems. The bandwidth per core is measured as the peak sustainable data rate in number of bits successfully routed per core per second at network saturation. The energy efficiency is measured as the packet energy, defined as the average energy (i.e. both switch and link energy) required to route an entire packet from source to destination successfully. It is measured by the sum of the energy dissipation of all the components in the multichip systems such as switches and links divided by the total number of successfully routed packets. For the multichip systems with wireline I/O whenever a flit traverses an inter-chip link, the energy dissipated by the I/O is added to the total sum. Conversely, in the wireless multichip systems, the wireless transceivers are always active, and hence their energy dissipation is added to the total energy dissipation.

In the following subsections, we demonstrate the performance of different multichip systems in terms of the available bandwidth per core and packet energy dissipation.

### A. Architectures for Comparison

We consider six multichip systems with different inter-chip connection configurations for a comparative performance evaluation. These configurations are shown in Table 3.1. Among these six configurations, four configurations use I/O based wireline chip-to-chip interconnection, and two configurations use wireless interconnection for chip-to-chip communication. In these arrangements, each multicore chip is considered to have 64 cores where each core is connected to a network switch. We also consider two different intra-chip topologies, Mesh and Small-World to evaluate the effect of the intra-chip network on the performance of the multichip system. The number of chips in the system is varied from one to four interconnected together yielding different system sizes of 64, 128, 192 and 256 cores collectively.

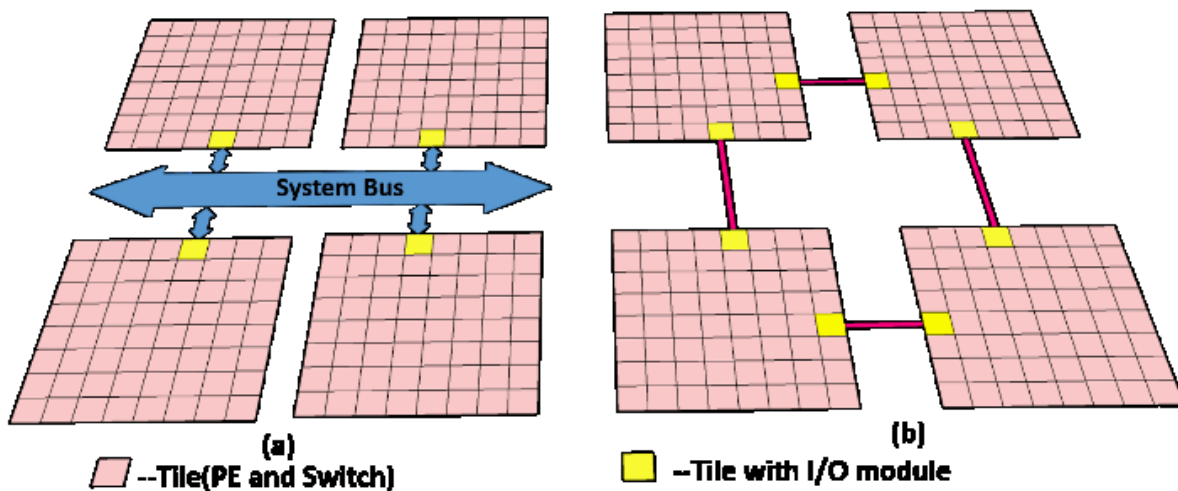


Figure 3.6. Conceptual view of (a) Bus I/O and (b) Network I/O based wireline configuration

Among the six configurations, four configurations use I/O based wireline chip-to-chip interconnection, and two configurations use wireless interconnection for chip-to-chip communication. Due to the large pitch of substrate-to-board pins [41], the number of pins dedicated for I/O operations is limited. Moreover, crosstalk between parallel inter-chip interconnects which can be several tens of millimeters long severely limits signal integrity. As shown in [76], signal integrity can be maintained in high-speed I/O based inter-chip communication only in the total absence of crosstalk. Therefore, to eliminate crosstalk, only a single inter-chip interconnect line is considered to exist between a pair of chips. To achieve this, only one switch along one edge of each chip (except the corner) is connected to the I/O module in the Bus I/O based wireline configurations. One of the middle switches is chosen as it is connected to three neighbors in the mesh based intra-chip NoC as shown in Figure 3.6 (a). For the small-world based configurations, the same switches are chosen for the I/O modules to implement the same inter-chip architecture.

To investigate the effect of increased bandwidth of the inter-chip wired links, we investigate the Network I/O configuration where we equip multiple switches in each chip with the I/O modules. However, between a particular pair of chips, there is only a single inter-chip link thus eliminating signal crosstalk. The chips are in turn connected in a mesh configuration among themselves via switches along the edges, using the I/O based inter-chip interconnects as shown in Figure 3.6 (b).

In Bus I/O based wireline configuration, inter-chip communication happens through a shared bus. For bus access, we have adopted an independent, guaranteed bandwidth arbitration appropriate for high-speed I/O buses, which combines a distributed Time Division Multiple Access

TABLE 3.1. MULTICHIP SYSTEMS WITH DIFFERENT INTER-CHIP INTERCONNECTION CONSIDERED IN THIS PAPER

<i>Architecture</i>	<i>Intra-chip configuration</i>	<i>Inter-chip configuration</i>
<i>Mesh+I/O(Bus)</i>	<i>Conventional grid based Mesh NoC</i>	<i>Bus-based I/O</i>
<i>Mesh+I/O (Network)</i>	<i>Conventional grid based Mesh NoC</i>	<i>Switching-based I/O</i>
<i>Small-World+I/O(Bus)</i>	<i>Small-world wireline NoC</i>	<i>Bus-based I/O</i>
<i>Small-World+I/O (Network)</i>	<i>Small-world wireline NoC</i>	<i>Switching-based I/O</i>
<i>Mesh+Token</i>	<i>Conventional grid based Mesh NoC</i>	<i>Token-based Wireless Links</i>
<i>Small-World+ Token</i>	<i>Small-world wireline NoC</i>	<i>Token-based Wireless Links</i>

(TDMA) approach with round robin access [77]. Simple slotted TDMA scheme is not realistic in a multichip system because it is impossible to achieve precise synchronization between multiple chips in current and future technologies. Therefore, an asynchronous and distributed access mechanism is necessary. However, a traditional request/grant based asynchronous centralized arbitration common in on-chip SoC busses is impractical as it needs additional control lines to the arbiter in addition to the data lines. In high-speed I/O as discussed before, implementing additional control (request/grant) lines would need additional I/O ports and pins and exacerbate the crosstalk noise causing severe signal integrity issues. Therefore, we enabled the distributed TDMA with a control flit broadcast to all the chips on the bus that passes the access to the next chip at the end of the transmission from the current chip. Each chip can access the bus for a maximum duration as given by (3.2) similar to the WIs to avoid bandwidth starvation. Also, the VC configurations of the switches attached to the bus are the same as in the WIs.

Unlike the Bus I/O based configuration, a wormhole based switching is adopted for the inter-chip communication in the Network I/O configuration. On the other hand, for both the wireless configurations, we have considered 4 WIs per chip located at the center of the subnets within the chips as discussed in the design methodology earlier.

### B. Achievable Performance

In this subsection, we evaluate the performance of the multichip systems with wireless interconnections. First, we evaluate the peak achievable bandwidth per core of different multichip systems at network saturation using uniform random traffic. The peak achievable bandwidth per core of these multichip systems is shown in Figure 3.7. It can be observed that the systems with wireless interconnections have higher bandwidth compared to all the wireline I/O interconnection for all system sizes. This is because the wireless nodes connect switches inside the chips directly

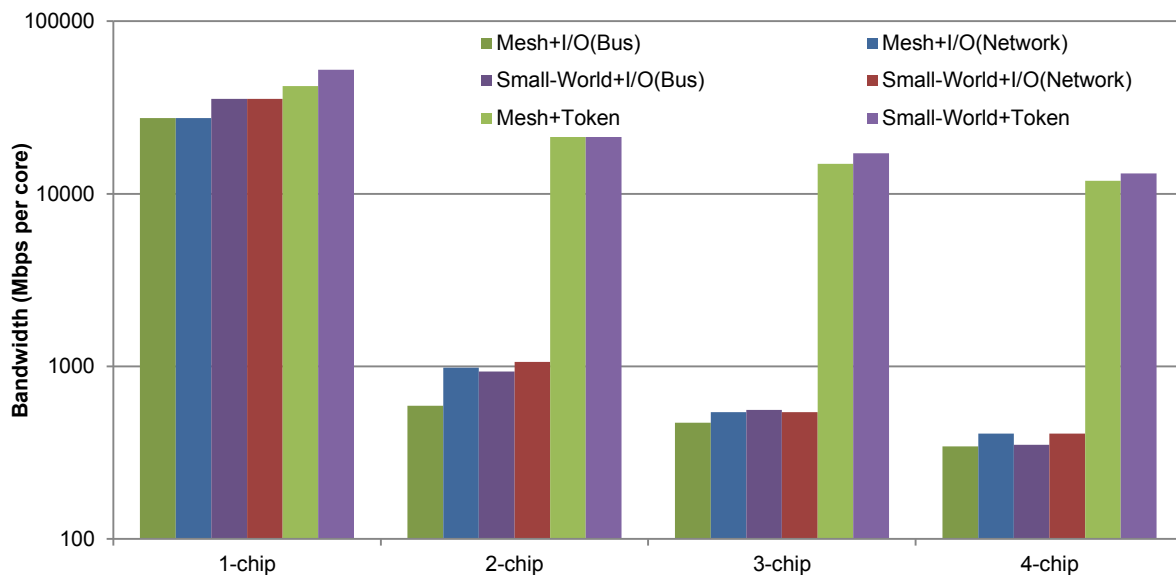


Figure 3.7. Peak achievable Bandwidth per core with varying system size for different configurations with uniform traffic.

over single-hop links for both intra as well as inter-chip data transfer. Therefore, even for a single-chip case, even when there is no inter-chip traffic the configurations with wireless interconnects have higher bandwidth compared to the complete wireline intra-chip NoCs. This is in agreement with several mm-wave wireless intra-chip NoC papers. On the other hand, for all the wireline I/O based systems the data packets need to [29][30][33] travel from internal cores to the peripheral I/O module and then, get routed over the inter-chip link and again travel to internal nodes at the destination chip. Among the wireline configurations, the Bus based multichip systems have the lowest performance and are not scalable due to the non-scalable bus-based interconnection. The Network I/O based wireline configuration has higher performance than the Bus. This is because the Network configuration allows concurrent communication between the adjacent chips. It can be observed that the wireless multichip system can sustain a bandwidth per core higher than 10 Gbps even for a 4-chip system. The degradation also seems to be asymptotic at 10 Gbps. However, with

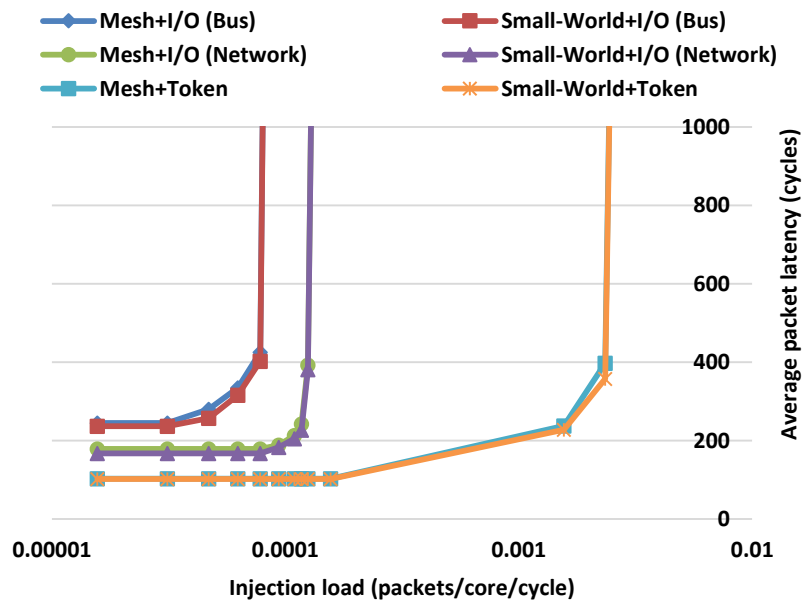


Figure 3.8. Average packet latency of various multichip systems.

the conventional I/O the bandwidth is more than  $10\times$  lower. This demonstrates the significantly higher bandwidth provided by the direct chip-to-chip wireless links.

Figure 3.8 shows the average packet latency for the various multichip systems with four chips with uniform random traffic. Due to different average distances between cores in the different multichip interconnection architectures, the latency characteristics are different. This is demonstrated by the average latencies at low injections loads. It can be observed that the wireless multichip has the lowest latency compared to the systems with inter-chip wireline interconnections. This is because of the shorter average path lengths due to WIs located inside the chips providing single hop links between cores located inside distant chips.

The performance of the Small-World NoC is higher than the Mesh-based NoC for both wired and wireless systems. This is due to direct one-hop connections between distant nodes on the chip. However, this gain is the most apparent in the single chip system. This is because, with an increase in the number of chips, the impact of the local NoC in each chip decreases on the overall system performance. We believe this trend to continue and hence, the importance of intra-chip NoC architecture to diminish compared to the inter-chip interconnection as the system size scales up.

### ***C. Packet Energy***

In this section, we compare the packet energy dissipation of different multichip systems interconnected with I/O based wireline interconnects and wireless interconnects. Figure 3.9 shows the packet energy dissipation of different multichip systems investigated in this paper. The packet energy dissipation for all system sizes is lower for the wireless multichip systems compared to all the I/O based multichip systems. The difference in packet energy between these wireline and

wireless multichip systems becomes more evident with an increase in system size as the packet energy dissipation for the I/O based multichip systems increase significantly with an increase in the number of chips. Alternatively, the packet energy in the wirelessly connected system does not increase as drastically. This is due to the direct energy-efficient wireless links between cores embedded in the multicore chips. Due to spatially uniform traffic, as the number of chips increase, the inter-chip traffic also increases in proportion from zero percentage in the single-chip scenario to 75% in the 4-chip case. This implies that 75% of the total number of packets generated uses the wireline I/O in case of the wired inter-chip interconnection systems. Because of this, a large proportion of traffic travels to and from the I/O modules using multi-hop wired paths over the intra-chip NoCs. This multi-hop path is reduced by use of the WIs deployed inside the chips. This is the main factor behind the gains in energy savings for the wireless multichip systems.

Among all the I/O based configurations, the configuration of network-based interconnect has lower packet energy dissipation. This is because, in the networked interconnection based

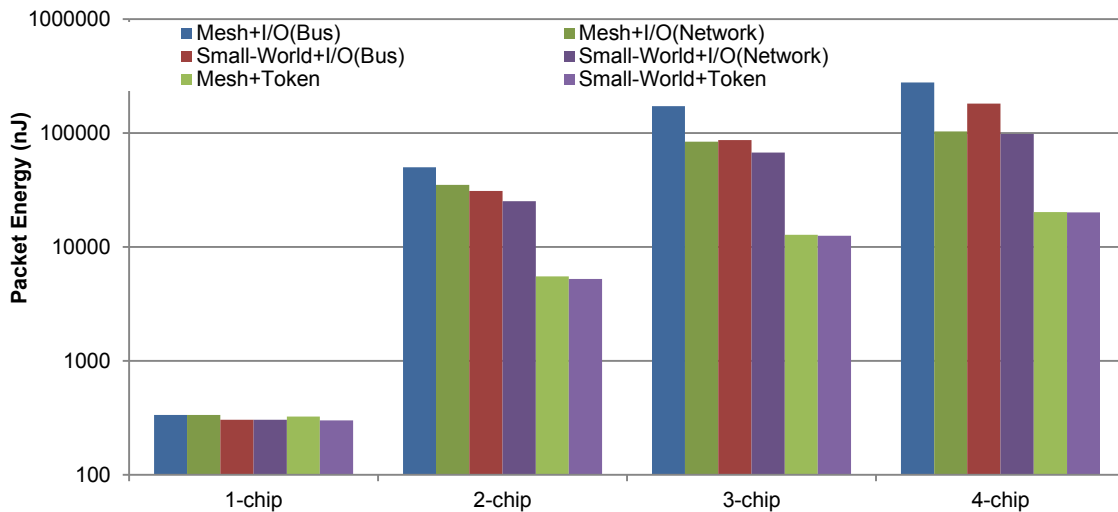


**Figure 3.9. Packet energy with varying system size for different configurations with uniform traffic.**

multichip systems, the I/O buffers are less congested compared to Bus configurations resulting in faster movement of data packets occupying buffers and interconnection resources for shorter durations. As both the performance and the energy efficiency of the network or switching based configuration is better than other I/O based configurations discussed in this paper, we consider this configuration as a baseline I/O based configuration for comparison in the following sections.

On the other hand, the Small-World NoC based wireless interconnection has lower packet energy compared to the Mesh NoC based wireless interconnection. This is because the Small-World nature of the topology reduces the average hop-count of the network by establishing long-range single-hop direct links. This effect is also demonstrated in recent literature [57][78][79]. Hence, in next sections, we consider the Small-World+Token architecture to evaluate the performance of the wireless multichip system.

#### ***D. Effect of Flit Width on Overall System Performance***

In this section, we analyze the effect of increasing flit width for Small-World+Token based wireless multichip system with uniform random traffic pattern and compare it with the Small-World+I/O (Network) architecture. A 2-chip system is considered in this subsection. For this experiment, we used four different flit sizes of 32, 64, 128, and 256 bits. This is because as noted in [80], higher flit widths beyond 128 are shown to provide marginal gains in performance of a NoC based system.

In the case of wireline intra-chip interconnections, widening physical channel width to accommodate larger flit width will increase the data rate on the wireline links. In the case of the conventional, I/O based inter-chip interconnect, the increase in flit-width translates into increasing the bandwidth of the interconnection by using multiple channels per link. However, signal

deterioration due to crosstalk coupling effects, microwave effects, and frequency-dependent losses in the transmission lines limits the number of parallel lines in the I/O modules. Here we only analyze the system-level performance metrics such as bandwidth per core and packet energy for these systems.

On the other hand, the data rate of the wireless links is governed by the speed of the transceiver and bandwidth of the antennas, which does not change with flit size. Hence, while the wireline communication becomes faster with an increase in flit size, the wireless communication speed remains constant. This results in a reduction in relative gains for the wireless multichip communication architecture with respect to the conventional I/O based system as shown in Figure 3.10. However, even with a flit width of 256 bits (8 parallel I/O channels per link), we see a relative improvement of 4.6x in data bandwidth and 3.1x in packet energy for a 2-chip system. In addition, we note that the reduction in relative gains for both bandwidth and packet energy display an

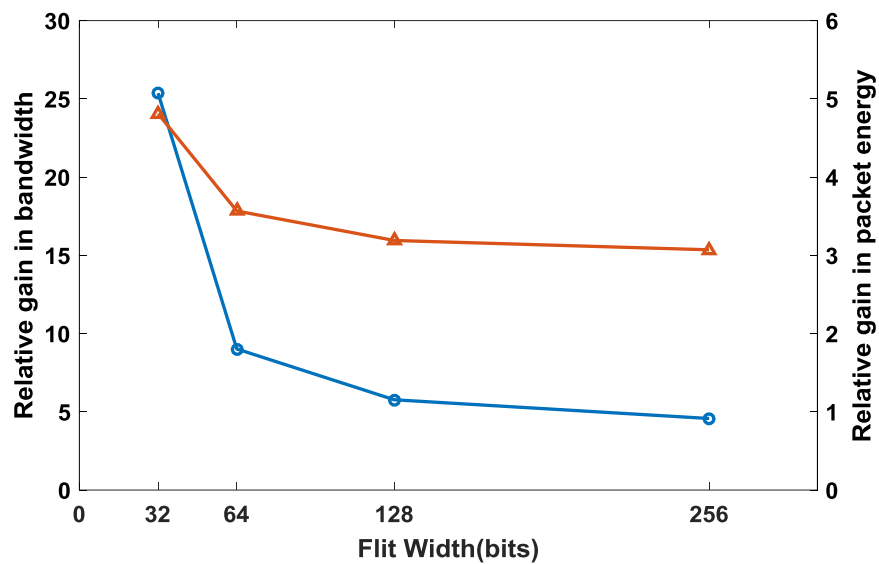


Figure 3.10. Relative gain in bandwidth and packet energy with different flit width for 2-chip system.

asymptotic behavior. This means that although the gains of using wireless interconnections decrease with increase in flit size the gain will stabilize beyond a point as the performance of the wireline interconnection does not continue to improve with flit size beyond 128 or 256 bits.

### 3.2.4 Deployment of the Wireless Interconnection with Scaling of System Size

In this section, we discuss the deployment methodology of the wireless interconnection for multichip systems when the system scales up. In our earlier experiments, we keep the number of WIs per chip constant and scale up the system i.e. increase the number of chips per system. However, in this approach, the total number of WIs keep increasing which will negatively affect the performance beyond a point as it will take increasingly longer time for each WI to possess the token and gain access to the medium. Hence, we have considered another alternative approach to deploying the WIs when system scales up. In this second method, we keep the total number of WIs per system constant and distribute the WIs among the chips. For the first approach, we consider

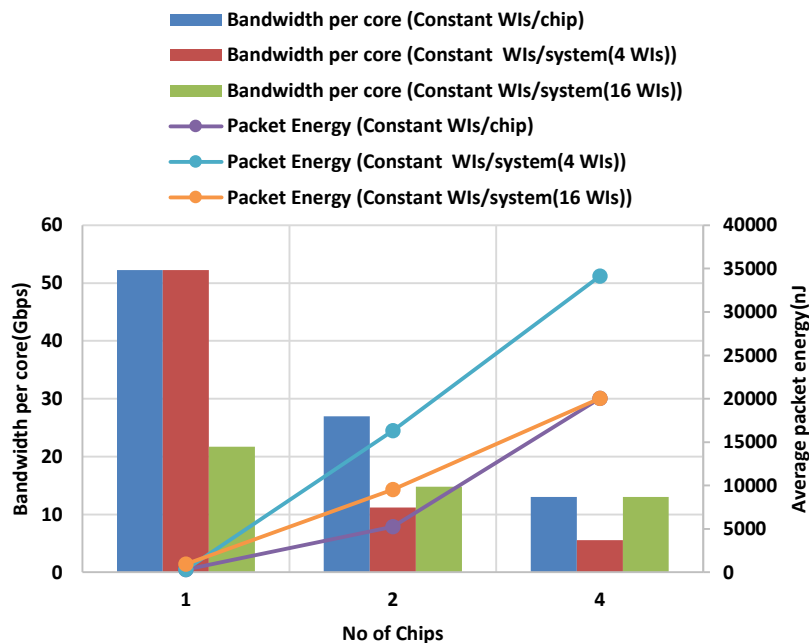


Figure 3.11. Bandwidth per core and Average packet energy for 1, 2, 4-chip systems for two different deployment approaches of WIs.

4WIs per chip and increase the system size whereas, in the second method, the same number of WIs is distributed among the chips of the system. In both cases, we evaluate the performance in terms of bandwidth per core and packet energy. However, in the second approach, we are distributing 4WIs among the chips that result in 1 WI per chip for a 4-chip system significantly degrading the performance. Hence, to study the deployment methodology more comprehensively, we consider another configuration with 16 WIs for the whole system and evaluate its performance.

The bandwidth per core and packet energy for 1, 2, and 4 chip systems for two different wireless interconnection deployment methodologies are shown in Figure 3.11. For this study, the Small-World+Token architecture is considered in all the cases. The peak bandwidth per core is higher for the system with a constant number of WIs per chip than that of the alternative approach. This is because in the first approach with increasing system size number of WIs also increases. It is true that increasing the number of WIs increase the token return period; it also helps to distribute the inter-chip traffic among the WIs. On the other hand, for the second approach with 4WIs for

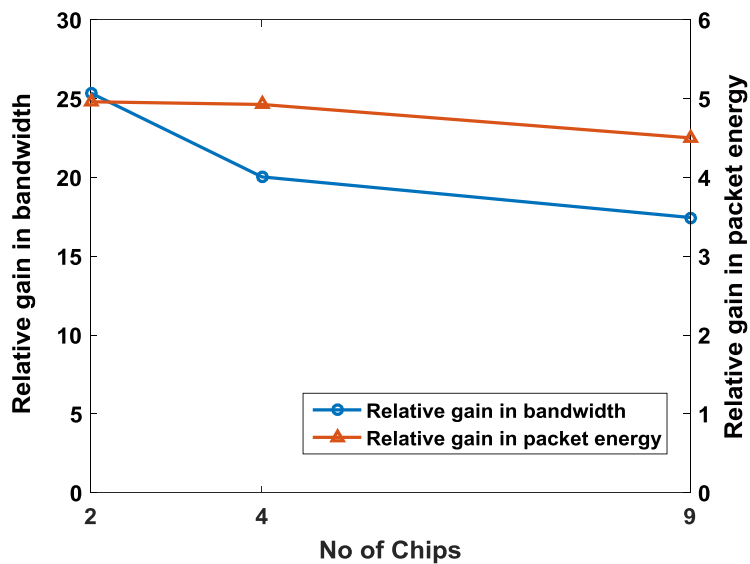


Figure 3.12. Relative gain in bandwidth and average packet energy with different system sizes.

the whole system, with increasing system size the volume of inter-chip communication increases whereas the number of WIs per chip decreases. This increases congestion at the wireless interfaces and adversely affects the bandwidth. This also causes a relative increase in the packet energy. To study the impact of the second methodology with a higher number of WIs, we deploy 16 WIs in the whole system. However, even in this case, the peak bandwidth per core is lower than that of the system with a constant number of WIs per chip. In the single-chip case, the performance with 16 WIs is lower than that with 4 WIs as each WI has to wait much longer for accessing the wireless channel. These two approaches are equal in peak bandwidth per core and packet energy in the 4-chip case because the two systems are identical. Hence, for the system sizes considered in this experiment, having a constant number of WIs per chip is a better deployment approach for the wireless multichip system.

To investigate the effect of this deployment policy on the scaling of system size and dimensions further, we evaluate a multichip system with 9 chips. Each chip is considered to be 20 mm x 20 mm, and a space of 10 mm is assumed between the edges of the chips as well as the edge of the substrate board. Thus, the overall dimensions of the board are 10 cm x 10 cm. Figure 3.12 shows the relative gains in bandwidth and average packet energy of the small-world based wireless multichip system with respect to small world based wireline (Network) multichip system for various system sizes. With the increase in number of chips and consequent increase in the number of WIs, the token-based wireless interconnection suffer a degradation in performance. However, it can be seen that the relative gains do not decrease significantly with increase in size because the performance of the wireline multichip systems also decreases with increase in size.

### 3.2.5 Performance Evaluation with Non-uniform Traffic Patterns

In this section, we analyze the bandwidth and packet energy in the Small-World+Token based multichip system with non-uniform traffic patterns and compare it with the Small-World+I/O (Network). We use the small-world based configurations in this section as they outperform the Mesh-based ones as demonstrated in the previous section. First, we use hotspot and transpose synthetic traffic pattern to evaluate these multichip systems. In the hotspot, 5% of all traffic generated from all cores has the same destination, which is the hotspot core. A single core was chosen randomly from the system as the hotspot. All other packets are destined to other cores following a uniform random distribution. This type of traffic pattern is fairly common for directory-based cache-coherent shared memory multiprocessor system where communication among the on-chip core and memory subsystem is more frequent [81]. Each core generates packet only destined to cores that are diametrically opposite to it in the whole system to generate the transpose traffic pattern. For example, the  $i_{th}$  core will only send data packets to the  $(N-i+1)_{th}$  core, where, N is the total number of cores in the entire system.

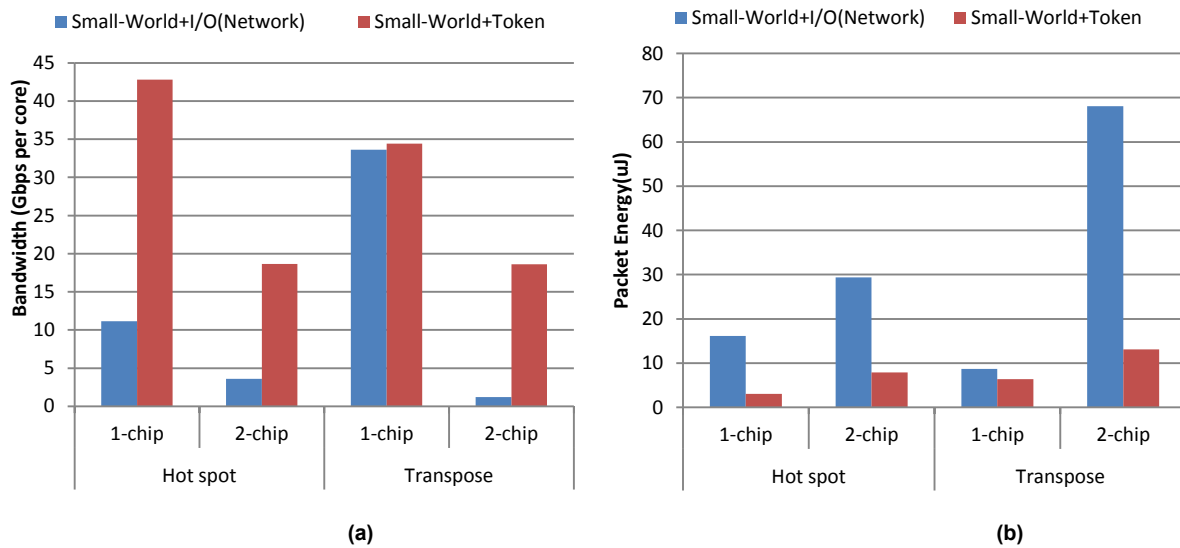


Figure 3.13. (a) Bandwidth per core and (b) Packet energy with non-uniform traffic for I/O based and wireless multichip systems.

The bandwidth per core and packet energy for the small-world NoC based multichip system for the one and two-chip cases are shown in Figure 3.13 (a) and (b) at network saturation respectively. As can be seen from results the wireless small-world system outperforms the I/O based multichip system for all the non-uniform traffic patterns. In the 2-chip system with both hotspot and transpose traffic patterns a significant portion of the traffic accesses the inter-chip communication medium. Hence, the distributed wireless interconnects improve the bandwidth and packet energy in both cases compared to the wireline inter-chip communication. In transpose traffic pattern, all data packets from all cores travel across the inter-chip communication medium. Hence, the relative gains of the wireless inter-chip interconnection are the most evident with this traffic pattern.

Our observations with the uniform and non-uniform traffic patterns indicate a strong correlation between the overall performance of the multichip system with that of the proportion of inter-chip traffic. However, it is hard to estimate or predict the proportion of inter-chip vs. intra-chip traffic in the set of applications suitable for modern and future multichip systems. Hence, we

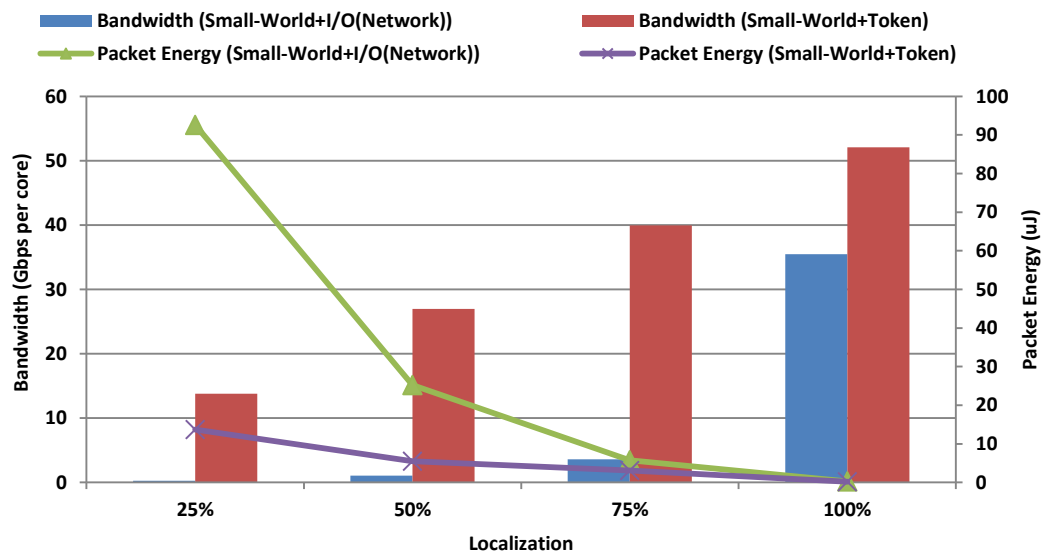


Figure 3.14. Bandwidth per core and Packet Energy for 2-chip I/O based and wireless multichip systems with varying localization

study the change in performance by varying the degree of localization in the traffic as a direct parameter. We define the localization parameter as the percentage of data packets from each core that has a destination randomly chosen from among the cores within the same chip. Figure 3.14 shows the bandwidth per core and packet energy respectively, as the localization parameter is varied from 25% to 100% for a 2-chip system with each chip having 64 cores interconnected with the small-world architecture. This captures the possible spectrum of traffic patterns while demonstrating how the performance depends on it. As the localization parameter increases, the performance of the multichip systems increases and the packet energy consumption decreases for both wireless as well as conventional I/O based systems due to lower dependence on the inter-chip communication fabric. More importantly, for low localization and increased inter-chip traffic, the role of the inter-chip interconnections become significant as one would expect and the gains of the wireless chip-to-chip links increases compared to the wired I/O system.

### **3.2.6 Comparative Evaluation with Respect to Emerging Multichip Integration Technologies**

In our prior sections, we considered simple token passing mechanism based wireless multichip system that outperforms wireline I/O based configurations. However, in token passing based wireless medium access mechanism, only a single transmitter can access the wireless channel at any given instant of time although multiple transceivers are deployed over the entire system. This limits the potential performance benefits of wireless architecture. Enabling simultaneous communication channels without any interference can ensure better utilization of the available bandwidth. This can be achieved by either designing a MAC protocol like Direct Sequence Spread Spectrum (DSSS) based CDMA channel access mechanism [34][42], or FDMA using novel

TABLE 3.2. ENERGY PER BIT AND AGGREGATE BANDWIDTH FOR DIFFERENT INTERCONNECT TECHNOLOGIES

	<i>Token-based Wireless interconnect</i>	<i>CDMA-based Wireless interconnect</i>	<i>CNT-based Wireless Interconnect</i>	<i>Inter-chip-photonic interconnect</i>
<i>Energy (pJ/bit)</i>	2.3	3.43	0.48	0.43
<i>Aggregate physical bandwidth (Gbps)</i>	16	6	160	160

antenna technology like Carbon Nanotube (CNT) based nano-antennas operating in THz frequency bands [30]. To study the potential performance improvement with these advanced techniques, we evaluate the same interconnection framework just replacing the token-based wireless transceivers with CDMA-based and CNT antenna based ones. In the CDMA-based medium access mechanisms, Walsh codes are used to create orthogonal code channels for multiple access. Due to this orthogonality between the code channels bits in one code channel are not affected by other channels. Transmitted bits are first encoded using the codeword, and at the receiving WI, the received bit is XORed with the code words to extract the transmitted data. We adopt the performance and power characteristics of the CDMA transceiver operating at 6 Gbps from [34] to estimate the performance of the system. For the CNT antenna technology, we consider Multi-Walled Carbon Nano Tube (MWCNT) antennas as they are shown to be in excellent quantitative agreement with traditional radio antenna theory [82]. These CNT antennas are excited using laser sources of different frequencies, which results in concurrent frequency channels supporting a data rate of 10 Gbps/channel [30].

Figure 3.15 shows the peak bandwidth per core and packet energy for the multichip systems with these different wireless interconnect technologies. For a fair comparison, we considered same

intra-chip architecture i.e. Small-World (SW) with same system size (4-chip) and the same number of WIs per chip (4 WIs). The raw energy/bit of the wireless technology and aggregate physical bandwidth provided by each of these technologies are summarized in Table 3.2. From Figure 3.15 it can be seen that SW+Token based system has the lowest bandwidth per core and highest packet energy among all the wireless configurations considered here. This is because only a single transmitter can access the wireless channel at any given instant of time. This increases the queuing delay for the packets yielding a lower bandwidth and higher packet energy. Designing complex MAC schemes like CDMA or using a novel antenna technology can improve this bandwidth to an extent due to concurrent communication among the WIs. However, in the CDMA-based system, these simultaneous communications happen to utilize the orthogonal Walsh code channels resulting in lower bandwidth per channel due to spectrum spreading effect of DSSS. Consequently, SW+CDMA provides lower bandwidth and consumes higher packet energy compared to SW+CNT based system. However, the improvement of the performance by implementing complex MAC or utilizing novel antenna technology does not come without a price. The

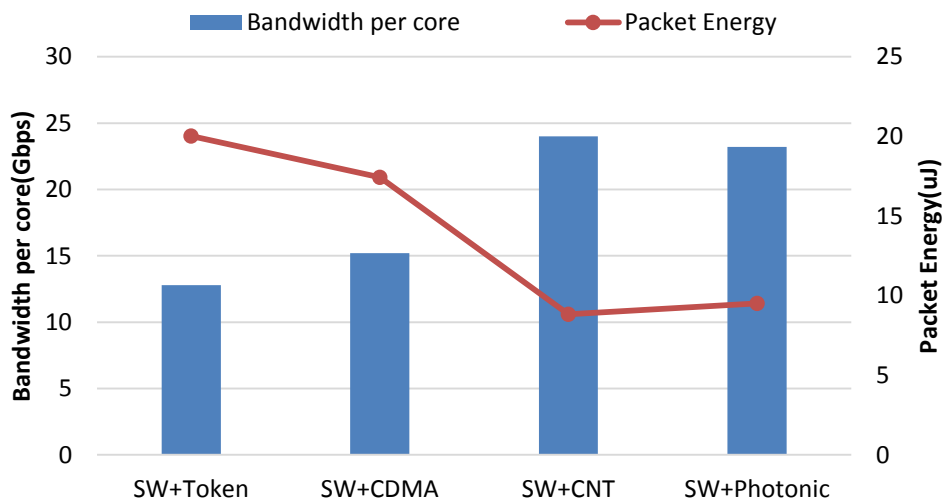


**Figure 3.15. Bandwidth per core and average packet energy for different interconnect technologies for 4-chip system**

transmitters are required to be synchronized to maintain the orthogonality among different code channels in CDMA-based MAC. This synchronization is difficult to achieve in a multichip environment as the WIs are distributed across different chips. Alternatively, integration of these CNT antennas with standard CMOS fabrication processes needs to overcome significant challenges [30]. Addressing these limitations by improving technology and designing efficient wireless medium access channel mechanism can exploit the full potential of the direct chip-to-chip wireless interconnects in future.

In recent literature, off-chip photonic interconnects has emerged as another enabling technology for chip-to-chip communication [12][13][83][84]. Next, we compare the wireless interconnection architecture with a photonic multichip system. For a fair comparison, we simulate the same 4-chip system. In this system as well, intra-chip architecture is same i.e. small-world. The only difference is in the inter-chip communication. In the photonic multichip system, the inter-chip communication happens through high bandwidth photonic interfaces. To connect these interface switches through a single waveguide, we consider these switches to be located at one edge of the chip. For our experiment, we consider four photonic interfaces per chip and one waveguide with 16-way Wavelength Division Multiplexing (WDM) channels having a bandwidth of 10 Gbps per channel [85]. The peak bandwidth per core and packet energy for the photonic system is shown in Figure 3.15. The power consumption of the laser sources is factored in the energy consumption per bit along with electro-optic conversions for both the photonic and the CNT-based multichip systems as shown in Table 3.2. The SW+Photonic outperforms both the token and CDMA-based wireless multichip system due to the presence of high bandwidth concurrent links. However, the performance of the photonic multichip system is lower than that of the CNT-based wireless system. As noted in Table 3.2 the physical bandwidth of both CNT-based

wireless multichip interconnection is considered to be the same as that of the photonic inter-chip waveguide. The energy per bit is also comparable. The gains in system bandwidth and packet energy comes from the fact that data packets can get routed from internal switches using the CNT-based wireless links. Whereas in the case of the photonic system, the data packets will have to reach the photonic interfaces of the chip in its periphery thereby affecting system level performance and packet energy negatively. Moreover, in the CNT-based wireless multichip system, intra-chip communication is also possible using the wireless channels without requiring any additional overheads. It is worth noting that the aggregate physical bandwidth of both the CNT-based wireless and the photonic interconnection framework can be increased by deploying more CNT-based antennas and using denser WDM respectively. This will improve the performance of both systems.

It is possible to improve the performance of the photonic multichip system by integrating the inter-chip waveguide with an intra-chip photonic NoC [13]. However, the challenges regarding integration of photonic devices, precise thermal tuning of electro-optic modulators and demodulators and a manufacturing process involving 3D technology for a separate photonic plane [39] need to be overcome.

Undoubtedly, the wireless multichip system with token-based MAC offers lower bandwidth compared to the other systems considered in this section. However, due to fabrication challenges and reliability concerns, implementing complex MAC or emerging novel interconnect technologies require further investigation. On the other hand, the token-based wireless system utilizing metal-zigzag antennas are CMOS compatible and outperforms conventional wireline I/O based inter-chip communication systems which make it a nearer term solution as the

communication backbone for designing such multichip systems providing significant gains in system performance.

### 3.2.7 Area Overheads

In this section, we estimate the corresponding area overheads of the various architectures studied in this paper. The number of wired intra-chip links in all configurations are same as that of a conventional Mesh NoCs i.e. number of intra-chip links in the small-world based architecture is constrained to be the same as that of the conventional Mesh. The only difference is the I/O modules, wireless transceivers and the area of ports associated with them. Figure 3.16 shows the total area overhead of the various interconnection architectures for different multichip configuration considered in this paper for a 4-chip system. In the case of token-based architectures, each transceiver occupies an area of  $0.3 \text{ mm}^2$  [28] whereas in I/O based architectures, each transceiver has an area of  $0.088 \text{ mm}^2$  [67]. For the wireless multichip systems of the largest

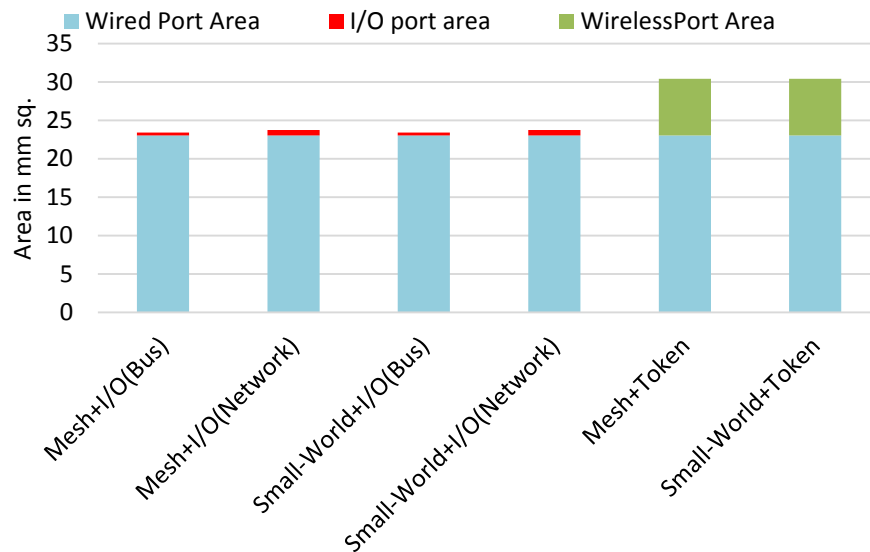


Figure 3.16. Area overheads of different wireline and wireless architecture considered in this paper

configuration, the total area of the interconnection network is 1.92% of the entire system while the wireless overhead is only 0.46% assuming each chip is  $20 \text{ mm} \times 20 \text{ mm}$ . The proportion of the various area overheads remains similar for other system sizes using the wireless interconnections, as the number of WIs per chip remains the same.

### **3.3 Summary**

High-performance computing environments and data centers employ modules with multiple multicore chips in a package or on board. The density and bandwidth of high-speed I/O for inter-chip interconnections are becoming the power-performance bottleneck for such multichip systems. In this work, we explore the advantages possible if inter-chip communication in multichip modules can be realized with state-of-the-art mm-wave wireless links operating in the 60GHz band. While the physical bandwidth of such wireless links is not necessarily higher compared to the high-speed serial I/O links, the wireless links are capable of establishing direct communication channels between cores in different chips via on-chip embedded antennas. Moreover, the wireless links can be used for a seamless data transfer between cores in the same chip as well to augment the traditional NoC backbone for intra-chip communications. These factors result in significant gains in performance and energy efficiency in both intra and inter-chip data communications. The energy-efficiency of the wireless interconnects have been improved by careful wireless data transfer protocol design to put unused WIs to sleep using power-gated transceivers. It can be further enhanced by using variable levels of power amplifications [86] depending upon the length of the wireless interconnects and associated path losses in the future.

## **Chapter 4      WIRELESS INTERCONNECT AS AN ENABLER FOR DATA COMMUNICATION ACROSS MICROCHANNEL BASED COOLING LAYER IN VERTICALLY INTEGRATED MULTICHIP SYSTEM**

Vertically integrated multichip system i.e. Three-dimensional Integrated Circuits (3D-ICs) have emerged as another feasible solution to overcome the performance limitation of 2D planar ICs [9]. Vertical interconnects realized using Through-Silicon-Vias (TSVs) provide high density, high bandwidth communication paths between the active layers of the 3D ICs greatly mitigating the global interconnect problems faced by planar ICs. However, utilizing the third dimension to provide additional device layers poses thermal challenges as stacking vertical layers increases the power dissipation density significantly, and the thermal footprint per unit area TSVs are used for both data as well as critical signals like clock and power delivery across the layers in a 3D ICs [16]. Conventional cooling techniques are limited in ability to extract heat only from the top or bottom of the entire 3D stack. Consequently, the design of aggressive and sophisticated cooling mechanisms are envisioned to alleviate the thermal issues in 3D ICs.

One such solution is where embedded inter-layer cooling microchannels or a cooling chip is inserted in between layers of the vertically stacked multichip system. Tuckerman and Pease [17] first proposed the use of microchannels to cool IC chips effectively. Introducing microchannels between the active layers of the 3D ICs and circulating cooled liquid through these channels can extract the heat from the interlayer regions and cool the 3D ICs more efficiently as compared to conventional cooling techniques. However, to increase the cooling capability of the microchannels

their effective thermal conductivity should be high, or conversely, they should have low thermal resistance. Short microchannel heights reduce their convective thermal resistance. However, short microchannels increase the pressure drop between the entry and exit points of the liquid causing thermal stresses [20]. These high stresses may compromise the mechanical integrity of the thin walls between TSVs and microchannels. Lowering the coolant flow rate to reduce the pressure drop has another disadvantage of higher temperature non-uniformity in the silicon substrate along the flow length. Moreover, large thermal gradients along the fluid flow direction inside microchannels can affect the structural reliability of the TSVs by inducing temperature related expansion and contraction due to a mismatch in coefficient of thermal expansion (CTE) between copper and silicon. To reduce the mechanical stresses and at the same time, to provide temperature uniformity and adequate cooling capabilities, the height and width of the microchannels need to be increased. Several dimensions of microchannels are suggested in literature ranging from 50  $\mu\text{m}$  to 1000  $\mu\text{m}$  in height and 100  $\mu\text{m}$  to 1000  $\mu\text{m}$  in width depending on desired pressure drop and cooling capabilities [21][22]. This, in turn, imposes significant restrictions on where and how many TSVs and microchannels can co-exist together. TSVs with Aspect Ratio ( $\text{AR}=\text{Height}/\text{Diameter}$ ) greater than 10 are tough to manufacture at high yield due to challenges related to etching, sidewall passivation, and formation, insulation, and filling of Vias [6] and co-dependency of the microchannels and electrical design makes the process even more complex. Wider microchannels occupy a significant portion of the floor area of the 3D IC severely restricting the freedom of placement and routing of TSV based links in 3D ICs. Moreover, increasing the microchannels height will eventually increase the die thickness and consequently, the height of TSVs that in turn will increase the diameter of the TSVs to maintain a fixed AR. Also, to reduce IR and  $Ldi/dt$  drop, TSVs used for power delivery network require higher diameter and pitch than

the signal TSVs. All these factors restrict the area available to route TSVs across the cooling layers and make the co-existence and co-design of TSVs and microchannels challenging especially when thousands of TSVs are required for interconnections in large chips with die areas higher than  $100\text{mm}^2$  [23].

In recent years on-chip wireless interconnects in the millimeter-wave frequency bands are demonstrated to be more energy-efficient compared to conventional wireline interconnect fabrics [28][29][30][31][33][34]. Moreover, wireless interconnects do not require physical layout of links and provide direct single-hop links between transceivers distributed across the chips. Based on these recent studies, we propose a wireless 3D NoC architecture to enable energy-efficient communication utilizing wireless links across interlayer microfluidic coolers. This will reduce the number of TSV based links across the microchannel layers as data transfer across the cooling layer

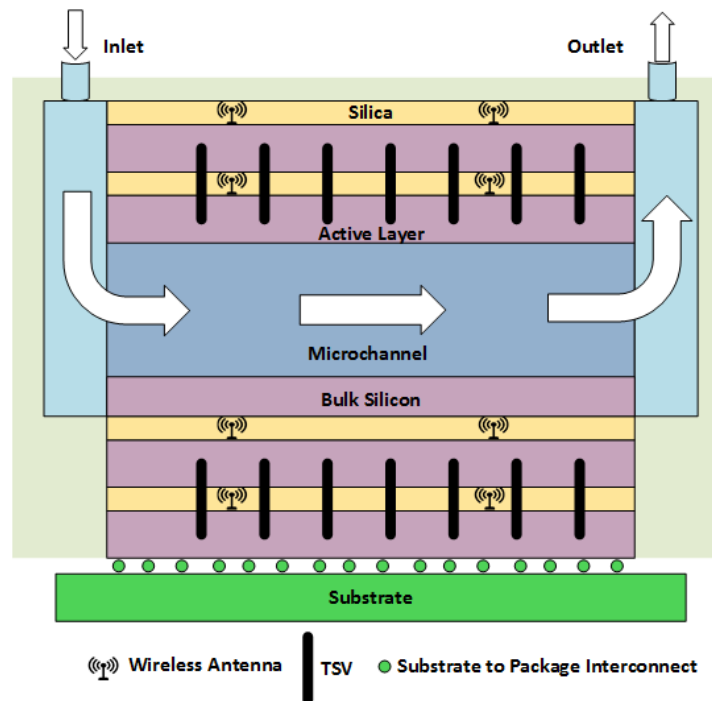


Figure 4.1. Side view of proposed 3D wireless NoC architecture with the interlayer cooling layer.

will only be achieved through wireless links. This will eliminate the need to place and route signal TSVs across the cooling layers. Therefore, the only TSV based links to be placed and routed across the cooling layers would be the power and clock delivery networks. This will significantly reduce the complexity of the co-design of TSV based interconnects and microchannel based interlayer cooling. Figure 4.1 shows the side view of the proposed wireless 3D NoC.

In this chapter, we first determine the dimensions of the microchannel for optimal thermal and hydraulic characteristics considering current trends in power consumption densities of 3D multicore ICs. Next, we design the wireless physical layer suitable for communication across the designed microchannel based coolers. Lastly, we evaluate the performance of a 3D wireless NoC designed with the above physical layer.

The specific contributions of this chapter are listed below:

1. Determining optimal dimensions of microchannel based interlayer coolers for 3D multicore ICs.
2. The design of on-chip antennas for the physical layer of the 3D wireless NoC suitable for communication across the above designed cooling layers.
3. The design of 3D Wireless NoC architectures for 3D multicore ICs with microchannel based cooling to reduce the number of TSVs across the cooling layers.
4. Evaluate the performance, energy consumption and thermal characteristics of 3D wireless NoCs equipped with microchannel cooling layers.
5. Comparison of the proposed 3D Wireless NoCs with respect to traditional 3D interconnection systems using TSVs.

6. Holistic comparative evaluation with the horizontally integrated wireless multichip module.
7. Present a discussion on the various trade-offs available for the proposed design.

## **4.1 Integrated Design Methodology for Wireless 3D NoC with Microchannel based Liquid Cooling**

In this research work, we propose to realize data communication links across the micro-channel cooling layer in the 3D NoC with the wireless interconnects. The design of the NoC architecture and the antennas will depend on the dimensions and characteristics of the cooling layers such that a reasonable trade-off between the cooling capacity and pressure drop is obtained. Based on those design specifications the methodology for designing the 3D Wireless NoC architecture and antennas will be discussed next.

### **4.1.1 Design of Microchannel Cooling Layer**

To enable efficient and powerful cooling in 3D IC systems, microchannel based liquid cooling needs to be employed between active layers of the 3D IC. The modular interlayer cooling chip needs to meet several design constraints. (i) The thermal performance should be high enough to dissipate heat fluxes of 100 to 500 W/cm<sup>2</sup>, which are expected from 3D multicore processors in the near future [20]. (ii) provide temperature uniformity along the flow length, and (iii) have low pressure drops across the channel to reduce the power required for pumping the fluid and reduce structural strain on the IC. Need to provide temperature uniformity along the flow length, and (iv) have high hydraulic performance, which corresponds to low pressure drops across the channel to reduce the power required for pumping the fluid and reduce structural strain on the IC. The number

of cooling layers, and how many active layers can be sandwiched between two cooling layers depends on the number of active layers, their heat flux and cooling capability of the microchannels.

The thermal and hydraulic performance are two important factors in 3D IC cooling as they determine the cooling capability and the mechanical stress on the IC package. The geometry of the microchannels governs both the thermal and hydraulic performance. Finding a trade-off between the cooling performance and reliability is not trivial because of the interdependence of the thermal and hydraulic performance and the microchannel geometry. Here we discuss the interdependence, which will guide the design of the microchannel geometry.

The thermal performance depends on the thermal resistance of the designed microchannels. The thermal resistance  $R_{th}$  is the ratio of the increment of the average surface temperature above the input temperature of the fluid to the total heat dissipated. For a fully developed flow under a constant heat flux and considering fluid flow to the parallel to the x-axis, the 1-D thermal resistance can be defined as:

$$R_{th} = \frac{\Delta T_{max}}{q'' A_s} = \frac{T_{s,avg} - T_{f,in}}{q'' A_s}. \quad (4.1)$$

Where  $\Delta T_{max} = T_{s,avg} - T_{f,in}$  is the maximum temperature rise in the microchannels i.e. the temperature difference between the peak temperature in the heat sink at the surface ( $T_{s,avg}$ ) and the fluid inlet temperature  $T_{f,in}$ ,  $A_s$  is the surface area, and  $q''$  is the heat flux at the channel wall. Fluid inlet temperature is used in *eqn. 4.1* to incorporate the impact of mass flow rate. Hence, the convective resistance ( $R_{conv}$ ) and the effective resistance due to temperature rise of the liquid ( $R_{heat}$ ) are both included in the analysis. Low values of the thermal resistance are desired for

micro-channels in order to achieve lower temperatures in the surfaces where heat must be dissipated.

On the other hand, as liquid flows through the microchannels, the pressure decreases from the inlet section to the outlet section due to frictional losses. This pressure drop needs to be overcome by an external pump circulating the liquid coolant. Thus, the hydraulic performance is quantified by the pumping power i.e. the power required to drive the coolant through the flow passages to achieve the desired flow rate required for cooling. The pumping power,  $W$  to overcome the flow resistance can be defined as:

$$W = \Delta p \cdot \dot{V}. \quad (4.2)$$

Where  $\Delta p$  is the difference between the pressure at the inlet and the pressure at the outlet of the microchannels,  $\dot{V}$  is the volumetric flow rate.

From these equations, we can see that a higher flow rate will reduce the temperature rise for a given heat input and hence, results in lower thermal resistance. This will improve the thermal performance. However, increasing the flow rate will increase the pressure drop and hence, pumping power. As a result, it can cause structural strain on the IC. Moreover, the pressure drop across the microchannel and thermal resistance depend on the geometry of the microchannel. All these factors complicate the overall design of the microchannel. In later sections, we perform numerical simulations to evaluate the thermal and hydraulic performance of the modular microchannel cooling chip to determine the optimal design. For the numerical analysis, the geometric parameters that were varied are the height of the microchannel,  $b$ , and the width of the microchannel,  $w$ . The width of fin between the micro-channels is  $w_f$ , and the microchannel pitch,

$p$  is defined to be  $(w+w_f)/2$ . Detailed results are presented in section 4.2.1. The results obtained from these experiments will be used to guide the architecture design methodology as discussed next.

#### 4.1.2 Proposed Topology of the 3D Wireless NoC Architecture

We propose to realize links across the microchannel cooling layer in the 3D IC with the wireless interconnects. The cores in the 3D multicore system will be interconnected using a NoC fabric through switches and links. In our proposed architecture, each core is connected to a NoC switch. Switches within a single layer are connected in a mesh topology with conventional copper wire based NoC links. To enable interlayer communication between layers that are not separated by a cooling layer, all the switches are equipped with TSV based links to switches vertically above or below itself.

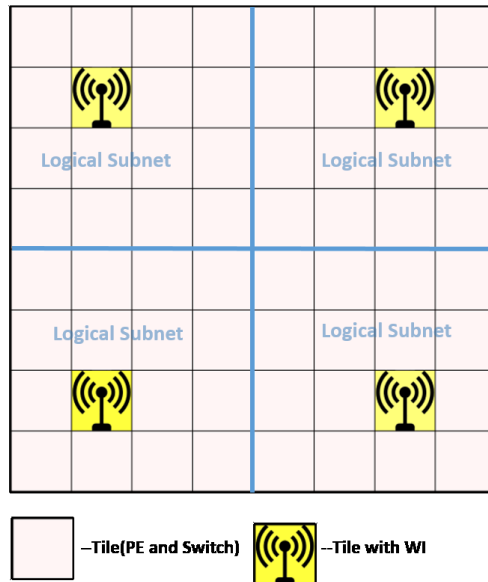


Figure 4.2. Top view of one active layer.

Communication channels across the cooling layer are realized through wireless links. For this purpose, each layer is logically divided into subnetworks or subnets, such that a particular switch in each subnet is equipped with a Wireless Interface (WI). The WIs are deployed in a switch at the center of the subnets to avoid long multi-hop paths from all cores in its subnet, assuming any core can transmit inter-chip data at some point during the operation of the system. This WI deployment strategy has been shown to provide the Minimum Average Distance (MAD) between all switches in an intra-chip NoC in [58]. All cores that need to send data across the cooling layer access the wireless channel through the WI in its subnet. The WIs are connected in an all-to-all fashion using the shared wireless band. The data is transferred to the WI in the subnet of the destination core from where it is routed to the final destination. To improve performance, data transfer within the same layer or in adjacent layers not separated by a cooling layer can also use the WIs depending on the adopted routing policy as discussed in section 4.1.4. In this way, a hybrid hierarchical 3D wireless, wireline and TSV based NoC architecture (3D-HiWiNoC) is formed. Figure 4.2 shows the top view of one active layer (vertical TSVs are not shown).

### **4.1.3 Physical Layer**

Several alternative technologies exist for realizing on-chip and off-chip wireless interconnections [29][30][31][32][35]. We envision the use on-chip embedded miniature antennas that can be fabricated with-in the chip to establish direct communication channels between internal switches of the chips. To realize such wireless channels, we choose on-chip metal zig-zag antennas which have been shown to be effective in establishing on-chip communication [27]. The chosen on-chip antenna has to provide the best power gain for the smallest area overhead. A linear dipole occupies a large area proportional to the wavelength of the carrier frequency. A patch antenna is directional

mostly radiating perpendicular to its plane. A log-periodic antenna can have higher power gains but is highly directional. We intend the chosen antenna to be compact as well as not directional. This is because we want to communicate between antennas that are located in different layers of the 3D IC and potentially at different angles with respect to each other's axes. A metal mm-wave zigzag antenna has been demonstrated to possess these characteristics as they are more compact compared to a linear dipole due to the zig-zag folding of the arms. In addition, such mm-wave antennas fabricated using top layer metals are CMOS process compatible making them suitable for near-term solutions to the wired interconnect problem [27]. Therefore, to realize such wireless channels, we choose on-chip metal zig-zag antennas which have been shown to be effective in establishing on-chip communication [29][32][33]. This antenna also has the negligible effect of rotation (relative angle between transmitting and receiving antennas) on received signal strength, making it most suitable for on-chip wireless interconnects, as each antenna has to communicate with other WIs in multiple directions. Such mm-wave 60GHz antennas are shown to have a bandwidth of 16GHz for on-chip communications links. The antennas are placed at the center of each subnet being fed from the WIs of its respective subnet in each layer. Consequently, the antennas need to be tuned best radiation characteristics in this 3D system with the microchannel based cooling layers separating active layers. The specific details of the designed antenna, and radiation characteristics depend on the dimensions of the cooling layers and are shown in section 4.2 under experimental results. The antennas are tuned to work in the mm-wave band with a carrier frequency of 60GHz.

#### 4.1.4 Seamless Flow Control and Routing

The routing protocol for the proposed 3D wireless system with microchannel based cooling is a seamless intra and inter-chip data communication mechanism. We adopt wormhole switching for wireline links in the proposed system where data packets are broken down into flow control units or flits [36]. All switches have bidirectional ports for all links attached to it. The WIs have an additional port equipped with the wireless transceivers to access the wireless physical channel. For the wireless links, we adopt the same wormhole switching with a slight modification as explained in the next subsection.

We use a forwarding table based routing algorithm over pre-computed shortest paths determined by Dijkstra's algorithm for both inter-chip and intra-chip data. Dijkstra's algorithm extracts a minimum spanning tree, which provides the shortest path between any pair of nodes in a graph. The exact minimum spanning tree depends on the chosen start node for the algorithm but the length of paths between any pair, along the tree does not rely on the start node. Hence, it is chosen randomly from among all the switches in the system. However, for a specific start node, the shortest path along the extracted tree is always unique as the minimum spanning tree eliminates loops inherently. Consequently, deadlock is avoided by transferring flits along the shortest path routing tree extracted by Dijkstra's algorithm, as it is inherently free of cyclic dependencies. The route computation overheads are reduced significantly, as the routing decisions are made locally based on the forwarding table only for determining the next hop and is done only for the header flit. The tail flits simply follow the reserved path as per wormhole switching.

#### 4.1.5 Wireless Communication Protocol and Transceiver

In mm-wave interconnects wireless bandwidth is limited by the state-of-the-art transceiver design and on-chip antenna technology. Multiple wireless transceivers need to access the wireless medium to communicate via the energy-efficient wireless interconnects to improve connectivity and performance. Consequently, multiple transceivers share a single wireless frequency channel. Therefore, an efficient and collision-free Medium Access Control (MAC) mechanism is needed. The authors in [29] have proposed such a distributed and low-overhead token-based MAC mechanism for on-chip wireless interconnects. The token-based MAC grants access to the shared wireless medium to a single WI resulting in a contention free communication using the wireless channel. However, in such a MAC only whole packets are transmitted to other WIs, to maintain the integrity of the wormhole switching [87]. This increases the buffer requirement and hence static power consumption in the WIs. Therefore, we propose a MAC mechanism that allows partial packet transmission from a WI while maintaining the integrity of the wormhole switching.

In the proposed MAC, instead of circulating a token at the end of each transmission, each WI broadcasts a control packet at the beginning of its transmission. The control packet consists of a header for identification and differentiation of data packets. In addition, to enable partial packet transmission and correct routing, the control packet has 3-tuples: (DestWI, PktID, NumFlits) for every partial packet that it will transmit. Each 3-tuple contains the information about the number of flits (i.e., NumFlits) to be transmitted from the WI to a particular destination (i.e., DestWI) along with the packet ID (i.e., PktID) of the packet, to which the flits belong. The PktID enables the destination WI to identify the VC number at the destination WI to put the flits, thus maintaining wormhole switching. In case the PktID does not exist at the destination WI, the WI reserves an

unoccupied VC. The number of output VC of the transmitting WI limits the number of 3-tuples in a control packet. The control packet is broadcast to all WIs. Therefore, the next WI in sequence computes the duration of the current transmission from the information in the control packet and transmits its control packet when the current transmission is completed. For this purpose, the WIs are numbered in a sequence. Thus, contention between WIs in accessing the channel is avoided. This control packet based MAC enables an energy-efficient operation of the WIs by using sleep transistors. We adopt the design of such sleepy transceivers from [65] to put particular receivers to sleep when the transmitted data is not intended for them based on the information in the control packets. This eliminates the overhead and layout complexity of the global signaling wires to carry the *sleep/wake* signals as in [65].

The WI transceiver circuitry has to provide a very wide bandwidth as well as low power consumption. The transceiver design is adopted from [28] where low power design considerations are taken into account at the architecture level. Non-coherent On-Off Keying (OOK) modulation is chosen, as it allows relatively simple and low-power circuit implementation. Next, we present the performance evaluations of the proposed wireless interconnection framework.

## **4.2 Experimental Results**

In this section, we determine the dimensions of the cooling layer, demonstrate the design of the on-chip antennas with suitable communication properties, and estimate performance and temperature profile of a 3D multicore IC incorporating the cooling layers and interconnected by wireless links across them.

### 4.2.1 Dimensions of the Cooling Channels

To capture the operating conditions in the microchannel cooling chip module, a heat flux,  $q''=100$  W/cm<sup>2</sup> is imposed at the upper and lower walls each, of a single microchannel unit. A single passage is modeled by considering symmetry planes along the length of the microchannel passing at mid-planes of the fins to avoid simulating the whole module. The total width of the computational domain is the pitch,  $p$  between mid-planes along the fins and the total length is 10 mm. Fully developed laminar flow at  $303$  K is considered at the inlet of the fluid passage, and the radiation effects are neglected in the entire computational domain. Deionized water is used as the cooling fluid flowing through the fluid passage, and the material of the microchannel is modeled as silicon. The dielectric property of deionized water enhances the radiation characteristics of wireless links making it a suitable choice. All properties for the materials are taken as constant and evaluated at  $303$  K, except the viscosity,  $\mu$  (Pa.s) of the deionized water, which is curve fitted by following equation:

$$\mu = 2.414 \times 10^{-5} (10^{247.8/(T[K]-140)}). \quad (4.3)$$

The numerical models are simulated using the finite volume software Fluent 14.5 [88], which provide accurate temperatures in the solid; and pressure, velocity, and temperature fields in the fluid using the assumptions above, A structured mesh consisting only of hexahedral elements is used to split the computational domain into several control volumes. The mass, momentum, and energy conservation equations are solved for each control volume. Convergence is considered when the residuals for the governing equations are less than  $10^{-6}$ . These microchannels are modeled and simulated by Jose-Luis Gonzalez-Hernandez using ANSYS Fluent 14.5 [88] under the supervision from Dr. Satish G. Kandlikar [74].

### A. Thermal Resistance

For this experiment, we consider the inlet temperature and the heat supplied to the layers are constant. Therefore, low values of the thermal resistance are desired for microchannels in order to achieve lower temperatures in the surfaces where heat must be dissipated. The mass flow rate in the simulations is selected such that the lowest mass flow rate needed to achieve the 80 °C surface temperature at the outlet is employed. The thermal resistance for the microchannel heatsinks modeled in this study is shown in Figure 4.3 for different heights of the microchannels as a function of the pitch. As the microchannel height increases, the thermal resistance also increases, leading to a lower thermal performance when the height is higher than 200  $\mu\text{m}$ . For heights of 10 and 100  $\mu\text{m}$ , thermal resistance values of 0.1 and 0.4 K/W, are obtained, respectively. It is observed that for a fixed microchannel height, the effect of the pitch on the thermal resistance becomes negligible when the pitch is greater than 2000  $\mu\text{m}$ .

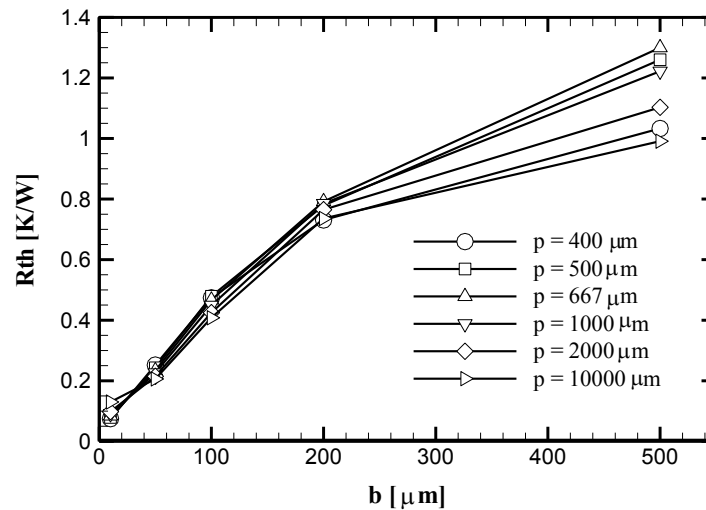


Figure 4.3. Thermal resistance variation for the microchannels.

## B. Pressure Drop and Pumping Power

The pressure field is obtained from the simulations as explained in section 4.2.1. The pressure drop is computed as the difference between the pressure at the inlet and the pressure at the outlet of the channels. In Figure 4.4, the pressure drop characteristics of the modeled microchannel heat sinks are shown. It is observed that the pressure drop decreases with increase in the height of the microchannel for all the pitches considered. The highest-pressure drops of the order of 1 MPa are observed for heights of 10  $\mu\text{m}$  which is the typical interlayer thickness in monolithic 3D ICs [20]. Such high hydraulic stress severely impacts the reliability of the 3D ICs [20]. The high slopes between a height of 10  $\mu\text{m}$  and 100  $\mu\text{m}$  indicate that a dramatic change in hydraulic performance is achieved between these microchannel heights. Beyond a microchannel height of 100  $\mu\text{m}$  the slope of the pressure drop plots become less steep and for a height higher than 200  $\mu\text{m}$  the effect of the microchannel height is negligible. Under these geometric parameters very low values for the pressure drop are achieved ( $\Delta P < 10$  kPa).

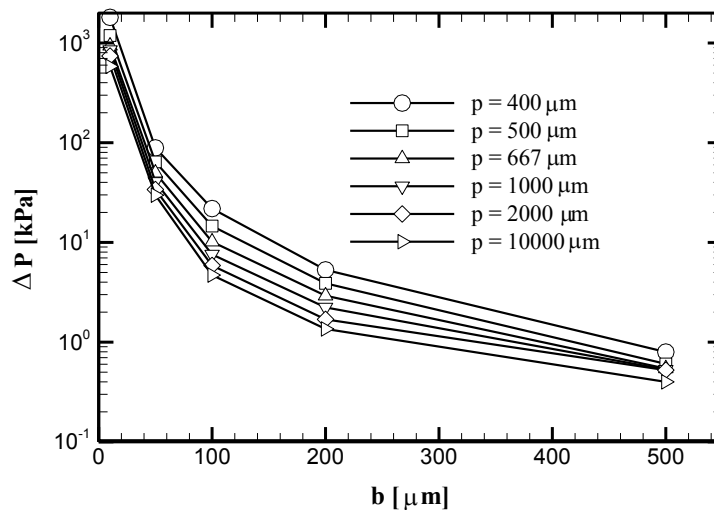


Figure 4.4. Pressure drop variation for the microchannels.

Figure 4.5 shows the pumping power required to drive the fluid through the cooling layer. For microchannel heights lower than  $100\ \mu\text{m}$ , the pumping power is very high ( $> 2\text{W}$ ), and it decreases almost exponentially as the value of  $b$  increases (taller microchannels). For a microchannel height of  $b = 100\ \mu\text{m}$ , the values of  $W$  are low enough ( $< 400\ \text{mW}$ ) to be attractive. Higher microchannel heights lead to a very low pumping power; however, the thermal resistance is high, which indicates a poorer thermal performance.

We observe that a height of  $100\ \mu\text{m}$  results in low thermal resistances and the pumping power remains low. Thus implementing  $b=100\ \mu\text{m}$  offers the best overall performances, providing a thermal resistance of  $\sim 0.4\ \text{K/W}$ . For a fixed microchannel height of  $100\ \mu\text{m}$ , the effect of varying the microchannel width on the thermal resistance is negligible for widths greater than  $800\ \mu\text{m}$ . Hence, a microchannel of  $100\ \mu\text{m}$  and pitch of  $800\ \mu\text{m}$  is recommended for high overall performances. While it is true that narrower channels result in higher heat transfer coefficients [46], these widths also result in higher pressure drops. Increasing the channel width while keeping

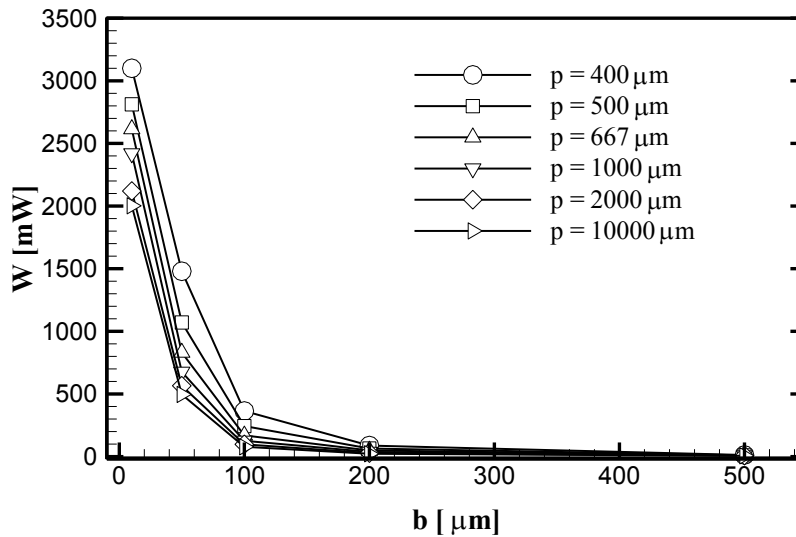


Figure 4.5. Pumping power variation for the microchannels.

TABLE 4.1. SUMMARY AND COMPARISON OF THE SINGLE-PHASE MICROCHANNEL GEOMETRIES IN THE LITERATURE

<i>Ref</i>	<i>Thermal Resistance (K/W)</i>	<i>Pressure Drop (kPa)</i>	<i>Flow rate (ml/min)</i>	<i>Microchannel Dimensions (<math>\mu\text{m}</math>)</i>
[17]	0.09	214	516	width=50 $\mu\text{m}$ height=320 $\mu\text{m}$
[45]	0.20	50	220	width=200 $\mu\text{m}$ height=100 $\mu\text{m}$
[46]	0.17	280	155	width= 50 $\mu\text{m}$ height=100 $\mu\text{m}$
[89]	0.32	70	96	width=200 $\mu\text{m}$ height=2000 $\mu\text{m}$
[90]	0.38	2.41	145	width= 560 $\mu\text{m}$ height=200 $\mu\text{m}$
<i>This work</i>	0.40	9	45	width=800 $\mu\text{m}$ height =100 $\mu\text{m}$

the flow rate per unit width results in a lower pressure drop with the same temperature rise throughout the chip. The somewhat lower heat transfer coefficients are more than offset by having considerably lower pressure drops in the wider channels. For 3D IC applications, the pressure drop is desired to be very low; thus, we recommend a channel width of 800  $\mu\text{m}$  for the subsequent analysis, we assume a height of 100  $\mu\text{m}$  for the microchannels for wireless link design and a corresponding thermal resistance of 0.4 K/W in the cooling layers.

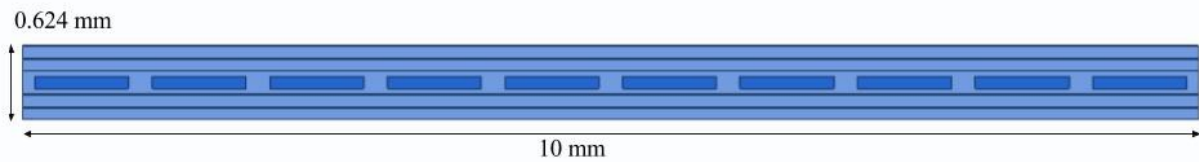
Table 4.1 shows the comparison of the performance for different microchannel configurations reported in the literature with respect to our design. Among the works surveyed here, our design has the highest thermal resistance. However, this thermal resistance is capable of cooling a heat flux of 200 W/cm<sup>2</sup>, while maintaining a surface temperature of 80 °C. The trade-off with thermal resistance, however, enables us to reduce the pressure drop and flow rate compared to earlier work significantly. This leads to a lower power required to drive the flow through the

channels. Therefore, we adopt the microchannel configurations with comparatively high widths and heights. However, this does not have any impact on TSV placement as we propose to establish communication across these microchannels using wireless interconnects. In the next subsections, we evaluate the impact of using wireless interconnects in the 3D NoC on its performance and energy efficiency.

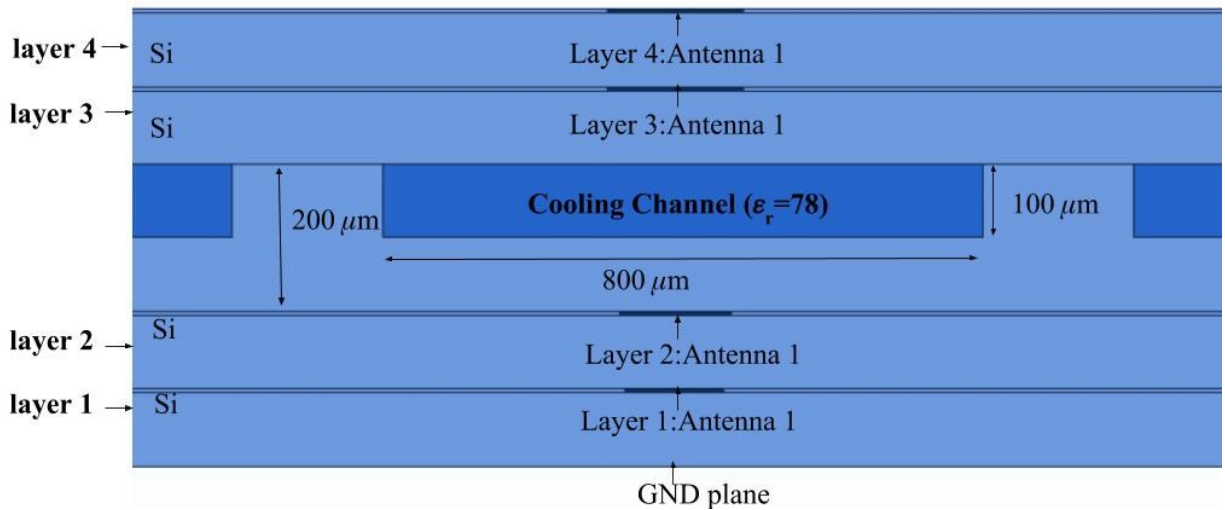
#### **4.2.2 Evaluation of the Hybrid 3D NoC Architecture in the Presence of Microchannel based Liquid Cooling**

According to the projection from ITRS, 3D stacked ICs will have 4 high-performance layers by 2020, where each layer is projected to dissipate more than  $100 \text{ W/cm}^2$  [6]. Hence, to evaluate performance and temperature characteristics of the proposed architecture, we consider a 64-core 3D chip consisting of 4 layers each of  $10 \text{ mm} \times 10 \text{ mm}$  footprint. For interlayer cooling, we have considered one cooling chip after every two active layers as our designed microfluidic cooling layer is capable of cooling a heat flux of  $200 \text{ W/cm}^2$ . We also evaluate the impact of increasing the frequency of insertion of the cooling layers to increase the cooling capability in section 4.2.4. Each layer consists of 16 cores and switches. In the 3D-HiWiNoC architecture, each layer is divided into 4 subnets with 4 cores in each. Therefore, there are 16 WIs, one in each subnet connected to antennas located at the center of each subnet. The NoC architecture is characterized using a cycle accurate simulator that models the progress of the data flits accurately per clock cycle accounting for those flits that reach the destination as well as those that are stalled. For each NoC simulation, ten thousand iterations were performed eliminating transients in the first thousand iterations. The width of all wired links is considered to be same as the flit size, which is considered to be 32 and 256 bits in this paper. We have considered the lower and higher end of flit sizes found

in modern NoC designs. We consider a moderate packet size of 64 flits for all our experiments. The particular NoC switch architecture has three functional stages, namely, input arbitration, routing/switch traversal, and output arbitration [69]. Each switch port has four virtual channels each with a buffer depth of 2 flits. The wireless ports have an increased buffer depth of 8 flits to avoid excessive packet dropping while waiting for the token [28]. The delay and energy dissipation of network switches are obtained from the post-synthesis RTL models using 65nm standard cell libraries from CMP (<http://cmp.imag.fr>) at 1V, using Synopsys. The NoC switches are driven by a clock of frequency 2.5 GHz. The delays and energy dissipation on the wired links were obtained through Cadence simulations taking into account the specific lengths of each link based on the established connections in the 10 mm x 10 mm layer following the topology of the NoCs. Each



(a)



(b)

Figure 4.6. (a) Full side view (b) view inside the box

device layer is considered to be 10  $\mu\text{m}$  thick whereas the cooling layer is considered as 100  $\mu\text{m}$  thick. The power dissipation and delay of the TSVs are adopted from [26]. The wireless transceiver adopted from [28] is shown to dissipate 36.7 mW sustaining a data rate of 16 Gbps while occupying an area of 0.3  $\text{mm}^2$  using TSMC 65-nm CMOS process.

#### ***A. Wireless Channel Modeling and Link Budget Analysis***

In this subsection, we discuss the radiation characteristics of the antennas that are designed to communicate across a cooling layer with microchannels of height 100  $\mu\text{m}$  and width of 800  $\mu\text{m}$ . These dimensions are chosen based on the results of the previous subsection.

##### ***A.1 Characteristics of the Antennas***

The characteristics of the antennas are simulated using HFSS [73], which solves Maxwell's equation in the entire volume of the model by automatically dividing the volume into tetrahedral elements and hence, considers both near field and far field of the antennas. The antennas are designed and tuned by Rounak Singh Narde under the supervision of Dr. Jayanti Venkatarman [74]. The detailed design model of a 3D IC can be seen in Figure 4.6. From the figure, it can be seen that four layers of Silicon substrate are placed on top of each other with silicon dioxide (silica) layer sandwiched in between. Moreover, there is an extra 200  $\mu\text{m}$  thick silicon layer in the midst of the IC consisting of cooling microchannels. The cooling layer is considered to be 200  $\mu\text{m}$  thick with 100  $\mu\text{m}$  tall microchannels embedded in them. The microchannels are considered 800  $\mu\text{m}$  thick with the microchannels walls being 200  $\mu\text{m}$  as widening the microchannels beyond 800  $\mu\text{m}$  alters the thermal characteristics marginally as noted in the previous subsections.

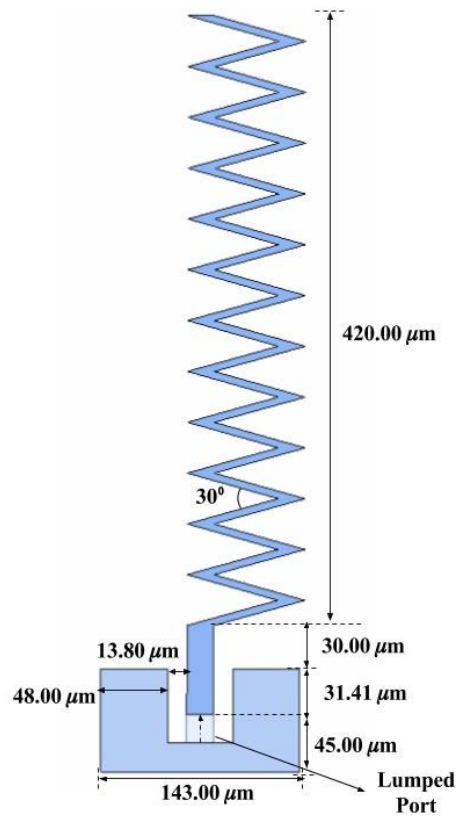


**Figure 4.7. Dimensions of the designed zig-zag antenna.**

We evaluated the communication capability of these antennas deployed on all the layers of the 3D IC both separated as well as not separated by the cooling layer. The antennas are placed assuming the wireless 3D NoC architecture as proposed in section 4.1.2 at the center of each subnet in each layer. Therefore, some pairs are separated only vertically while other pairs are separated both vertically as well as horizontally (in hubs that are not vertically aligned).

The metal antennas are considered to be embedded in the midst of a 6  $\mu\text{m}$  layer of silica. Figure 4.7 shows the specific dimensions of the antenna and its coplanar feed structure. A trace width of 5  $\mu\text{m}$  and thickness of 2  $\mu\text{m}$  is used for all arms of the antenna. All the antennas are tuned to resonate at 60 GHz with low return losses of at least -16 dB. Figure 4.8 shows the return loss

for the proposed antenna system. We have observed that at low frequencies below 10 GHz there is no resonance in these antennas as the return loss is 0 dB. This demonstrates that there is no radiation from the antennas at those frequencies. This eliminates the possibility of interference with clock or other electrical signals in the IC mostly in those frequency bands lower than 10 GHz.

As described in earlier sections, we have considered a 64 core system with 4 active layers and one cooling layer for our system level simulation where each active layer is divided into 4 subnets resulting in total 16 WIs. The worst case path loss is seen for antennas those are placed in lower layer i.e. close to the metallic ground plane. Figure 4.9 shows insertion loss for one antenna placed in the lower layer. From the figure, it can be seen that the transmission for the antennas, which are in the near field i.e. placed vertically on top of each other, are better than other pairs. This effect is also demonstrated in [91] that transmission is much higher in near field than in the

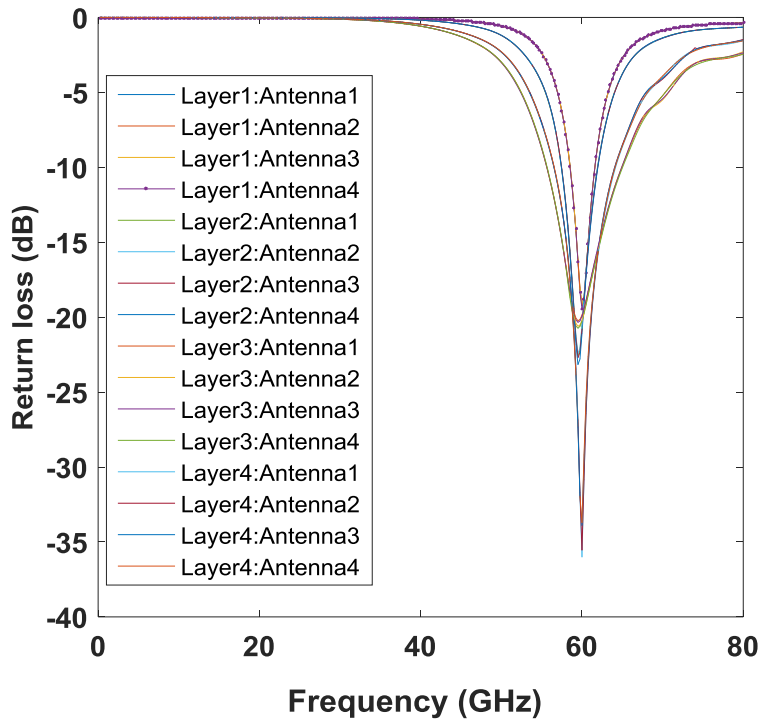


Figure 4.8. Return losses of all 16 antennas.

far field. The worst case path loss is -48.6 dB between antennas that are deployed in the first layer (closest to the ground plane) and the third layer. The cooling layer separates these layers. Also, these antennas are in subnets that are diagonal across from each other along the planar dimension. In the next subsection, we estimate the reliability of wireless communication using this antenna system and existing on-chip mm-wave transceivers from literature [28].

### A.2 Link Budget Analysis

In this subsection, we present a link budget analysis to estimate the Bit Error Rate (BER) in the wireless communication channel in the 3D IC with cooling layers. The following equation gives the transmitted power,  $P_t$  in dBm on the wireless channels:

$$P_t = SNR + PL + N_f. \quad (4.4)$$

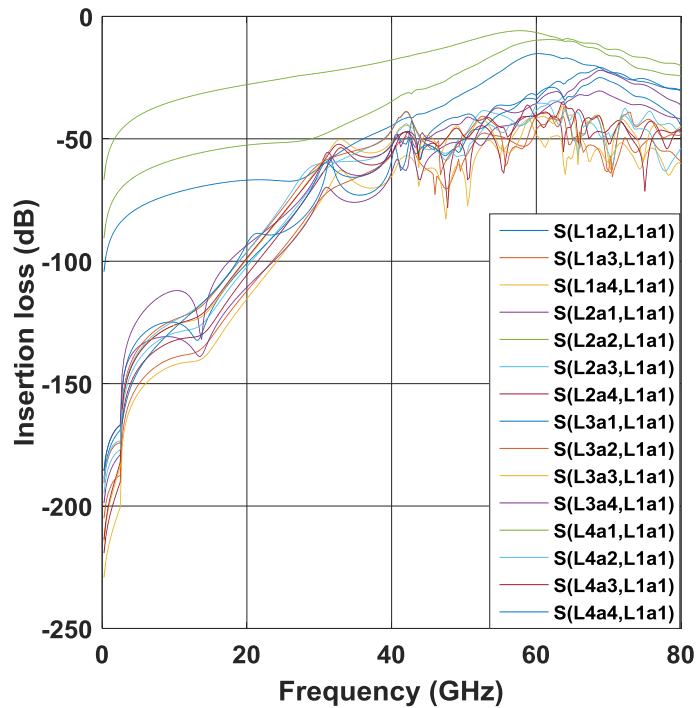


Figure 4.9. The insertion loss of antenna 1 in layer1.

Where,  $SNR$  is the signal to noise ratio at the receiver in dB,  $PL$  is the path loss in dB and  $N_{floor}$  is the receiver noise floor in dBm. The worst-case path loss,  $PL$  obtained from Figure 4.9 is -48.6 dB. The noise floor of the receiver is given by,

$$N_{Floor} = 10 \log kTB + NF. \quad (4.5)$$

Where  $k$  is the Boltzmann constant,  $T$  is the temperature,  $B$  is the bandwidth of the receiver and  $NF$  is the noise figure of the receiver in dB. The noise figure of the adopted receiver is 13 dB [29]. This makes the receiver noise floor -62.68 dBm at 50 °C for a BW of 16 GHz. Using the power output of 0 dBm by the transmitter adopted from [28], the received SNR turns out to be 16.846 dB. In the non-coherent OOK modulation scheme adopted in the transceiver, this achieves a BER of about  $10^{-12}$ , which is comparable to conventional interconnects in multicore SoCs.

### ***B. Temperature and Performance Characteristics of 3D Wireless NoC Architectures with Synthetic Workload***

In this section, we evaluate the temperature profiles and performance of 3D multicore chips interconnected with various NoC architectures and employing microchannel based cooling as well as conventional cooling with synthetic workloads and traffic scenarios. To capture the impact of the power dissipation of the cores on-chip temperatures, we use predictive power models proposed in [92] to estimate the power profile of the individual cores for synthetic workloads. According to [92], the chip power density in the 65nm technology node is 0.5 W/mm<sup>2</sup>. We consider a 64-core chip consisting of 4 layers each of 10 mm x 10 mm. Hence, based on the tile-based floorplan each core is estimated to dissipate 2.645 W. Using these power profiles of the cores and obtaining the power profile of the NoC with uniform random traffic, the network switches and links are arranged on a 10 mm x 10 mm layer. These floor plans, along with the power profiles, are used in a thermal

modeling tool, HotSpot3D [93] to obtain the thermal profiles. We use a sampling interval of 100k cycles, and all simulations are initialized with ambient temperature. Specifically, we consider the following configurations:

1. 3D Mesh NoC with TSV with a conventional air-cooled heat sink (3D-MTSV) adopted from [94]. For this architecture, each switch is connected to its cardinal neighbors as well as its vertical neighbors above and below itself.
2. Token-based 3D Hierarchical Wireless NoC with interlayer cooling (3D-THiWiNoC) as proposed here.

### ***B.1 Temperature Evaluation with Synthetic Workload***

The power dissipation of the cores, the power dissipation of the NoC switches, and interconnects, as well as the impacts of the cooling infrastructures, are considered for evaluation of the temperatures. The maximum chip temperature can be either the temperature of a core, link or switch. For interlayer cooling, we have considered one cooling chip after every two active layers. It is important to note that, we did not incorporate any dynamic thermal management technique for this experiment as our goal was to study the effectiveness of two cooling approaches (conventional forced air-cooling and inter-layer liquid cooling) considered in this subsection. Table 4.2 shows the maximum chip temperature for each of the architectures studied here for two different flit sizes. For interlayer coolers, we used a thermal resistance of 0.4 K/W. As noted in section 4.2.1, a thermal resistance of 0.4K/W is obtained by optimizing the width and height of the microchannels such that the pressure drop across them is not too high. From the table, it can be seen that for flit size of 32 bits, maximum steady state temperature of the 3D-MTSV reaches 102.17°C with forced-air cooling based conventional heat sink whereas, with interlayer layer

TABLE 4.2. PEAK TEMPERATURE OF TWO ARCHITECTURES CONSIDERED HERE

	<i>Flit size (32 bits)</i>		<i>Flit size (256 bits)</i>	
	<i>3D-MTSV</i>	<i>3D-THiWiNoC</i>	<i>3D-MTSV</i>	<i>3D-THiWiNoC</i>
<i>Thermal resistance (K/W)</i>	<i>1*</i>	<i>0.4</i>	<i>1*</i>	<i>0.4</i>
<i>Peak chip temperature (°C)</i>	<i>102.7</i>	<i>65.12</i>	<i>158.1</i>	<i>67.81</i>

\* *Convictional cooling only*

cooling, it decreases by 35.5% for 3D-HiWiNoC architecture. On the other hand, increasing flit size eventually will increase the power dissipated by interconnects (links and switches) as described in next section. Because of this, for flit size of 256 bits, maximum steady state temperature for 3D-MTSV reaches to 158.1°C with conventional forced air-cooling based heat sinks. Whereas for the same flit sizes, the maximum steady state temperature remains below 68°C. Again, no additional DTM/DPM mechanism was considered in these cases. The interlayer microfluidic cooling channels are more efficient in heat removal from the stacks of active layers. In contrast with conventional convection cooling heat is only removed from the top surface of the 3D IC trapping the heat in internal layers making temperatures rise dramatically in response to similar power dissipation profiles

## ***B.2 Performance Evaluation with Synthetic Workload***

In this section, we evaluate the proposed token-based 3-D hierarchical WiNoC architecture for a system size of 64 cores with uniform random traffic distribution in terms of energy cost per bit and peak network bandwidth and compare it with 3D wireline mesh architecture for two different flit sizes of 32 bits and 256 bits respectively. Energy cost per bit is the energy dissipated in transferring

one bit completely from source to destination at network saturation. Peak bandwidth is the maximum achievable data rate for the NoC. The bandwidth is measured as the average number of bits successfully arriving per core per second. From the Figure 4.10, it can be seen that for 3D-MTSV architecture yields maximum bandwidth for both flit sizes compared to wireless architecture with liquid cooling. This is because number of active links in wireless architecture is less than 3D-MTSV as this architecture eliminates the TSV based interconnects for data communication across the cooling layers. In the 64-core system divided into 4 layers with 16 cores each, there are cooling layers after every 2 layers. This implied that in the WiNoC architecture, 16 TSV based links connecting the vertically adjacent switches across the cooling layer is eliminated. This results in a loss of an aggregate physical bandwidth of 1.2 Tbps for flit size of 32 bits (16 links with 32 bits each @ 2.5 GHz). The additional wireless bandwidth of 16 Gbps helps to interconnect the two segments across the cooling layer. The removal of the interlayer TSV based connections across the cooling chip results in bandwidth degradation by approximately the same amount of the loss in the bisectional bandwidth of the removed TSV based links. On the other hand, for flit size of 256 bits, 3D-MTSV architecture shows nearly 7.6x improvement over flit sizes of 32 bits whereas, in 3D-THiWiNoC architecture, it is about 6.2x. This is because widening physical channel width to accommodate larger flit increases the data rate of the wireline links and TSVs. However, the data rate of the wireless links is governed by the speed of the transceiver and bandwidth of the antennas, which does not change with flit size. Hence, while the wireline communication becomes faster with an increase in flit size, the wireless communication speed remains constant resulting in a lower relative improvement in bandwidth with an increase in flit size compared to a completely wired NoC. However, wider TSV based vertical links have a significant impact on the area required to route them and consequently, increase the challenges of

place and route of these communication channels across the cooling layers. The interlayer wireless links alleviate this problem significantly, as is discussed later in section 4.2.6.

The WiNoCs, on the other hand, can reduce the energy cost per bit compared to the wireline TSV based 3D NoCs for both flit sizes. This is because long-range data transfer between different layers of the 3D NoC between switches, which are also separated by several millimeters in the planar dimension, can be accomplished in a single hop using the wireless links. In contrast, in the 3D mesh architectures, data transfer over even short vertical distances happen over multi-hop paths over multiple switches resulting in higher energy dissipation compared to the 3D-THiWiNoCs for both flit sizes. In addition, the interlayer cooling chip reduces the temperature due to increased cooling capacity. Therefore, while the bandwidth of the WiNoCs is less than that of the 3D mesh, the packet energy, and peak temperatures are significantly reduced.

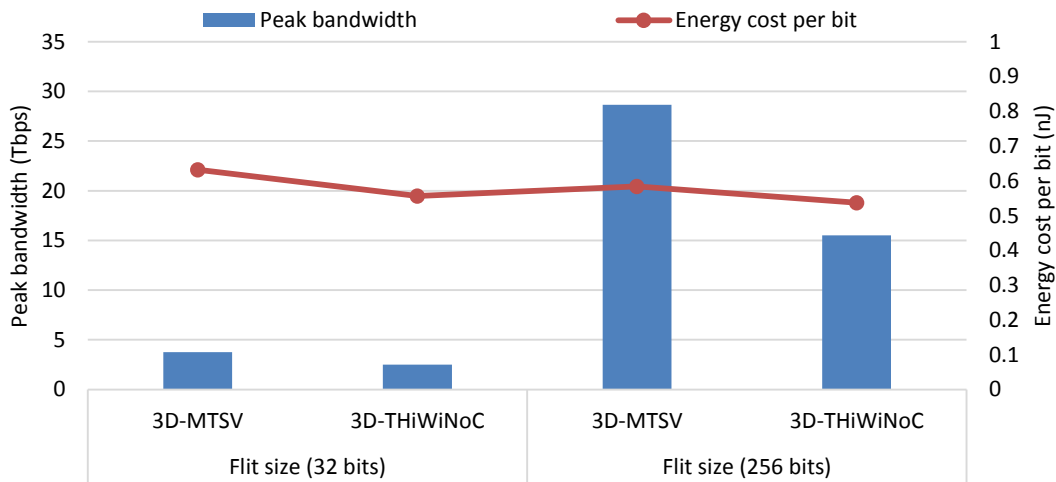


**Figure 4.10. Peak bandwidth and energy cost per bit for different 3D NoC architectures.**

### 4.2.3 Temperature and Performance Characteristics of 3D NoC Architectures with Real Application-based Workloads

In this section, we evaluate the performance and thermal characteristics of 3D multicore ICs interconnected by the proposed token-based 3D-THiWiNoC and 3D-MTSV architectures in the presence of real application-based workloads mapped onto a 64 core chip mentioned architectures. We use GEM5 [95], a full system simulator to obtain detailed processor and network-level information on SPLASH-2 [96] and PARSEC [97] benchmarks and HotSpot3D [93] to obtain detailed thermal profiles. We consider a system of 64 alpha cores running Linux within the GEM5 platform for all experiments. The memory system is MOESI\_CMP\_directory, setup with private 64KB L1 instruction and data caches and a shared 64MB (1MB distributed per core) L2 cache. The processor-level utilization statistics generated by the GEM5 simulations are incorporated into McPAT simulator [98] to determine the processor-level power statistics. The traffic interaction patterns for each benchmark obtained from Gem5 are used in the NoC simulator to get the NoC

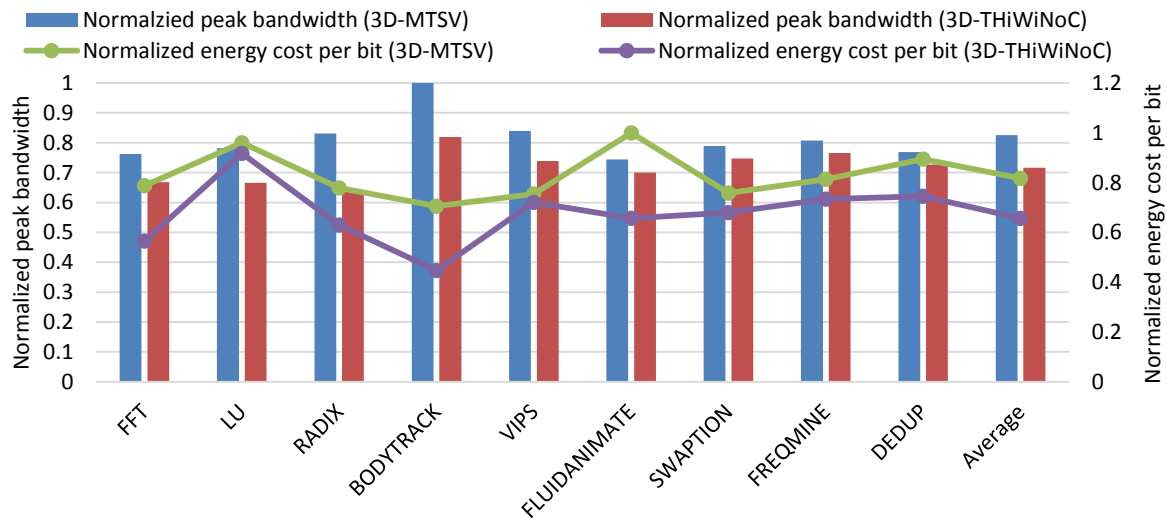
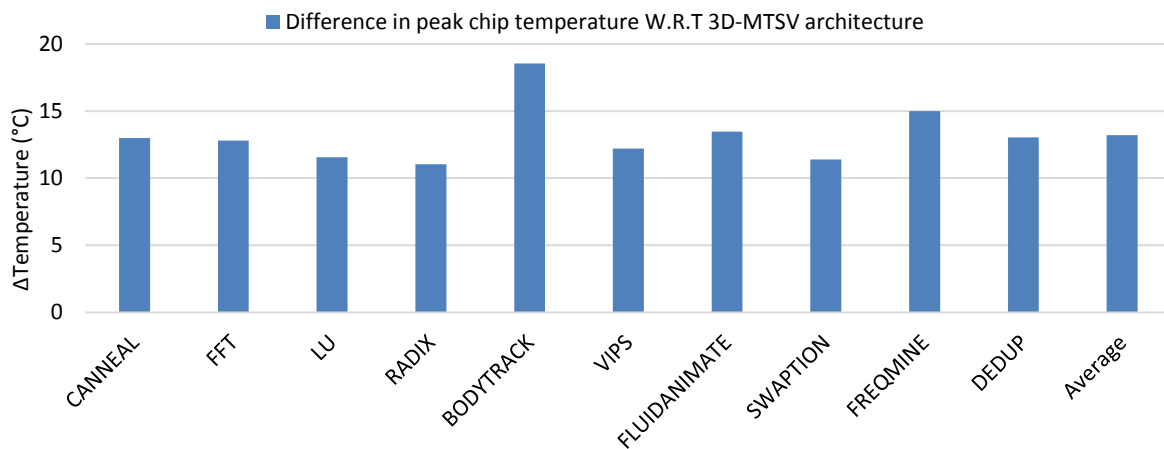


Figure 4.11. Normalized Peak bandwidth and energy cost per bit in the presence of real application traffic.

performance in terms of peak bandwidth, average network latency, and average energy cost per bit. Similar to previous experiments, we consider cooling chip after every two layers.

Figure 4.11 and 4.12 show the normalized peak bandwidth & energy cost per bit and difference in peak chip temperature ( $\Delta T$ ) of two architectures considered here in the presence of different real application traffics. As number of vertical links is less in 3D-THiWiNoC architecture than that in the 3D-MTSV, peak bandwidth of the 3D-THiWiNoC is lower than that of 3D-Mesh-TSV for all real life application traffics. However, the presence of single hop energy efficient wireless links reduces the energy cost per bit compared to the wireline TSV based 3D NoCs.

Also, the presence of the interlayer cooling chip can reduce the peak temperature due to increased cooling capacity which can be seen from Figure 4.12. With cooling chip after every two layers, 3D-THiWiNoC architecture shows on average 13 degrees and a maximum of 18 degrees reduction in peak temperature compared to 3D-MTSV architecture with conventional fan based air-cooled heat sink. We observe that although the peak bandwidth in 3D-THiWiNoC is less than



**Figure 4.12. Peak chip temperature in presence of real application traffics.**

that of wireline 3D-MTSV architecture, it achieves lower energy cost per bit and peak temperatures for all the application-specific workloads.

#### 4.2.4 Increasing Cooling Capacity of the Interlayer Coolers and its Impact on Performance of the 3D Wireless NoC

In this section, we study the impact of various techniques for increasing the cooling capacity of the interlayer coolers in case the power consumption profiles of the 3D IC layers require. The cooling capability of the microchannels can be increased by increasing the flow rate of the coolant fluid through the microchannels. However, that results in an increase in pressure drop. However, the flow rate can only be increased such that the resultant pressure drop is within acceptable limits of hydraulic stress that the 3D IC can sustain. Otherwise, the microchannel heights will need to be increased requiring the antennas to be retuned for the altered dimensions. Hence, we study the increase in cooling capacity by increasing the frequency of insertion of the cooling layers in this section.

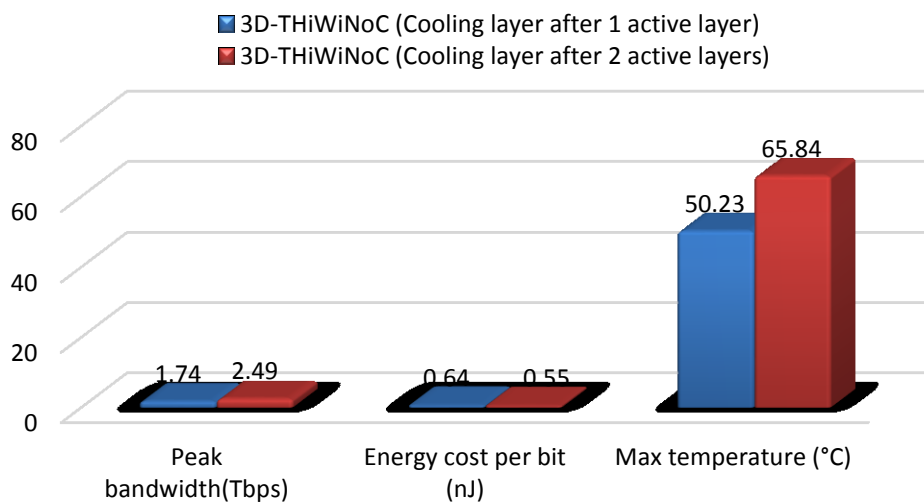


Figure 4.13. The impact of frequency of the cooling layers.

The frequency of insertion of the cooling layers signifies the number of active device layers between the cooling layers. The impact of varying the frequency of the cooling layers on performance, energy dissipation and maximum chip temperatures of token-based 3D-THiWiNoC architecture. We have considered uniform random traffic with maximum injection load for this experiment. Figure 4.13 shows the effect of varying the frequency of cooling layers from one after every active layer to one cooling layer after every 2 layers on maximum chip temperature, peak bandwidth, and energy cost per bit. From the figure, it can be seen that increasing the frequency of cooling layers reduce the maximum chip temperature to a great extent for both architectures considered for the experiment. With cooling chip after every 1 layer, with a thermal resistance of 0.4W/K, maximum temperature reduces to 50.23°C for token-based 3D-THiWiNoC from around 65°C for the same NoCs with one cooling layer after every two layers. However, increasing the frequency of cooling layer have a diminishing effect on performance for wireless 3D architecture. This is because in token-based 3D-THiWiNoC architecture with a cooling chip after every active layer, the number of active links is 33.33% less than 3D wireline mesh architecture, to accommodate microchannel liquid cooling chip, which in turn reduces performance. For cooling chip after every two active layers, due to augmentation of TSV based links, the performance of the Token-based 3D-THiWiNoC architecture increases. However, decreasing the frequency of cooling layers increases maximum chip temperature because of the increased stacking of layers.

#### **4.2.5 Comparison with Alternative Wireless Communication Mechanism**

In this section, we evaluate the performance of the proposed wireless multichip system coupled with an alternative wireless communication mechanism i.e. Direct Sequence Spread Spectrum (DSSS) based Code Division Multiple Access (CDMA) channel access mechanism and compared

the performance in terms of bandwidth and energy cost per bit with token-based 3D-TWiNoC architecture.

In token passing based wireless medium access mechanism, only a single transmitter can access the wireless channel at any given instant of time. This limits the performance benefits of the wireless interconnection although multiple transceivers are deployed over the entire system. However, it is possible to design sophisticated MAC mechanisms which will enable multiple WIs to share this wireless channel without any interference and ensure optimal utilization of the available bandwidth. In order to enable multiple concurrent communication between the WIs, authors in [34] proposed a DSSS based CDMA channel access mechanism for a wireless NoC. In the CDMA-based medium access mechanisms, Walsh codes are used to create orthogonal code channels for multiple access. Due to this orthogonality between the code channels bits in one code channel is not affected by other channels. Transmitted bits are first encoded using the code-word, and at the receiving WI, the received bit is XORed with the code words to extract the transmitted

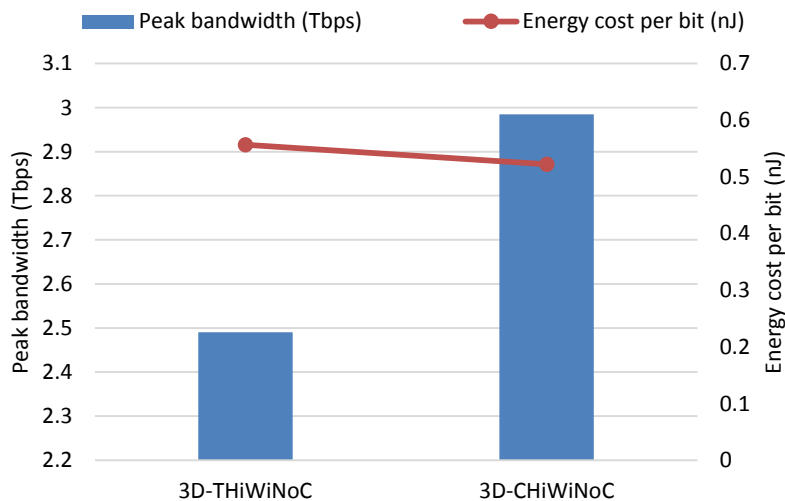


**Figure 4.14. Peak bandwidth and energy cost per bit for different wireless communication mechanisms.**

TABLE 4.3. ENERGY PER BIT FOR A SINGLE POINT-TO-POINT LINK AND POSSIBLE AGGREGATE BANDWIDTH FOR DIFFERENT WIRELESS COMMUNICATION PROTOCOLS

	<i>Token-based wireless interconnect</i>	<i>CDMA based wireless interconnect</i>
<i>Energy (pJ/bit)</i>	2.3	3.43
<i>Aggregate physical bandwidth (Gbps)</i>	16	6
<i>Transceiver area (mm<sup>2</sup>)</i>	0.3	0.4

data. We adopt the performance and power characteristics of the CDMA transceiver from [34] to estimate the performance of the system. The raw energy/bit of the wireless technology for a single point-to-point link and aggregate physical bandwidth provided by each of these technologies are summarized in Table 4.3.

Figure 4.14 shows the peak achievable bandwidth and energy cost per bit for token-based and CDMA-based 3D Wireless NoC (3D-CHiWiNoC) architecture. For a fair comparison, we considered same network topology and the same number of WIs per layer in both cases. From the figure, it can be seen that the peak achievable bandwidth of the CDMA-based 3D-HiWiNoC is 19.86% higher than the token-based counterparts. This is because in CDMA concurrent wireless communication is possible in different orthogonal code channels whereas in token passing only one wireless communication is possible at a time. Similarly, the energy cost per bit of the CDMA-based 3D-CHiWiNoC is also lower than the token-based 3D-THiWiNoC architecture. This is because, in the token-based system when the number of WIs is increased, token returning period to the WIs also increase. This result in higher energy cost per bit in the token-based system as

packets has to wait longer in the wireless buffers before getting transmitted via the wireless interconnect.

However, the improvement of the performance by implementing sophisticated MAC does not come without a price. Reliability can be an issue for the CDMA-based 3D-CHiWiNoC architecture, as CDMA requires the transmitters to be synchronized with each other so that the transmitted data is perfectly aligned with respect to other transmitters to maintain the orthogonality between the code words. Such synchronization is difficult to achieve in a 3D environment as the WIs are distributed across different layers and require further investigation.

#### 4.2.6 Area Overheads

In this section, we estimate the comparative area overheads of the signal TSVs through microchannel based cooling layer. TSVs for power and clock networks are not considered here. We have considered a moderate size signal TSV with diameter 2  $\mu\text{m}$  and pitch 4  $\mu\text{m}$  to calculate

TABLE 4.4. AREA OVERHEAD FOR THE SIGNAL TSVS THROUGH MICROCHANNEL COOLING LAYER.

	<i>Flit size of 32 bits</i>		<i>Flit size of 256 bits</i>	
	<i>3D-MTSV</i>	<i>3D-THiWiNoC</i>	<i>3D-MTSV</i>	<i>3D-THiWiNoC</i>
<i>Required area for place and route of signal TSVs (mm<sup>2</sup>)</i>	2.016	0	16.352	0
<i>Available area for place and route of all the TSVs through microchannel walls (mm<sup>2</sup>)</i>	20	20	20	20
<i>Percentage of occupied area for place and route of signal TSVs through microchannel walls</i>	10.08%	0%	81.76%	0%

the area overhead. The optimal width of each microchannel is found to be 800  $\mu\text{m}$  in section 4.2.1 keeping 20  $\text{mm}^2$  area available for place and route of all the TSVs through the interlayer cooler. Table 4.4 shows the area required for the signal TSVs to route through the microchannel walls. From the table, it can be seen that for flit size of 32 bits, 10.08% area is occupied by the signal TSVs for place and route through the interlayer cooling layer. As a result, 89.92% of area is available for power and clock delivery TSVs to place and route. Whereas, for flit size of 256 bits, the signal TSVs occupy an area of 16.352  $\text{mm}^2$  out of 20  $\text{mm}^2$  available area keeping only 18.24% area to properly route the power and clock TSVs which might not be sufficient. On the other hand, in the case of wireless 3D NoC architecture with interlayer cooling, we are eliminating the entire signal TSVs across the microchannels keeping the entire 20  $\text{mm}^2$  area for power and clock delivery TSVs. This, in turn, will reduce the complexity of the co-design of TSV based interconnects and microchannel based interlayer cooling significantly.

#### **4.2.7 Trade-off Analysis**

From all the results we can conclude that the 3D-THiWiNoC with 256 bits per flit and microchannel based interlayer coolers provides the best trade-offs in performance, energy consumption per bit and temperature. While the fully wired TSV based counterpart provides higher bandwidth, it imposes severe challenges to co-design and place and route of the TSV based links across the cooling layers, due to its high area requirements. The same fully wired architecture with 32 bits per flit has lower area requirements for the vertical links but has lower bandwidth and higher energy consumption as well as worse temperature compared to the 3D-THiWiNoC with 256 bits per flit. The 3D-THiWiNoC with 256 bits per flit enjoys the benefit of the wide TSV based vertical links among adjacent layers while enabling communication across the cooling layer

with the wireless links. Moreover, utilizing wireless interconnect for data communication across the cooling layer relaxes the height restrictions of the microchannels, and therefore, results in lower pressure drop across the cooling layer. This, in turn, leads to a lower power requirement to drive the flow through the channels and increases structural stability.

Increasing the frequency of cooling layer have a diminishing effect on performance for wireless 3D architecture. This is because in token-based 3D-THiWiNoC architecture with a cooling chip after every active layer, to accommodate microchannel liquid cooling chip, the number of active links is reduced compared to 3D wireline mesh architecture. This, in turn, reduces the performance of the 3D wireless NoC. For cooling chip after every two active layers, due to augmentation of TSV based links, the performance of the Token-based 3D-THiWiNoC architecture increases. However, decreasing the frequency of cooling layers increases maximum chip temperature because of the increased stacking of layers.

Compared to other contactless wireless interconnect such as capacitive/inductive coupling based links, the energy consumption per bit for mm-wave wireless links do not increase with communication distance. This makes mm-wave wireless interconnect feasible solution for data communication across microchannels cooling layers with heights of 100  $\mu\text{m}$ .

In terms of the wireless communication protocol, in token passing based wireless medium access mechanism, only a single transmitter can access the wireless channel at any given instant of time. This limits the performance benefits of the wireless interconnection although multiple transceivers are deployed over the entire system. Complex MAC mechanism like CDMA can enable better performance compared to the token passing based method. However, the requirement of precise synchronization in CDMA links is difficult to achieve in a large 3D multicore chip. The

loss of synchronization will introduce inter-channel interference resulting in unreliable performance and require further investigation.

#### 4.2.8 Holistic Comparison of the Vertically Integrated Wireless System with Horizontally Integrated Wireless Multichip System

In this section, we perform a holistic comparison of the wireless 3D system with respect to the wireless multichip system in terms of performance, energy efficiency, and temperature.

Horizontal integration or Multi-Chip Module (MCM) is another way of integrating multiple chips where chips are placed horizontally on the same substrate or interposer within a package and are considered as a predecessor to monolithic 3D integration. Conventionally, MCM systems are interconnected by C4 bumps coupled with in-package transmission lines [41]. However, signal quality deteriorations due to microwave effects, crosstalk coupling effects, signal reflections, and frequency-dependent lines losses in the transmission line restrict the possible

TABLE 4.5. PERFORMANCE COMPARISON WITH THE HORIZONTALLY INTEGRATED WIRELESS MULTICHIP MODULE.

	<i>Wireless MCM System</i>	<i>3D-THiWiNoC (Cooling layer after 2 active layers)</i>	<i>3D-THiWiNoC (Cooling layer after 2 active layers)</i>
<i>Peak Bandwidth (Tbps)</i>	1.737	2.491	1.738
<i>Energy Cost per Bit (nJ)</i>	0.64	0.55	0.64
<i>Temperature (°C)</i>	71.31	65.84	50.23

performance benefits of the multichip system [10]. To improve performance and energy efficiency, [87] proposes to use wireless interconnects for data transfer between chips in an MCM system. Due to the analogous nature of the wirelessly connected MCM [87], and the 3D wireless NoC integrating multiple layers with the same mm-wave technology we compare the two systems in terms of their performance, energy-efficiency, and thermal profiles.

For a fair comparison, same number and location of wireless interconnect, and same token-based wireless medium access mechanism is considered in both 3D and MCM systems. In addition, the intra-layer NoC architecture and intra-chip NoC architecture for the individual chips in the MCM are considered to be identical. The routing and switching protocol in the two systems are also same with same NoC switch design adopted in both. Table 4.5 shows the peak bandwidth, energy cost per bit, and temperature for 4-chip wireless MCM and the 3D-THiWiNoC architectures at network saturation using uniform random traffic. For 3D-THiWiNoC architecture, we have considered two different configurations: cooling layers after every active layer and cooling layer after every 2 active layers. It is important to note that inserting cooling chip after every active layer will eliminate all the data TSVs utilizing solely wireless interconnections for data communication across cooling layer and will result in identical topology for wireless MCM and 3D-THiWiNoC architecture. Consequently, these two systems are equal in peak bandwidth and energy cost per bit as can be seen from Table 4.5. However, the cooling layers after every active layer result in a much better thermal characteristic. The 3D-THiWiNoC with cooling chip after every two layers has higher bandwidth and lower energy cost per bit compared to other configurations, due to augmentation of TSVs for data communication between active layers, which are not separated by a cooling layer. On the other hand, its thermal characteristics are worse than the 3D-THiWiNoC with cooling layers between every active layer. Both 3D-THiWiNoC

TABLE 4.6. HOLISTIC COMPARISON OF BOTH MULTICHIP INTEGRATION TECHNIQUES IN VARIOUS DOMAINS.

	<i>3D Wireless Multichip System with Microchannel Cooling</i>	<i>Wireless MCM System</i>
<i>Projected Performance</i>	<i>Higher compared to wireless MCM systems</i>	<i>Outperforms conventional wireline interchip communication systems</i>
<i>Form Factor</i>	<i>Smaller footprint due to the vertical stacking</i>	<i>Larger footprint due to horizontal integration</i>
<i>Design Flow</i>	<i>Requires new EDA tools</i>	<i>Can utilize existing EDA tools</i>
<i>Manufacturing</i>	<i>Challenging</i>	<i>Contemporary</i>
<i>Testing</i>	<i>New methods</i>	<i>Contemporary</i>
<i>Device Impact</i>	<i>Stress from TSV fabrication</i>	<i>None</i>
<i>Cost</i>	<i>High (initially)</i>	<i>High Volume Manufacturing (HVM) possible at low cost</i>

configurations have lower peak chip temperature compared to wireless MCM system due to the presence of microchannels that are more efficient in heat removal compared to traditional fan based air-cooled heat sinks. Therefore, it can be observed that the 3D-THiWiNoC can provide identical or better performance compared to a wireless MCM for better thermal characteristics.

While improvement in energy efficiency and temperature profile is possible in the 3D wireless NoC architecture with microchannel based liquid cooling, however, to take full advantages of 3D integration, more research is necessary to address various challenges in multiple areas including TSV fabrication, testing, and CAD tool development. Table 4.6 shows the holistic comparison of both multichip integration techniques. Fabrication of TSVs requires additional process steps, and these additional steps make TSV manufacture at high yield extremely difficult. In addition, to maintain good conductivity and minimize resistance, the TSVs between dies must be aligned precisely. Moreover, there are limited number of Electronic Design Automation (EDA) tools available to design and test 3D integrated ICs. On the other hand, a horizontally stacked wireless multichip system utilizing metal-zigzag antennas are CMOS compatible and do not require any additional fabrication steps. Moreover, the wireless planar multichip system outperforms conventional wireline interchip communication systems.

### **4.3 Summary**

In this chapter, we present a wireless 3D NoC architecture that enables energy-efficient on-chip data transfer along with liquid cooling technology suitable for 3D multicore ICs. We designed the on-chip antennas to establish wireless communication across cooling layers depending upon the dimensions of the microchannels for best trade-offs in thermal and hydraulic performance. The hybrid wireless and wireline 3D NoC architecture was designed using these antennas. We demonstrate that with wireless 3D NoC coupled with a cooling layer with microchannels can improve the thermal characteristics of the 3D IC compared to 3D NoCs with TSVs and conventional cooling significantly while also reducing the energy cost per bit. This is due to a reduction in multi-hop communication in both planar and vertical directions in a wireless 3D NoC.

However, due to the removal of TSV based high bandwidth links across the cooling layer, the bandwidth of this wireless NoC is lower than the 3D Mesh.

## **Chapter 5      CONCLUSION    AND    FUTURE    RESEARCH DIRECTIONS**

The aim of this work is to demonstrate the potential of mm-wave wireless interconnects to overcome the challenges of multichip integration. This chapter concludes the work accomplished in this dissertation by summarizing significant contributions. It also points towards various promising future directions originating from this research work.

### **5.1    Conclusion**

The multichip system has emerged as a feasible solution to overcome the physical constraint of the area, yield, and scalability limitations of the single chip multiprocessor system. However, as a new technology, disintegrating multiple systems needs to overcome few key challenges to be widely accepted and depending on the integration approaches, these challenges are diverse in nature. In the case of the horizontal integration, the difficulties lie in the inter-chip communication whereas, in vertical integration, the challenge is to find an enabling technology to communicate across the cooling layer. Wireless interconnect can be a promising solution to deal with these challenges. This dissertation proposes the design methodologies to utilize wireless interconnects as the communication backbone for both horizontally and vertically integrated multichip system.

For the horizontally integrated multichip system, this work explores the advantages possible if inter-chip communication in multichip modules can be realized with state-of-the-art mm-wave wireless links operating in the 60GHz band. The wireless links are capable of establishing direct communication channels between cores in different chips via on-chip embedded

antennas. Moreover, the wireless links can be used for a seamless data transfer between cores in the same chip as well to augment the traditional NoC backbone for intra-chip communications. These factors result in significant gains in performance and energy efficiency in both intra and inter-chip data communications. The energy-efficiency of the wireless interconnects have been improved by careful wireless data transfer protocol design to put unused WIs to sleep using power-gated transceivers. It can be further enhanced by using variable levels of power amplifications [86] depending upon the length of the wireless interconnects and associated path losses in the future.

As for vertical integration, this dissertation proposes to use wireless interconnect to enable energy-efficient on-chip data transfer across the cooling layers. We designed the on-chip antennas to establish wireless communication across cooling layers depending upon the dimensions of the microchannels for best trade-offs in thermal and hydraulic performance. Using these antennas, the hybrid wireless and wireline 3D NoC architecture are designed. From all the results we can conclude that the 3D-THiWiNoC with 256 bits per flit and microchannel based interlayer coolers provides the best trade-offs in performance, energy consumption per bit and temperature. While the fully wired TSV based counterpart provides higher bandwidth, it imposes severe challenges to co-design and place and route of the TSV based links across the cooling layers due to its high area requirements. The same fully wired architecture with 32 bits per flit has lower area requirements for the vertical links but has lower bandwidth and higher energy consumption as well as worse temperature compared to the 3D-THiWiNoC with 256 bits per flit. The 3D-THiWiNoC with 256 bits per flit enjoys the benefit of the wide TSV based vertical links among adjacent layers while enabling communication across the cooling layer with the wireless links. Hence, this architecture is suitable for applications and environments that have strict constraints on energy consumption and temperature of the system and do not require extremely high bandwidths. This method of

reducing both energy and temperature of a 3D multicore IC is orthogonal and can co-exist with other dynamic thermal and power management mechanisms like DVFS which will provide further enhanced control and trade-offs in the power-performance-temperature spectrum of the chip. Moreover, dynamic control of the cooling capability of microchannels can be achieved by micro-pumps, which can dynamically vary the flow rates in the channels. Such a mechanism together with DVFS can be designed for a more holistic dynamic thermal control of a 3D multi-core chip in the future.

When compared to the planar multichip module as an alternative to monolithic 3D integration with interlayer coolers, we find out that the monolithic 3D-THiWiNoC (with cooling layer after 2 active layers) has better performance, energy per bit as well as temperature compared to the planar counterpart. This is because of the TSV based links that interconnect the active layers not separated by the cooling layer. The microchannel based coolers help in reducing the temperature in the 3D-THiWiNoC. While improvement in energy efficiency and temperature profile is possible in the 3D-THiWiNoC architecture, there have several other challenges. Fabrication of TSVs requires additional process steps, and these additional steps make TSV manufacture at high yield extremely difficult due to challenges related to etching, sidewall passivation, and formation, insulation, and filling of Vias. In addition, to maintain good conductivity and minimize resistance, the TSVs between dies must be aligned precisely. On the other hand, a horizontally stacked wireless multichip system utilizing metal-zigzag antennas are CMOS compatible and do not require any additional fabrication steps. Moreover, the wireless planar multichip system outperforms conventional wireline interchip communication systems. Hence, it is a nearer term alternative as the communication backbone for multichip systems providing significant gains in performance over conventional wireline system. On the other hand,

going forward with matured TSV fabrication process, 3D-HiWiNoC with microchannel cooling can be future alternative as it provides better performance, energy per bit as well as temperature compared to the planar counterpart.

## **5.2 Future Research Directions**

The opportunities for progressing the research performed for this dissertation work will be discussed in the following sections.

### **5.2.1 Energy-Efficient Multi-gigabit Transceiver Design for Intra and Inter-Chip Wireless Interconnects**

The main enabling technology for inter and intra-chip wireless interconnection proposed in this dissertation is the physical layer design comprising of the transceiver circuits and antennas. To compete with state-of-the-art technologies the power consumption of the transceiver circuits should be a minimum while providing the maximum possible data rates. Trends indicate a target link energy efficiency of  $<1$  pJ/bit at data rates of  $>10$  Gbps [43][99]. Consequently, mm-wave transceiver with non-coherent OOK modulation are suitable for such wireless communication technologies [29][99] due to its low complexity and power consumption. In [100] a 60-GHz transceiver system with 2.5 Gbps data rate is implemented in 90-nm CMOS process that has an energy efficiency of 114 pJ/bit. In [101] authors proposed the design of a transceiver with the bit-energy efficiency of 6.26 pJ/bit, with a data rate of 10.7 Gb/s. However, it requires an onboard Yagi–Uda antenna on a non-silicon substrate, which can result in integration difficulties. Moreover, none of the transceiver implementation meets all the desirable specifications of the wireless interconnects i.e. high multi-gigabit data rate and high energy efficiency [43][99].

Therefore, an energy-efficient mm-wave transceiver suitable for both intra and inter-chip application is yet to be demonstrated.

### **5.2.2 Traffic-Aware Medium Access Mechanism for Multi-Chip System**

The MAC for intra-chip WiNoC has been identified by all research groups as one of the main challenges in the design particularly, dynamic mechanisms which are adaptive to changes in the system. Utilizing the full potential of the novel mm-wave interconnect technology in a multichip system requires overcoming two critical design challenges: i) design of efficient, simple and fair MAC mechanism, and ii) managing the wireless bandwidth effectively. Moreover, intra and inter-chip traffic can have very different characteristics and requirements. Information exchange between components in such multichip environments can be either control information or data exchange. Control information required for tasks such as cache coherency protocol, synchronization, thread migrations typically require sporadic but low latency time sensitive communication. Whereas, read and writes between processing engines and memory elements and require a higher volume of data exchange. Consequently, the data exchange in the multichip system can vary from low load extremely sporadic yet latency sensitive data transfer to high load high throughput data exchange.

Due to the distributed and low-overhead implementation, and fairness in channel access, a Token passing based Time Division Multiple Access (T-MAC) is used in many intra-chip architectures [29][32][33]. The MAC should also manage the sharing of the wireless communication medium depending on traffic variation in the intra and inter-chip communication to maximize performance. In a token-based MAC, a single WI possessing the token gains access to the wireless medium to transmit for a certain number of time slots. However, in the multichip

environment, the traffic demand through the switches vary both temporally and spatially depending on the application [102][103]. Therefore, the MAC for such multichip system should be able to allocate transmission slots dynamically to WIs in response to sudden and large variations in traffic. Hence, energy-efficient dynamic MAC mechanisms that can predict the traffic demand of the WIs and respond accordingly by adjusting transmission slots of the WIs need to be developed.

### **5.2.3 A Wireless Interconnection Framework for Multichip System with In-Package Memory**

Multichip computing modules with several chips integrated with memory banks can be found in a wide range of platform based designs from servers to embedded systems. These chips can be processing chips such as multicore chips, CPUs or GPUs or a heterogeneous mix of such chips (For example AMD's Fusion Accelerated Processor Units (APUs)) depending upon desired functionality. Due to scaling up of a number of individual computing nodes by several orders of magnitude in these systems, the interconnection between them has become increasingly complex. Moreover, to satisfy the memory bandwidth demands, integration of in-package memory has become a norm in these systems. Integrating memory within a single package can be done either by placing memory which itself will possibly be vertically stacked on top of a multicore die i.e. monolithic 3D integration [9] or placing them side-by-side on the same substrate or interposer i.e. 2.5D integration [8]. However, in 3D stacked approach, the amount of memory that can be integrated into the package is limited by the size of multicore die (increasing the die size generally reduces yield, and hence, increases manufacturing cost). In addition, the multicore processing chips need to be thinned to accommodate TSVs through it, which can induce die-cracking and

structural yield issues. Moreover, as the integration of the memory will essentially block the path of heat flow of the multicore die, the average die temperature of such system can become prohibitively high [104]. As a result, this approach requires sophisticated thermal management techniques. On the other hand, in horizontal or 2.5D integration, the amount of memory that can be integrated is not bound by the size of the multicore die, rather limited by the size of substrate board or interposer. As a result, it can provide more memory capacity. Moreover, this integration technique will allow disintegration of a large multicore processing chip into several smaller processing chips. Consequently, for the same computational capabilities (i.e. same number of cores and memory sizes), this disintegration will lower the total manufacturing cost considering the fact that smaller die size will eventually result in higher yield and better packing of the rectangular die on a circular wafer [8]. It also enables an easy integration of heterogeneous chips and technologies on the same platform. All these benefits over 3D stacking make 2.5D integration a nearer term solution for a multichip system with in-package memory integration.

Recent trends according to the ITRS (<http://www.itrs2.net/>) predict that the pitch of the I/O interconnects in ICs is not scaling as fast as the gate lengths or pitch of on-chip interconnects. This implies a gap in density and performance of traditional I/O systems relative to on-chip interconnections. The wiring complexity of both on-chip and off-chip interconnects exacerbates the problem by posing design challenges, crosstalk, and signal integrity issues. Moreover, in the case of disintegrated processing chips, cores that were previously on the same chip are now on different processing chips. Therefore, inter-chip communication becomes critical and a potential bottleneck. These factors reduce the efficiency in terms of energy consumption as well as latency and bandwidth of the data transfer between communicating components such as processing cores and memory blocks in a multichip system. Therefore, we need an energy efficient, seamless,

scalable interconnection network that spans across distances of a few millimeters (single chip) to several centimeters (on a multichip environment). Integrated inter and intra-chip photonic interconnections is a promising solution to the off-chip interconnection challenges of traditional I/O. However, the pitch of photonic interconnects does not scale well due to the limitations in size of silicon photonic devices. Moreover, this technology is challenging to integrate with standard CMOS processes typically requiring a separate photonic device layer with large footprints on the chip. Research in recent years has demonstrated that on-chip and off-chip wireless interconnects are capable of establishing radio communications within as well as between multiple chips. Using such on-chip antennas embedded in the chip, Wireless Network-on-Chip (NoC) architectures are shown to improve energy efficiency and bandwidth of on-chip data communication in multicore chips. As a future direction, we propose to use such wireless interconnects to establish a seamless communication backbone which enables data exchange between chips in a multichip system with in-package memory. The same communication protocols used for on-chip data transfer in the intra-chip NoC will be used for off-chip data as well, eliminating the need for protocol transfer. Wireless transceivers will be deployed inside each chip and memory stack, which will be capable of establishing direct one-hop communication with other such transceivers in the system. Hence, the benefits of the design methodologies outlined in this dissertation can be further exploited for such multichip systems with several multicore processing chips and memory stacks.

#### **5.2.4 60 GHz mm-wave Wireless Interconnects to Enable Contactless Testing**

Aggregating multiple smaller chips can overcome the physical limitations in the area, power density, and yield of a single chip multiprocessor system. However, a major concern in multichip integration is the quality of the arriving dies and wafers before stacking. The yield and

consequently, the cost benefits of the multichip system largely depend on the availability of the known good dies. This is because the overall manufacturing yield of the multichip system is a function of the yields of the bare die being stacked. State-of-the-arts chip manufacturing process consists of numerous fabrication steps, and defects can induce in any of these steps. The lifecycle of a chip starts after getting the masks of the circuit design. These masked are then used to fabricate the circuits on a silicon wafer. After the fabrication, the circuits first go through the wafer testing to check functional defects by applying the special test vectors. After wafer testing, the dies are then packaged individually after separating from the wafer using laser dicing. These packaged dies then undergo assembly or packaging test to check the package induced defects. Finally, the packaged dies that pass the packaging test are then assembled onto a substrate (preferably on a PCB board) to make the final product, and the product level testing is done to check the interconnections and the assembly process. In each stage of the testing, the faulty ones are marked to thrown away. As a result, it is very important to catch these defects at the early stages of the life cycle of a chip to save cost and ensure quality. Detecting a defect late in the life cycle is not only decrease cost significantly but also, it hinders the overall reputation of the company, especially if the consumer notices it after delivery. Hence, the chip manufacturing company aims to reach the highest possible coverage in the wafer test in order to minimize the yield losses at the later stages. However, wafer testing in multichip integration needs to overcome several serious difficulties.

In wafer testing, probing dies typically requires a contact to be made between the Automatic Test Equipment (ATE) and die, as the ATEs must be connected to the primary input/output of the Device-Under-Test (DUT) during the test. These connection are made through a set of mechanical probes or probe cards. However, the frequent physical contacts between the probe card and the wafer-under-test have several shortcomings. The probe needles and contact

points can suffer deformation, and debris accumulates on the probe card also affect test outcome. Abrasive cleaning can be used to remove the debris. However, this can damage the probe needles [105][106]. Moreover, stress applied by these probe needles can cause die cracks. In addition, the reduction in feature sizes and the increasing demand for parallel multisite testing limit the benefits of the probe cards [107]. Several wireless or contactless test methods are proposed in the recent literature to overcome the limitation of wafer testing [105][108][109]. However, these methods utilize the near field communication of the antennas and hence, need to be aligned precisely due to the proximity requirements. Mm-wave wireless interconnect realized by metallic zigzag antennas fabricated using top layer metals are CMOS process compatible making them suitable for wafer testing. Moreover, it has been noted in many earlier works that the mm-wave wireless antennas are not directional and hence can be used for broadcast type transmission over the shared wireless channel. This property gives an additional advantage as wireless interconnects can provide a broadcast-capable medium to distribute any kind of test contents faster and efficiently. In our proposed multichip integration methodology using wireless interconnects, the intra-chip interconnection is a hybrid one, consisting both wired and wireless links. For the wafer testing, we will equip the probe card with multiple wireless transceivers operating at 60 GHz carrier frequency. These wireless transceivers will be used to send the test vectors to the chips and to get the testing outcome. As we are envisioning a shared broadcast medium, the probe card can send the test vectors to multiple dies at the same time as all the transceiver will be tuned to work on the same frequency and can reduce the testing time significantly.

## APPENDIX A

### PUBLICATIONS

Following is a list of publications published in reputed journals and conferences during this research.

#### Journals:

- J1. **M. S. Shamim**, N. Mansoor, R. S. Narde, V. Kothandapani, A. Ganguly and J. Venkataraman, "A Wireless Interconnection Framework for Seamless Inter and Intra-Chip Communication in Multichip Systems," In *IEEE Transactions on Computers*, vol. 66, no. 3, pp. 389-402, March 1 2017.
- J2. H. Mondal, S. Gade, **M. Shamim**, S. Deb, and A. Ganguly, "Interference-Aware Wireless Network-on-Chip Architecture using Directional Antennas," In *IEEE Transactions on Multi-Scale Computing Systems*, vol. PP, no. 99, pp.1-1.
- J3. N. Mansoor, A. Vashist, M. Ahmed, **M. S. Shamim**, S. Mamun, and A. Ganguly. "A Traffic-Aware Medium Access Control Mechanism for Energy-Efficient Wireless Network-on-Chip Architectures." In *IEEE Transactions on Computers*. (Under review).
- J4. **M. S. Shamim**, R. S. Narde, J. Hernandez, A. Ganguly, J. Venkatarman, S. G. Kandlikar. "Evaluation of Wireless Network-on-Chip Architectures with Microchannel-Based Cooling in 3D Multicore Chips." In *IEEE Transactions on Computers*. (Under review).

## Conferences:

- C1. **M. S. Shamim**, J. Muralidharan, and A. Ganguly. "An Interconnection Architecture for Seamless Inter and Intra-Chip Communication Using Wireless Links." In *Proceedings of the 9th International Symposium on Networks-on-Chip (NOCS '15)*, Article 2, 8 pages, 2015.
- C2. **M. S. Shamim**, N. Mansoor, A. Samaiyar, A. Ganguly, S. Deb, and S.S. Ram. "Energy-efficient wireless network-on-chip architecture with log-periodic on-chip antennas." In *Proceedings of the 24th edition of the great lakes symposium on VLSI (GLSVLSI)*, 2014.
- C3. **M. S. Shamim**, A. Mhatre, N. Mansoor, A. Ganguly and G. Tsouri, "Temperature-aware wireless network-on-chip architecture," In *Proceedings of International Green Computing Conference*, pp. 1-10, Dallas, TX, 2014.
- C4. **M. S. Shamim**, A. Ganguly, C. Munuswamy, J. Venkatarman, J. Hernandez, S. G. Kandlikar. "Co-design of 3D wireless network-on-chip architectures with microchannel-based cooling" In *Proceedings of the Sixth International Green Computing and Sustainable Computing Conference (IGSC)*, pp. 1-6, 2015, Las Vegas, NV, 2015.
- C5. N. Mansoor, **M. S. Shamim**, and A. Ganguly, "A demand-aware predictive dynamic bandwidth allocation mechanism for wireless network-on-chip," In *Proceedings of the ACM/IEEE International Workshop on System Level Interconnect Prediction (SLIP)*, pp. 1-8, Austin, TX, 2016.

## **Work-in-Progress (WiP)/Poster Presentation:**

- P1. **M. S. Shamim**, N. Mansoor, M. Ahmed, M. Dhull, A. Ganguly, "An Energy-Efficient Integration Methodology for Multichip Systems: A Low-Latency Wireless Interconnection Approach," Accepted for poster presentation as Work-in-Progress (WiP) at Design and Automation Conference (DAC), Austin, TX, 2017.
- P2. **M. S. Shamim**, N. Mansoor, A. Ganguly, "Energy-Efficient Wireless Interconnection Framework for Multichip Systems with In-package Memory Stacks," Accepted for poster presentation at Golisano College of Computing & Information Science Research Showcase, Rochester, NY, 2017.

## BIBLIOGRAPHY

- [1] M. J. Flynn, "Very high-speed computing systems," In *Proceedings of the IEEE*, vol.54, no.12, pp. 1901-1909, Dec. 1966.
- [2] L. Benini, and G. De Micheli, "Networks on chips: a new SoC paradigm," In *Computer*, vol.35, no.1, pp. 70-78, Jan. 2002.
- [3] D. Wentzlaff *et al.*, "On-Chip Interconnection Architecture of the Tile Processor," In *Proceedings of the IEEE Micro*, vol.27, no.5, pp. 15-31, Sep./Oct. 2007.
- [4] S.R. Vangal *et al.*, "An 80-Tile Sub-100-W TeraFLOPS Processor in 65-nm CMOS," In *IEEE Journal of Solid-State Circuits*, vol.43, no.1, pp.29-41, Jan. 2008.
- [5] J. Howard *et al.*, "A 48-Core IA-32 message-passing Processor with DVFS in 45nm CMOS," In *Proceedings of the IEEE International Solid-State Circuits Conference (ISSCC)*, San Francisco, CA, pp. 108-109, 2010.
- [6] International Technology Roadmap for Semiconductors (ITRS), online: <http://www.itrs2.net/itrs-reports.html>
- [7] S. Beamer *et al.*, "Designing multi-socket systems using silicon photonics." In *Proceedings of the International Conference on Supercomputing (ICS)*, pages 521- 522, 2009.
- [8] A. Kannan, N. E. Jerger, and G. H. Loh. "Enabling interposer-based disintegration of multi-core processors." In *Proceedings of the 48th International Symposium on Microarchitecture (MICRO-48)*, Pages 546-558, 2015.
- [9] A.W. Topol *et al.*, "Three-dimensional integrated circuits," In *IBM Journal of Research and Development*, vol.50, no.4.5, pp.491-506, July 2006.
- [10] K. C. Yong; W. C. Song; B. E. Cheah; M. F. Ain, "Signaling analysis of inter-chip I/O package routing for Multi-Chip Package," In *Proceedings of the 4th Asia Symposium on Quality Electronic Design (ASQED)*, vol., no., pp.243-248, July 2012.
- [11] IBM Power Systems for High-Performance Computing System, URL: <http://www-03.ibm.com/systems/power>
- [12] R. Hendry; D. Nikolova; S. Rumley; K. Bergman, "Modeling and Evaluation of Chip-to-Chip Scale Silicon Photonic Networks," In *Proceedings of the 22nd Annual Symposium on IEEE High-Performance Interconnects (HOTI)*, vol., no., pp.1-8, 26-28 Aug. 2014
- [13] X. Wu *et al.*, "UNION: A Unified Inter/Intrachip Optical Network for Chip Multiprocessors," In *Proceedings of the IEEE Transactions on Very Large Scale Integration (VLSI) Systems*, vol.22, no.5, pp. 1082-1095, May 2014.

- [14] Y. Pan *et al.*, "Firefly: Illuminating future network-on-chip with nanophotonics." In *Proceedings of the 36th annual international symposium on Computer architecture (ISCA)*, 2009.
- [15] S. Gunther, F. Binns, D. M. Carmean, J. C. Hall. "Managing the Impact of Increasing Microprocessor Power Consumption". In *Intel Technology Journal*, vol.5, no.1, 2001.
- [16] H. Mizunuma; Lu Yi-Chang; Yang Chia-Lin. "Thermal Modeling and Analysis for 3-D ICs With Integrated Microchannel Cooling." In *IEEE Transactions on Computer-Aided Design of Integrated Circuits and Systems*, vol.30, no.9, pp. 1293 – 1306, 2011.
- [17] D. B. Tuckerman, and R. F. W. Pease. "High-performance heat sinking for VLSI." In *IEEE Electron Device Letters*, vol. 2, no. 5, pp. 126-129, 1981.
- [18] K. Puttaswamy and G. H. Loh. "Thermal analysis of a 3D die-stacked high-performance microprocessor." In *Proceedings of the 16th ACM Great Lakes Symposium on VLSI*, pp. 19-24, 2006.
- [19] B. Dang, M. S. Bakir, D. C. Sekar, C. R. Jr. King, and J. D. Meindl, "Integrated Microfluidic Cooling and Interconnects for 2D and 3D Chips" In *IEEE Transactions on Advanced Packaging*, vol.33, no.1, pp. 79–87, 2010.
- [20] S. G. Kandlikar. "Review and Projections of Integrated Cooling Systems for Three-Dimensional Integrated Circuits." In *Journal of Electronic Packaging*, 2014.
- [21] S. Ndao, Y. Peles, and M. K. Jensen, "Multi-objective thermal design optimization and comparative analysis of electronics cooling technologies," In *International Journal of Heat and Mass Transfer*, vol.52, pp. 4317–4326, Sep. 2009.
- [22] D. Liu and S. V. Garimella, "Analysis and optimization of the thermal performance of microchannel heat sinks," In *International Journal of Numerical Methods for Heat & Fluid Flow*, vol.15, no.1, pp. 70–26, 2005.
- [23] Young-Joon Lee *et al.*, "Co-design of signal, power, and thermal distribution networks for 3D ICs," In *Proceedings of the Design, Automation & Test in Europe Conference & Exhibition*, pp. 610-615, 2009.
- [24] H. Matsutani *et al.*, "Low-latency wireless 3D NoCs via randomized shortcut chips," In *Proceedings of the Design, Automation and Test in Europe Conference and Exhibition (DATE)*, vol., no., pp.1,6, 24-28 March 2014.
- [25] N. Miura, D. Mizoguchi, T. Sakurai and T. Kuroda, "Analysis and design of inductive coupling and transceiver circuit for inductive inter-chip wireless superconnect," in *IEEE Journal of Solid-State Circuits*, vol.40, no.4, pp. 829-837, April 2005.
- [26] J. Ouyang, J. Xie, M. Poremba, and Y. Xie, "Evaluation of using inductive/capacitive-coupling vertical interconnects in 3D network-on-chip," In *Proceedings of the IEEE/ACM International Conference on Computer-Aided Design (ICCAD)*, pp. 477-482, 2010.

- [27] J. J. Lin *et al.*, "Communication Using Antennas Fabricated in Silicon Integrated Circuits," in *IEEE Journal of Solid-State Circuits*, vol.42, no.8, pp. 1678-1687, Aug. 2007.
- [28] K. Chang *et al.*, "Performance evaluation and design trade-offs for wireless network-on-chip architectures," In *ACM Journal on Emerging Technologies in Computing Systems (JETC)*, vol.8, no.3, pp. 23:1–23:25, Aug. 2012.
- [29] S. Deb, A. Ganguly, P. P. Pande, B. Belzer, and D. Heo, "Wireless NoC as Interconnection Backbone for Multicore Chips: Promises and Challenges," In *IEEE Journal on Emerging and Selected Topics in Circuits and Systems*, vol.2, no.2, pp. 228–239, 2012.
- [30] A. Ganguly *et al.*, "Scalable Hybrid Wireless Network-on-Chip Architectures for Multicore Systems," In *IEEE Transactions on Computers*, vol.60, no.10, pp. 1485–1502, 2011.
- [31] S. Abadal, E. Alarcón, A. Cabellos-Aparicio, M. Lemme, M. Nemirovsky, "Graphene-enabled wireless communication for massive multicore architectures," In *IEEE Communications Magazine*, vol.51, no.11, pp.137,143, Nov. 2013.
- [32] D. Zhao and Y. Wang, "Sd-mac: Design and synthesis of a hardware efficient collision-free QoS-aware mac protocol for wireless network-on chip," In *IEEE Transactions on Computers*, vol.57, no.9, pp. 1230–1245, 2008.
- [33] D. DiTomaso, A. Kodi, S. Kaya, and D. Matolak, "iWISE: Inter-router Wireless Scalable Express Channels for Network-on-Chips (NoCs) Architecture," in *Proceedings of the 19th IEEE Annual Symposium on High-Performance Interconnects (HOTI)*, pp. 11–18, 2011.
- [34] V. Vijayakumaran *et al.*, "CDMA Enabled Wireless Network-on-Chip." In *ACM Journal on Emerging Technologies in Computing Systems (JETC)*. vol.10, no. 4, June 2014.
- [35] H. H. Yeh and K. L. Melde, "60 GHz multi-antenna design in Multi-Core system," In *Proceedings of the IEEE Antennas and Propagation Society International Symposium (APSURSI)*, pp. 1-2, 2012.
- [36] J. Duato, S. Yalamanchili, and L. NI, "Interconnection Networks-An Engineering Approach," *Morgan Kaufmann*, 2002.
- [37] U.Y. Ogras and R. Marculescu, "It's a small world after all": noc performance optimization via long-range link insertion," In *IEEE Transactions on Very Large Scale Integration (VLSI) Systems*. vol.14, no.7, pp. 693-706, July 2006.
- [38] A. Kumar, L. S. Peh, P. Kundu, and N. K. Jha, "Express virtual channels: towards the ideal interconnection fabric," in *Proceedings of the 34th annual international symposium on Computer architecture (ISCA)*. ACM, New York, NY, USA, 150-161, 2007.
- [39] D Vantrease *et al.*, "Corona: System Implications of Emerging Nanophotonic Technology." In *Proceedings of the 35th Annual International Symposium on Computer Architecture (ISCA)*. IEEE Computer Society, Washington, DC, USA, 153-164, 2008.

- [40] M. F. Chang *et al.*, "CMP network-on-chip overlaid with multi-band RF-interconnect," In *Proceedings of the IEEE International Symposium on High-Performance Computer Architecture*, Salt Lake City, UT, pp. 191-202, 2008.
- [41] J. E. Jaussi, M. Leddige, B. Horine, F. O'Mahony and B. Casper, "Multi-Gbit I/O and interconnect co-design for power efficient links," In *Proceedings of the IEEE 19th Conference on Electrical Performance of Electronic Packaging and Systems (EPEPS)*, pp. 1-4, 2010.
- [42] M. S. Shamim, J. Muralidharan, and A. Ganguly. "An Interconnection Architecture for Seamless Inter and Intra-Chip Communication Using Wireless Links." In *Proceedings of the 9th International Symposium on Networks-on-Chip (NOCS '15)*. ACM, New York, NY, USA, Article 2, 8 pages, 2015.
- [43] S. Laha, S. Kaya, D. W. Matolak, W. Rayess, D. DiTomaso and A. Kodi, "A New Frontier in Ultralow Power Wireless Links: Network-on-Chip and Chip-to-Chip Interconnects," in *IEEE Transactions on Computer-Aided Design of Integrated Circuits and Systems*, vol.34, no.2, pp. 186-198, Feb. 2015.
- [44] U. Chandran and D. Zhao, "Cost-optimal design of wireless pre-bonding test framework," In *Proceedings of the 27th IEEE International System-on-Chip Conference (SOCC)*, pp. 324-329, 2014.
- [45] L. Biswal, S. Chakraborty and S. K. Som, "Design and Optimization of Single-Phase Liquid Cooled Microchannel Heat Sink," in *IEEE Transactions on Components and Packaging Technologies*, vol.32, no.4, pp. 876-886, Dec. 2009.
- [46] M. M. Sabry, A. Sridhar, J. Meng, A. K. Coskun and D. Atienza, "GreenCool: An Energy-Efficient Liquid Cooling Design Technique for 3-D MPSoCs Via Channel Width Modulation," in *IEEE Transactions on Computer-Aided Design of Integrated Circuits and Systems*, vol.32, no.4, pp. 524-537, April 2013.
- [47] M. M. Sabry, A. K. Coskun, D. Atienza, T. Š Rosing and T. Brunschwiler, "Energy-Efficient Multi-objective Thermal Control for Liquid-Cooled 3-D Stacked Architectures," in *IEEE Transactions on Computer-Aided Design of Integrated Circuits and Systems*, vol.30, no.12, pp. 1883-1896, Dec. 2011.
- [48] H. B. Jang, I. Yoon, C. H. Kim, S. Shin and S. W. Chung, "The impact of liquid cooling on 3D multi-core processors," In *Proceedings of the IEEE International Conference on Computer Design*, pp. 472-478, 2009.
- [49] B. Shi, and A. Srivastava. "TSV-constrained micro-channel infrastructure design for cooling stacked 3D-ICs". In *Proceedings of the ACM international symposium on International Symposium on Physical Design*, pp. 113-118, 2012.
- [50] W. R. Davis *et al.*, "Demystifying 3D ICs: the pros and cons of going vertical," in *IEEE Design & Test of Computers*, vol.22, no.6, pp. 498-510, Nov.-Dec. 2005.
- [51] A. More, and B. Taskin. Wireless interconnects for inter-tier communication on 3D ICs. In *Proceedings of the European Microwave Conference (EuMC)*, pp. 105-108, 2010.

- [52] S. B. Lee *et al.*, "A scalable micro wireless interconnect structure for CMPs," In *Proceedings of ACM Annual International Conference on Mobile Computing and Networking*, pp. 20-25, 2009.
- [53] K. Duraisam, R. G. Kim, P. P. Pande, "Enhancing performance of wireless NoCs with distributed MAC protocols," In *Proceedings of the 16th International Symposium on Quality Electronic Design (ISQED)*, vol., no., pp.406-411, 2-4 Mar. 2015.
- [54] Piro *et al.*, "Initial MAC Exploration for Graphene-enabled Wireless Networks-on-Chip," In *Proceedings of the ACM First Annual International Conference on Nanoscale Computing and Communication (NANOCOM)*, ACM, New York, NY, USA, 2014.
- [55] J. Chen; Y. H. Lai, "A study of CSMA-based and token-based wireless interconnects network-on-chip," In *Proceedings of the IEEE International Conference on Communication Problem-Solving (ICCP)*, vol., no., pp.205-209, 5-7 Dec. 2014.
- [56] N. Mansoor, P. J. S. Iruthayaraj and A. Ganguly, "Design Methodology for a Robust and Energy-Efficient Millimeter-Wave Wireless Network-on-Chip," in *IEEE Transactions on Multi-Scale Computing Systems*, vol.1, no.1, pp. 33-45, Jan.-Mar. 1, 2015.
- [57] A. Ganguly, P. Wettin, K. Chang, and P. Pande, "Complex network inspired fault-tolerant NoC architectures with wireless links," in *Proceedings of the Fifth IEEE/ACM International Symposium on Networks on Chip (NoCS)*, pp. 169–176, 2011.
- [58] M. Yuan, W. Fu, T. Chen, and M. Wu, "An exploration on quantity and layout of wireless nodes for hybrid wireless network-on-chip." In *Proceedings of the IEEE Conference on High-Performance Computing and Communications*, pp. 100–107, Aug 2014.
- [59] T. Petermann and P. De Los Rios, "Spatial small-world networks: a wiring cost perspective," 2005. *arXiv:cond-mat/0501420v2*.
- [60] M.S. Shamim, N. Mansoor, A. Samaiyar, A. Ganguly, S. Deb, and S.S. Ram. "Energy-efficient wireless network-on-chip architecture with log-periodic on-chip antennas." In *Proceedings of the 24th edition of the great lakes symposium on VLSI (GLSVLSI '14)*, 2014.
- [61] H. Mondal; S. Gade; M. Shamim; S. Deb; A. Ganguly, "Interference-Aware Wireless Network-on-Chip Architecture using Directional Antennas," in *IEEE Transactions on Multi-Scale Computing Systems*, vol.PP, no.99, pp.1-1, 2016.
- [62] T. Kagami, H. Matsutani, M. Koibuchi, Y. Take, T. Kuroda and H. Amano, "Efficient 3-D Bus Architectures for Inductive-Coupling ThruChip Interfaces," In *IEEE Transactions on Very Large Scale Integration (VLSI) Systems*, vol.24, no.2, pp. 493-506, Feb. 2016.
- [63] N. Mansoor and A. Ganguly, "Reconfigurable Wireless Network-on-Chip with a Dynamic Medium Access Mechanism," In *Proceedings of the 9th International Symposium on Networks-on-Chip (NOCS)*, 2015.
- [64] N. Mansoor, MS. Shamim, and A. Ganguly, "A demand-aware predictive dynamic bandwidth allocation mechanism for wireless network-on-chip," In *Proceedings of the*

- ACM/IEEE International Workshop on System Level Interconnect Prediction (SLIP)*, , pp. 1-8, Austin, TX, 2016.
- [65] H. K. Mondal, and S. Deb, "An energy-efficient wireless network-on-chip using power-gated transceivers," In *Proceedings of the 27th IEEE International System-on-Chip Conference (SOCC)*, pp. 243–248, Sept 2014.
- [66] H. K. Mondal and S. Deb, "Energy efficient on-chip wireless interconnects with sleepy transceivers," In *Proceedings of the 8th International Design and Test Symposium (IDT)*, pp. 1–6, Dec. 2013.
- [67] G. Balamurugan *et al.*, "A Scalable 5–15 Gbps, 14–75 mW Low-Power I/O Transceiver in 65 nm CMOS," In *IEEE Journal of Solid-State Circuits*, vol.43, no.4, pp. 1010-1019, Apr. 2008.
- [68] Chip MultiProjects. Retrieved Nov. 2015, from <http://cmp.imag.fr>
- [69] P.P. Pande, C. Grecu, M. Jones, A. Ivanov, R. Saleh, "Performance evaluation and design trade-offs for network-on-chip interconnect architectures," In *IEEE Transactions on Computers*, vol.54, no.8, pp.1025-1040, Aug. 2005.
- [70] FR4 EPOXY URL: <http://www.sunstone.com/pcb-capabilities/pcb-manufacturing-capabilities/pcb-materials/fr-4-material>
- [71] Lopez, Aida L. Vera et al. "Novel low loss thin film materials for wireless 60 GHz application." In *Proceedings of the 60<sup>th</sup> IEEE Electronic Components and Technology Conference (ECTC)*, 2010.
- [72] M. Schwartz, W. R. Bennett, and S. Stein, "Communication Systems and Techniques." *IEEE Press., 1996*.
- [73] HFSS URL: <http://www.ansys.com/Products/Simulation+Technology/Electronics/Signal+Integrity/ANSYS+HFSS>
- [74] Personal Communication with Rounak, Dr. Jayanti, Jose-Luis, and Dr. Kandlikar.
- [75] S. Deb, A. Ganguly, K. Chang, P. Pande, B. Beizer and D. Heo, "Enhancing performance of network-on-chip architectures with millimeter-wave wireless interconnects," In *Proceedings of the 21st IEEE International Conference on Application-specific Systems Architectures and Processors (ASAP)*, pp. 73-80, 2010.
- [76] K. C. Yong; W. C. Song; B. E. Cheah; M. F. Ain, "Signaling analysis of inter-chip I/O package routing for Multi-Chip Package," in *Proceedings of the 4th Asia Symposium on Quality Electronic Design (ASQED)*, vol., no., pp.243-248, 10-11 July 2012.
- [77] P.J. Koopman and B.P. Upender, "Time Division Multiple Access without a Bus Master," In *United Technologies Research Center, US, Technical Report RR-9500470*, 1995.

- [78] P. Wettin *et al.*, "Performance evaluation of wireless NoCs in presence of irregular network routing strategies," In *Proceedings of the Design, Automation, and Test in Europe Conference and Exhibition (DATE)*, vol., no., pp.1-6, 24-28 Mar. 2014.
- [79] M. S. Shamim, A. Mhatre, N. Mansoor, A. Ganguly and G. Tsouri, "Temperature-aware wireless network-on-chip architecture," In *Proceedings of the International Green Computing Conference*, pp. 1-10. Dallas, TX, 2014.
- [80] J. Lee, C. Nicopoulos, S. J. Park, M. Swaminathan and J. Kim, "Do we need wide flits in Networks-on-Chip?," In *Proceedings of the IEEE Computer Society Annual Symposium on VLSI (ISVLSI)*, pp. 2-7, 2013.
- [81] V. Soteriou, Hangsheng Wang, and L. Peh, "A Statistical Traffic Model for On-Chip Interconnection Networks," In *Proceedings of the 14th IEEE International Symposium on Modeling, Analysis, and Simulation of Computer and Telecommunication Systems*. pp. 104-116, 2006.
- [82] K. Kempa *et al.*, "Carbon Nanotubes as Optical Antennae," In *Advanced Materials*, vol. 19, pp. 421-426, 2007.
- [83] P. Grani, S. Bartolini, E. Furdiani, L. Ramini and D. Bertozzi, "Integrated cross-layer solutions for enabling silicon photonics into future chip multiprocessors," In *Proceedings of the 19th International Mixed-Signals, Sensors, and Systems Test Workshop (IMS3TW)*, pp. 1-8, 2014.
- [84] K. Pranay *et al.*, "Silicon-photonic network architectures for scalable, power-efficient multi-chip systems." In *Proceedings of the 37th annual international symposium on Computer architecture (ISCA)*. ACM, New York, NY, USA, 117-128, 2010.
- [85] P. Dong *et al.*, "Wavelength-tunable silicon microring modulator." *Optics Express*, vol.18, no.11, pp.10941-10946, 2010.
- [86] A. Mineo, M. S. Rusli, M. Palesi, G. Ascia, V. Catania, and M. N. Marsono, "A closed-loop transmitting power self-calibration scheme for energy efficient WiNoc architectures," In *Proceedings of the Design, Automation Test in Europe Conference (DATE)*, Mar. 2015.
- [87] M. S. Shamim, N. Mansoor, R. S. Narde, V. Kothandapani, A. Ganguly and J. Venkataraman, "A Wireless Interconnection Framework for Seamless Inter and Intra-Chip Communication in Multichip Systems," In *IEEE Transactions on Computers*, vol. 66, no. 3, pp. 389-402, March 1, 2017.
- [88] Fluent 14.5 URL:  
<http://www.ansys.com/Products/Simulation+Technology/Fluid+Dynamics/Fluid+Dynamic+s+Products/ANSYS+Fluent>
- [89] H.Y. Zhang *et al.*, "Single-phase liquid cooled microchannel heat sink for electronic packages," In *Applied Thermal Engineering*, vol. 25, no. 10, Pages 1472-1487, July 2005.

- [90] D. Lorenzini-Gutierrez, S.G. Kandlikar, "Variable Fin density flow channels for effective cooling and mitigation of temperature non-uniformity in three-dimensional integrated circuits." In *Journal of Electronic Packaging*, vol. 136, no. 02, 2014.
- [91] H. G. Schantz, "Near field propagation law & a novel fundamental limit to antenna gain versus size," In *Proceedings of the IEEE Antennas and Propagation Society International Symposium*, pp. 237-240, 2005.
- [92] W. Huang, R.S. Mircea, S. Gurumurthi, R. J. Ribando, and K. Skadron. "Interaction of scaling trends in processor architecture and cooling." In *Proceedings of the 26th Annual IEEE SEMI-THERM*, pp. 198-204, 2010.
- [93] J. Meng, K. Katsutoshi, and A. K. Coskun. "Optimizing energy efficiency of 3-D multicore systems with stacked DRAM under power and thermal constraints." In *Proceedings of the 49th ACM Annual Design Automation Conference*, 2012.
- [94] B.S. Feero, P.P. Pande. "Networks-on-Chip in a Three-Dimensional Environment: A Performance Evaluation" In *IEEE Transactions on Computers*, vol.58, no.1, pp. 32-45, 2009.
- [95] N. Binkert *et al.*, "The GEM5 Simulator," *ACM SIGARCH Computer Architecture News*, vol.39, no.2, pp. 1-7, 2011.
- [96] S.C Woo; M. Ohara; E. Torrie; J.P. Singh; and A. Gupta; "The SPLASH-2 Programs: Characterization and Methodological Considerations," In *Proceedings of the Annual International Symposium on Computer Architecture*, pp. 24-36, 1995.
- [97] C. Bienia, "Benchmarking Modern Multiprocessors," *Ph.D. Dissertation, Princeton Univ.*, Princeton NJ, Jan. 2011.
- [98] S. Li; J.H. Ahn; R.D. Strong; J.B. Brockman; and D.M. Tullsen; "McPAT: an Integrated Power, Area, and Timing Modeling Framework for Multicore and Manycore Architectures," In *Proceedings of the. of the International Symposium on Microarchitecture*, pp. 469-480, 2009.
- [99] X. Yu, H. Rashtian, S. Mirabbasi, P. P. Pande and D. Heo, "An 18.7-Gb/s 60-GHz OOK Demodulator in 65-nm CMOS for Wireless Network-on-Chip," in *IEEE Transactions on Circuits and Systems I: Regular Papers*, vol. 62, no. 3, pp. 799-806, March 2015.
- [100] Jri Lee, Yenlin Huang, Yentso Chen, Hsinchia Lu and Chiajung Chang, "A low-power fully integrated 60GHz transceiver system with OOK modulation and on-board antenna assembly," In *Proceedings of the IEEE International Solid-State Circuits Conference - Digest of Technical Papers*, pp. 316-317,317a, San Francisco, CA, 2009.
- [101] W. Byeon, C. H. Yoon, and C. S. Park, "A 67-mW 10.7-Gb/s/60-GHz OOK CMOS transceiver for short-range wireless communications," In *IEEE Transactions on Microwave Theory and Techniques*, vol. 61, no. 9, pp. 3391–3401, Sep. 2013.

- [102] A. K. Mishra, N. Vijaykrishnan, and C. R. Das, "A case for heterogeneous on-chip interconnects for CMPs," In *Proceedings of the 38th Annual International Symposium on Computer Architecture (ISCA '11)*, San Jose, CA, pp. 389-399, 2011.
- [103] M. Badr and N. E. Jerger, "SynFull: Synthetic traffic models capturing cache coherent behaviour," In *Proceedings of the ACM/IEEE 41st International Symposium on Computer Architecture (ISCA '14)*, Minneapolis, MN, pp. 109-120, 2014.
- [104] G.H. Loh, N.E. Jerger, A. Kannan, and Y. Eckert. "Interconnect-Memory Challenges for Multi-chip, Silicon Interposer Systems." In *Proceedings of the ACM MEMSYS*, pp. 3-10, 2015.
- [105] E. J. Marinissen *et al.*, "Contactless testing: Possibility or pipe-dream?," In *Proceedings of the Design, Automation & Test in Europe Conference & Exhibition*, pp. 676-681, 2009.
- [106] W. R. Mann, F. L. Taber, P. W. Seitzer and J. J. Broz, "The leading edge of production wafer probe test technology," In *Proceedings of the International Conference on Test*, pp. 1168-1195, 2004.
- [107] C. W. Wu, C. T. Huang, S. y. Huang, P. c. Huang, T. y. Chang and Y. t. Hsing, "The HOY Tester-Can IC Testing Go Wireless?," In *Proceedings of the International Symposium on VLSI Design, Automation and Test*, pp. 1-4, 2006.
- [108] B. Moore *et al.*, "Non-contact Testing for SoC and RCP (SIPs) at Advanced Nodes," In *Proceedings of the IEEE International Test Conference*, pp. 1-10, Santa Clara, CA, 2008.
- [109] B. Moore *et al.*, "High throughput non-contact SiP testing," *2007 Proceedings of the IEEE International Test Conference*, pp. 1-10, Santa Clara, CA, 2007.
- [110] M. S. Shamim, A. Ganguly, C. Munuswamy, J. Venkatarman, J. Hernandez and S. Kandlikar, "Co-design of 3D wireless network-on-chip architectures with microchannel-based cooling," In *Proceedings of the Sixth International Green and Sustainable Computing Conference (IGSC)*, pp. 1-6, Las Vegas, NV, 2015.